March, 2000

Nonlinear Optics of Semiconductor Materials

Koichi Okamoto

Kyoto University – Venture Business laboratory

Nonlinear Optical Effect

Sum/Different frequency generation, Harmonic generation, Parametric amplification, Two photon absorption, Stimulated Raman scattering, Four wave mixing, Self focusing, phase conjugation, etc.

The nonlinear optical response is given by the polarization ***P***(t) as a power series in the electric field vector ***E*** as

$$\boldsymbol{P} / \varepsilon_o = \Sigma\, \chi_{ij}^{(1)} \boldsymbol{E}_j + \Sigma\Sigma\, \chi_{ijk}^{(2)} \boldsymbol{E}_j \boldsymbol{E}_k + \Sigma\Sigma\Sigma\, \chi_{ijkl}^{(3)} \boldsymbol{E}_j \boldsymbol{E}_k \boldsymbol{E}_l + \ldots$$

The time varying profiles of the nonlinear optical response indicate the many processes in several materials,

femto — pico — micro — milli — second — min — hour — **Time** →

Electronic polarization	Thermal dynamics	Clustering, Aggregation
Electron transfer	Volume, structure change	Molecular harmonic effect
Energy transfer	Density change	Nano particle growth
Carrier Dynamics	Ultrasonic, Acoustic wave	Crystal growth
Excitation Dynamics	Chemical reaction	Phase Transfer
Molecular vibration	Molecular translation	Metal diffusion

Carrier Dynamics

Currently, Semiconductor-based optical/electrical materials and devices have been developed and used for wider application fields

Optical properties of semiconductor materials are controlled by the **dynamics of carriers and/or excitons**

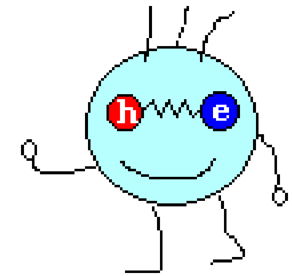

Mr. Exciton

Designed by Dr. Suda in Kyoto Univ.

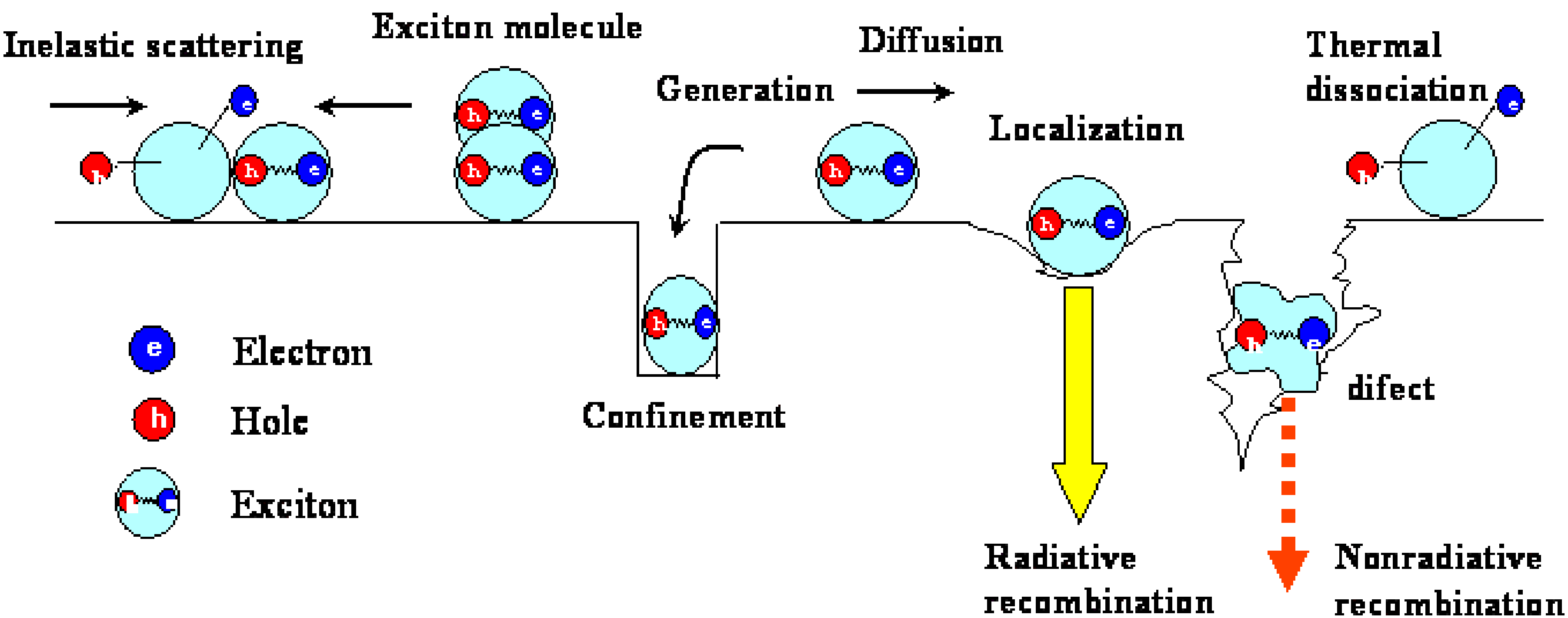

Molecular Dynamics

Optical properties of solutions are controlled by the molecular dynamics

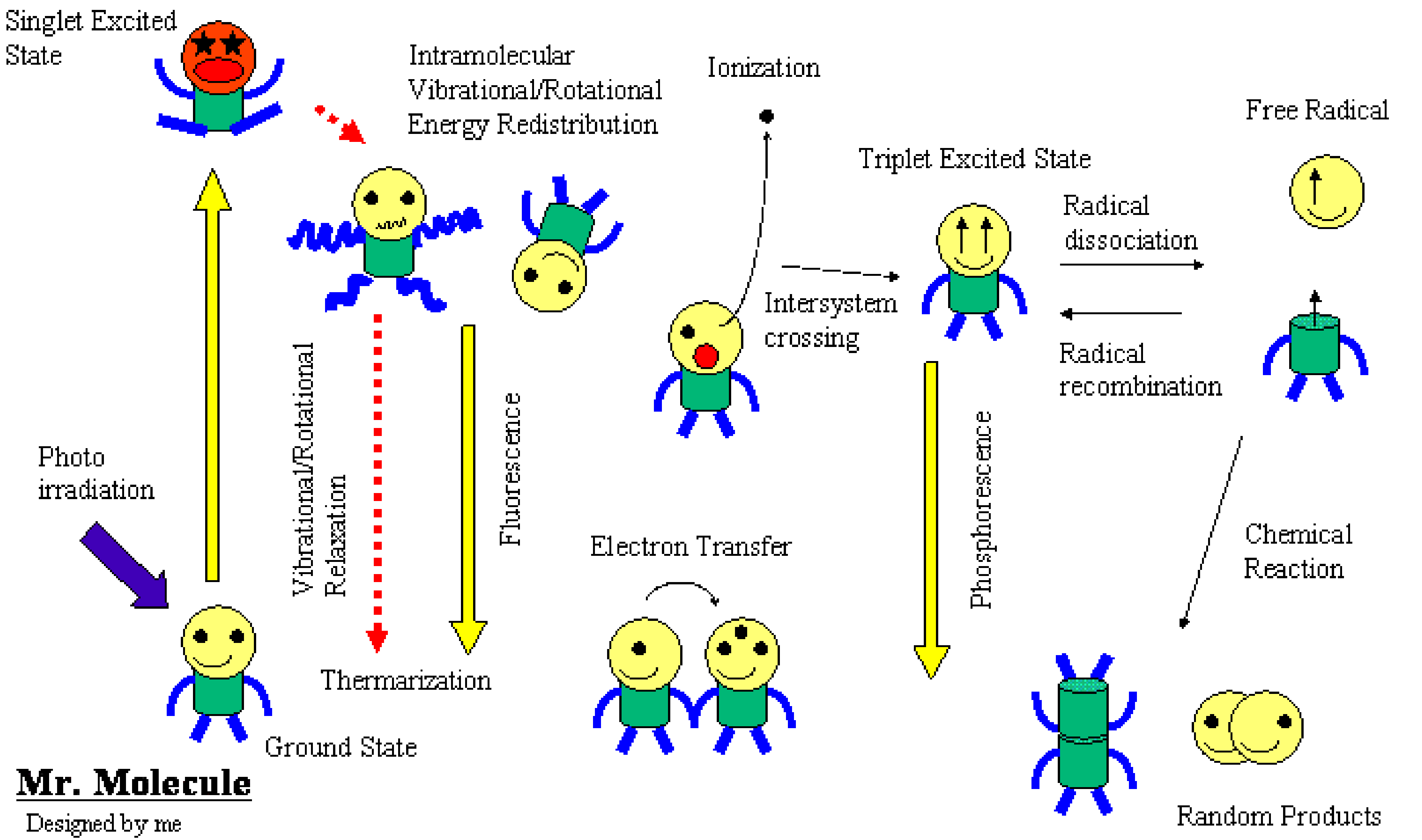

ZnSe Homoepitaxial Layers

ZnSe homoepitaxial layer

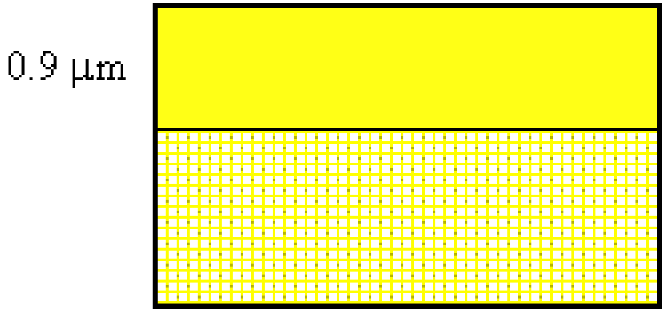

ZnSe Homoepitaxial layer (HL)

grown by Molecular Beam Epitaxy (MBE)

Low defects, dislocation, deformation

↓

Very strong emission and nonlinearity

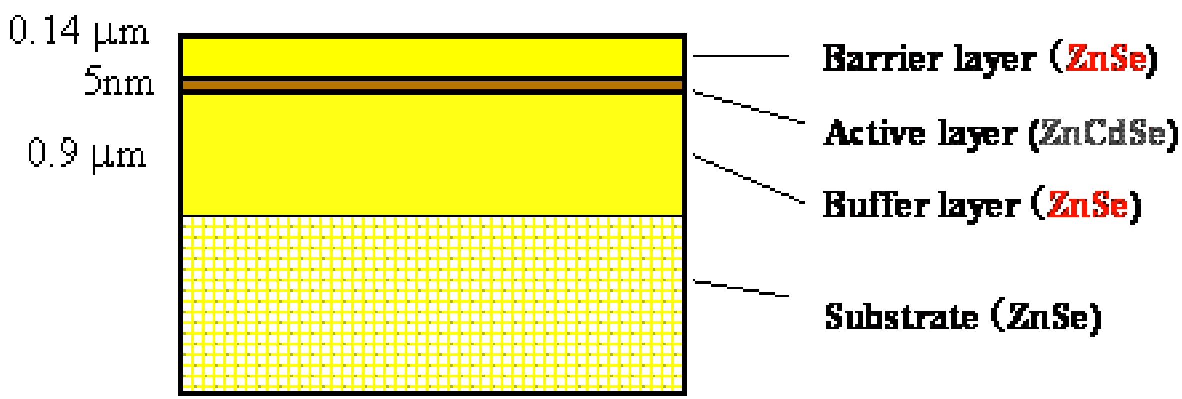

ZnCdSe/ZnSe Quantum Well (QW)

The reason of the strong emission of ZnSe homoepitaxial layer is still unknown

Emission Spectrum

HeCd Laser

325nm 3W/cm^{-2}

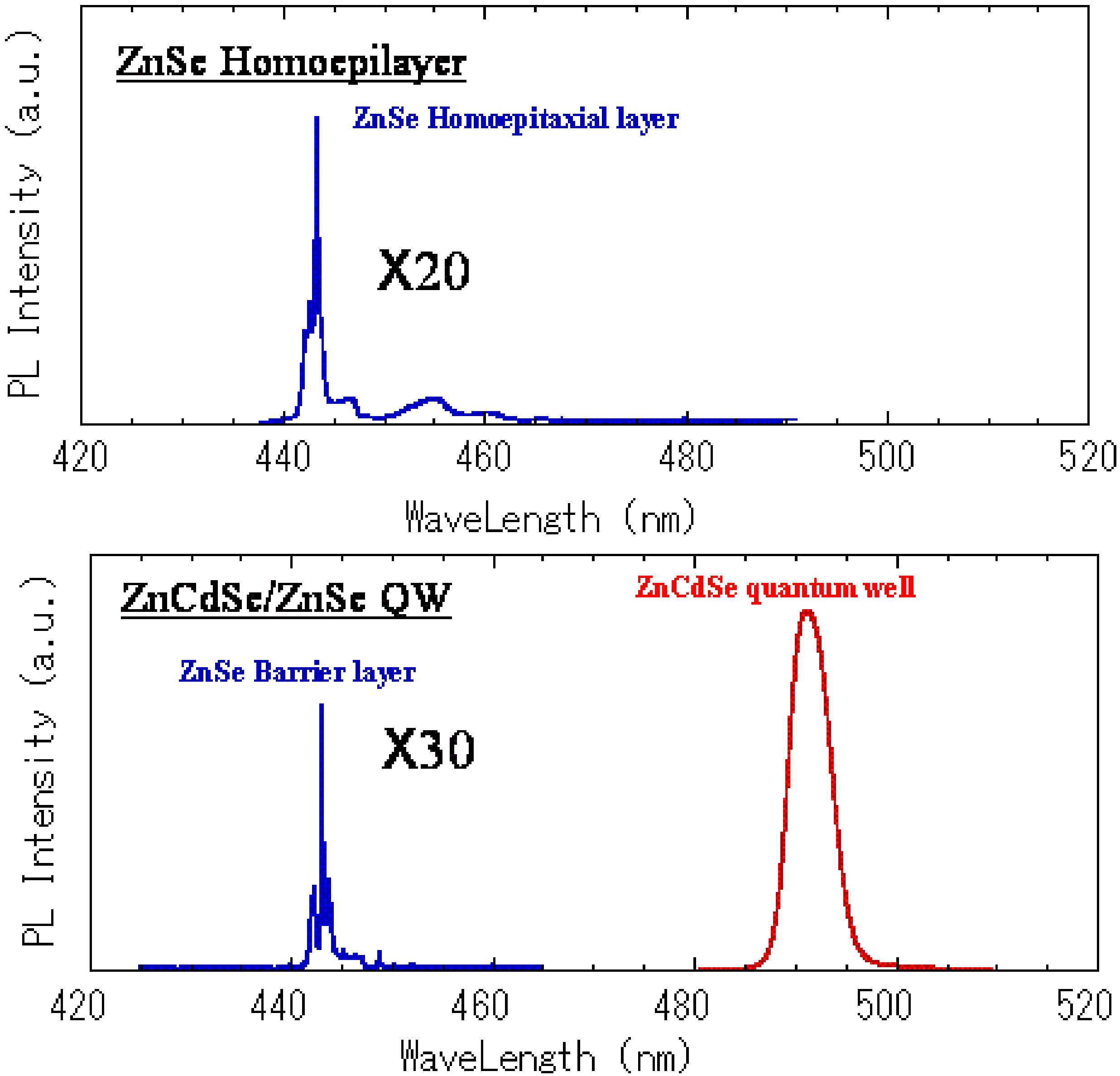

Time-Resolved Photoluminescence

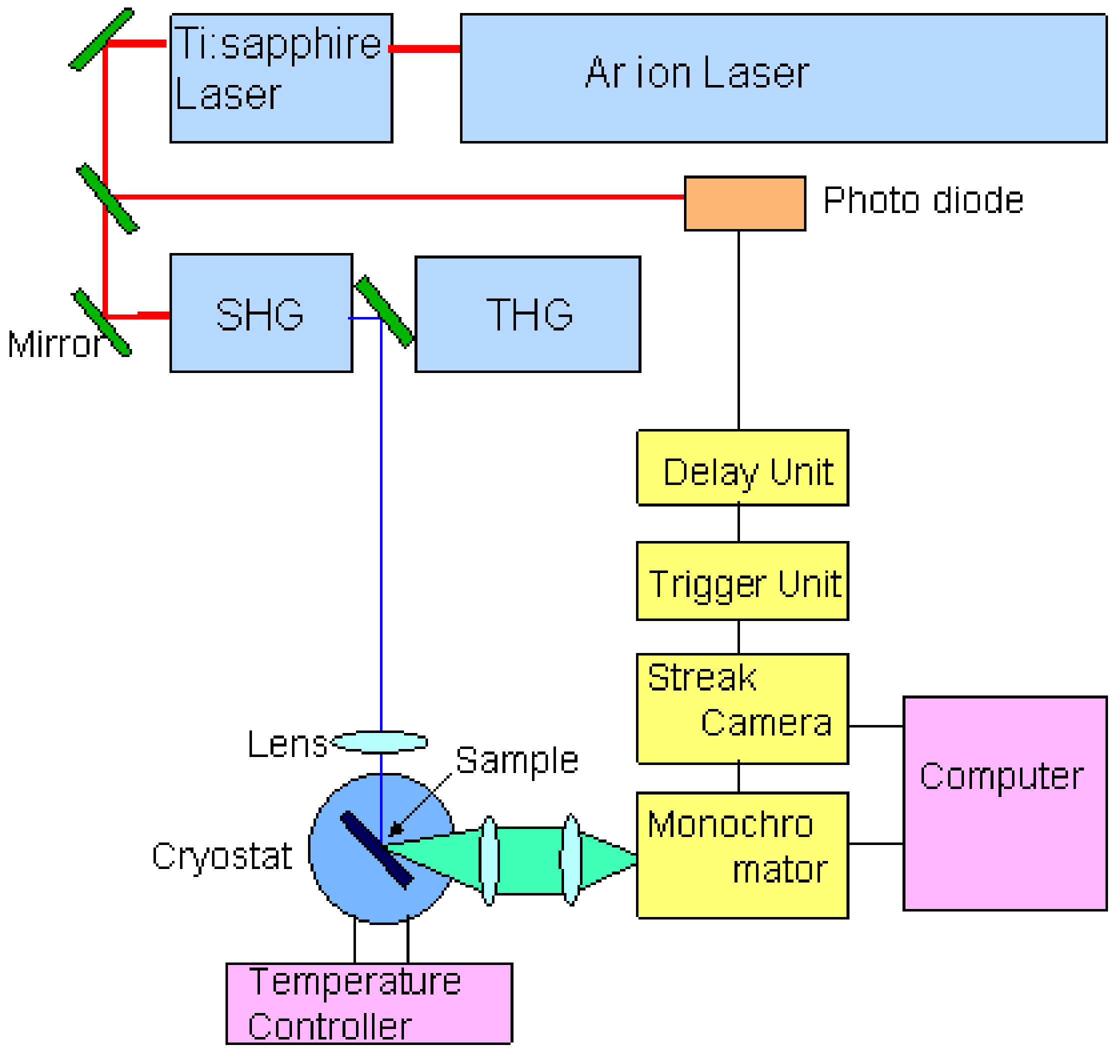

Mechanism of Streak Scope

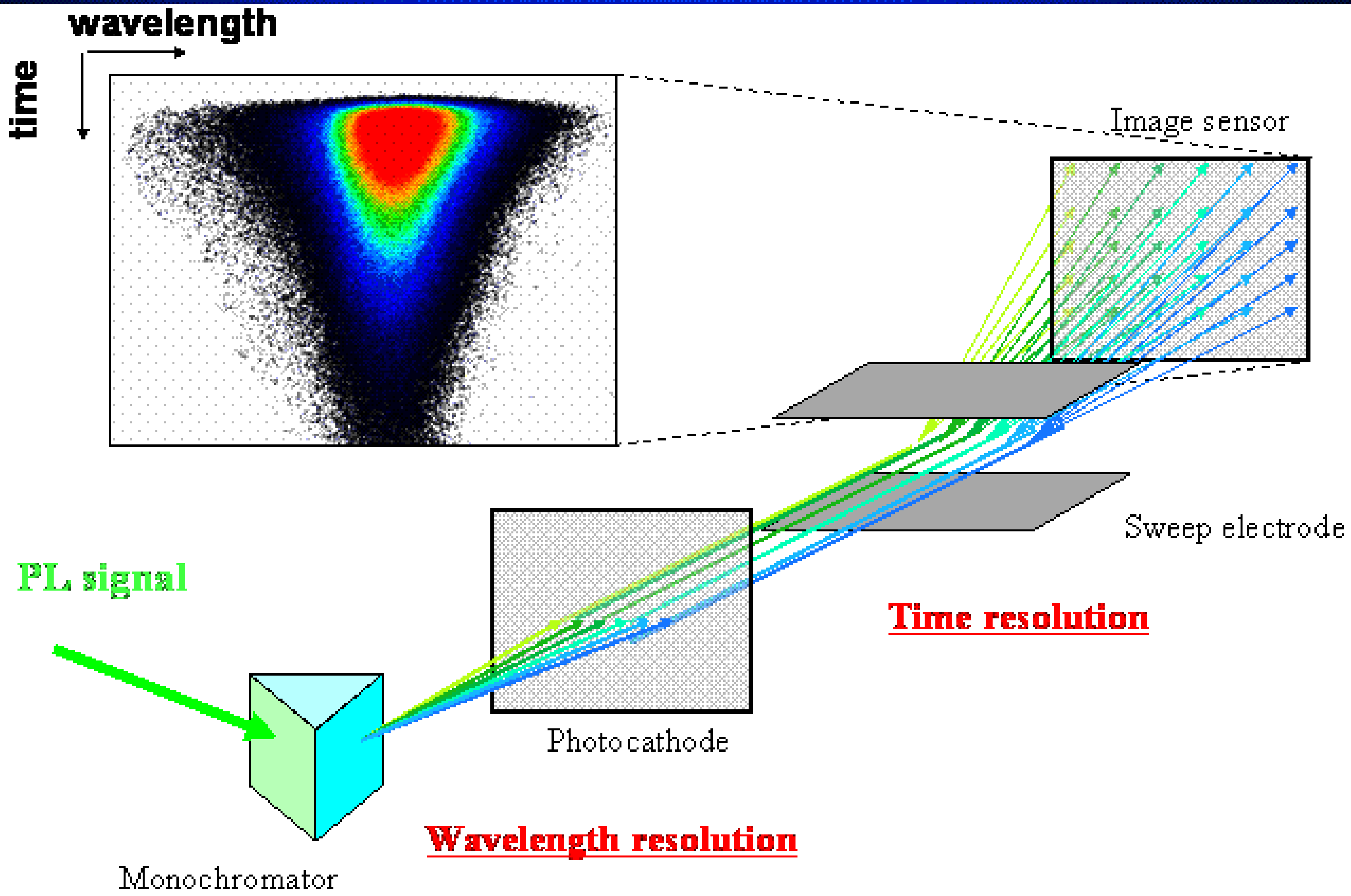

Analysis of Streak Image

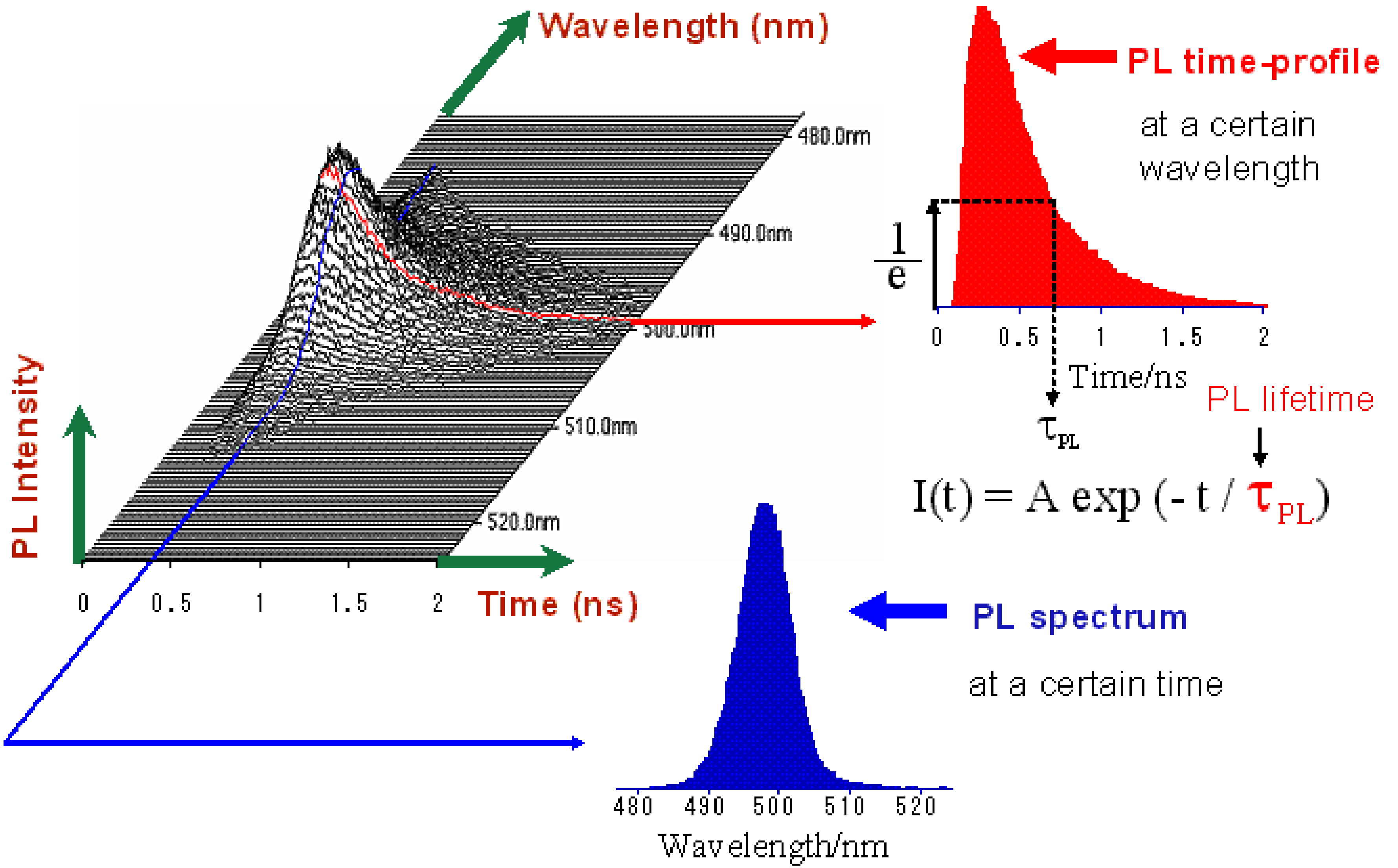

Sample Structures

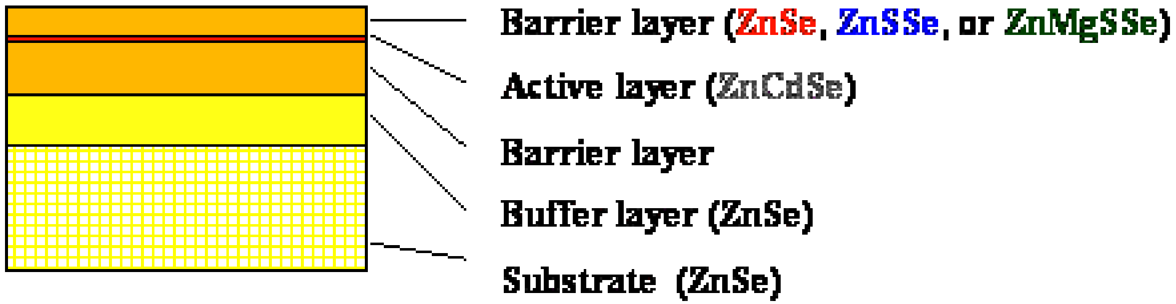

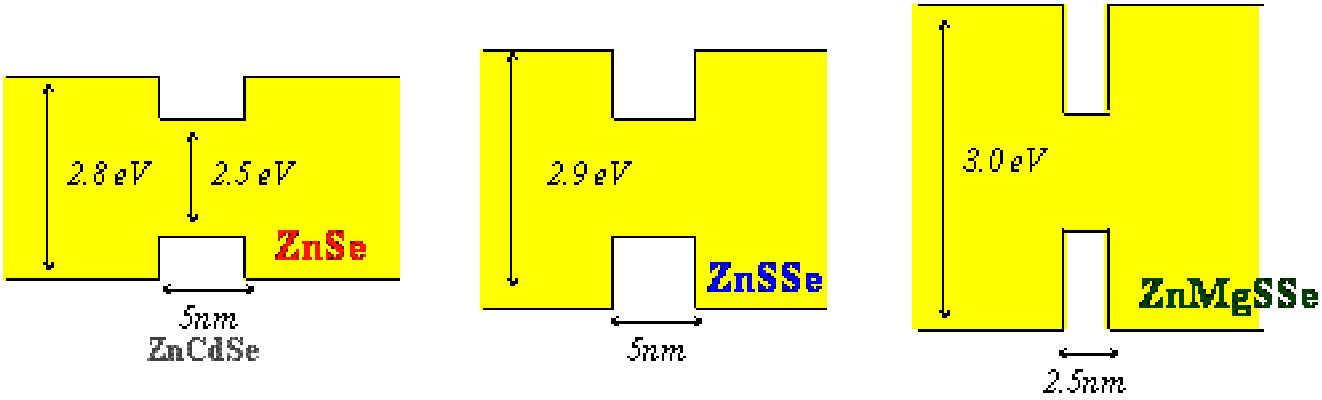

ZnSe(0.14 μm) / $Zn_{0.75}Cd_{0.25}Se$(5nm) / ZnSe (0.9 μm)/ZnSe sub.

ZnSSe(0.1 μm) / ZnCdSe(5nm) / ZnSSe(0.9 μm) / ZnSe(0.9 μm) / ZnSe sub. (S:12%),

ZnMgSSe(0.1 μm) / ZnCdSe(2.5nm) / ZnMgSSe(0.9 μm) / ZnSe(0.6 μm) / ZnSe sub. (S:7%, Mg:6%)

PL under low power excitation

© Koichi Okamoto

Excitation Power: 1mW, Carrier density : ~10^{16} cm^{-3}

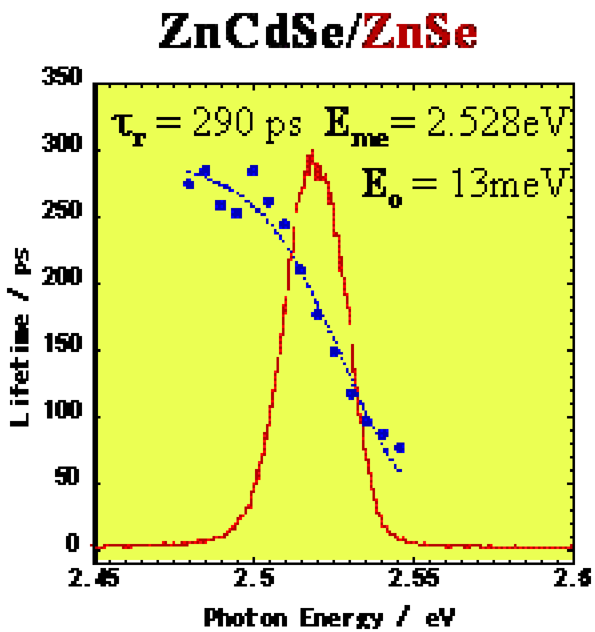

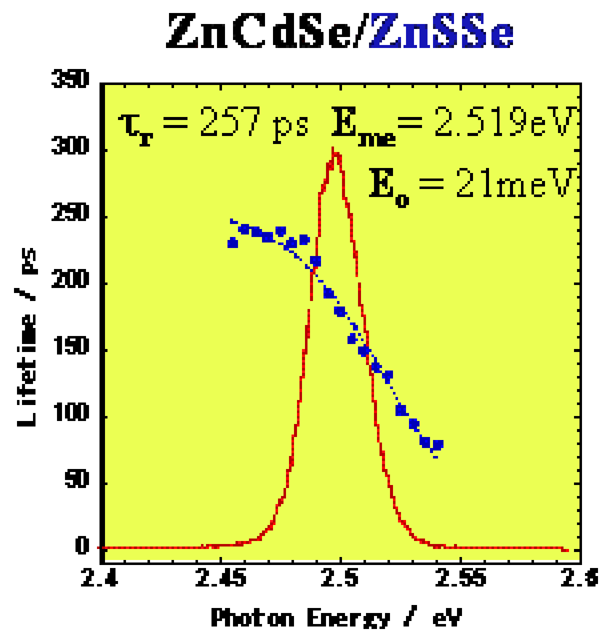

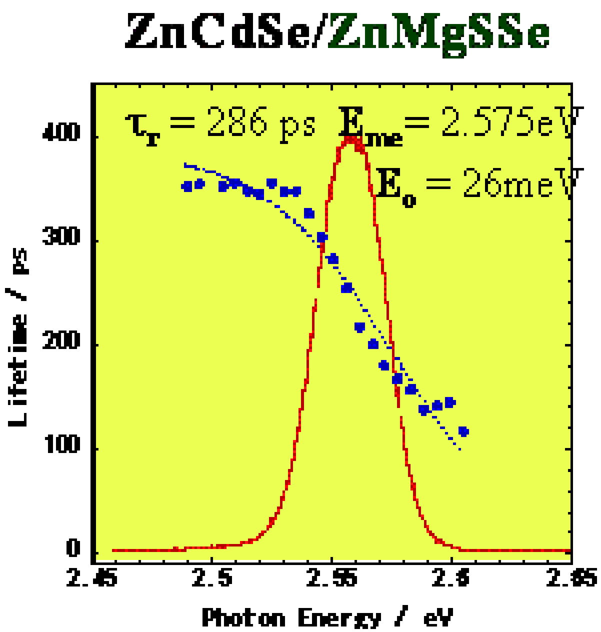

PL lifetimes are shorter at shorter wavelength ➡ Localization effect of excitons

$$\tau(E) = \frac{\tau_r}{1 + \exp[(E - E_{me}) / E_o]}$$

(Equation of Courdon & Lavallard)

τ_r : Lifetime without the localization

E_{me} : Mobility edge

E_o : Localization Energy

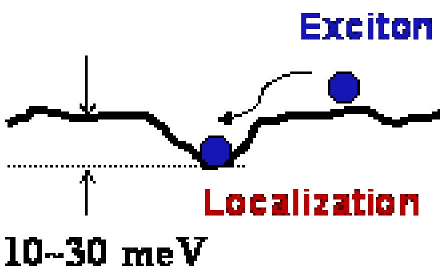

PL under high power excitation

Excitation Power: 100mW, Carrier density : ~10^{18} cm^{-3}

ZnCdSe/ZnSe

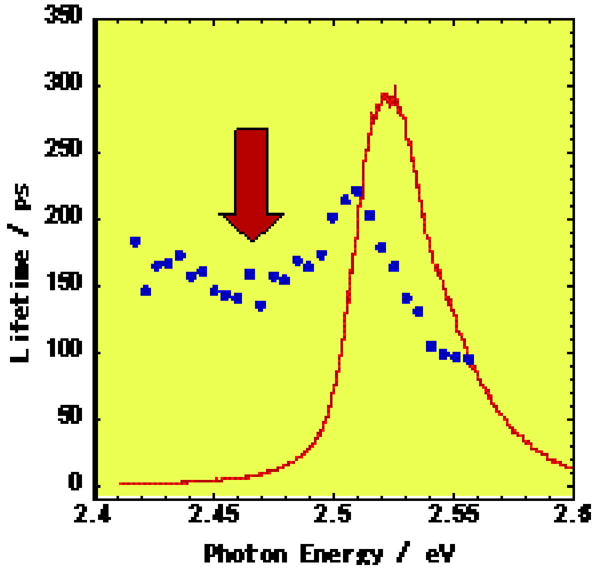

ZnCdSe/ZnSSe

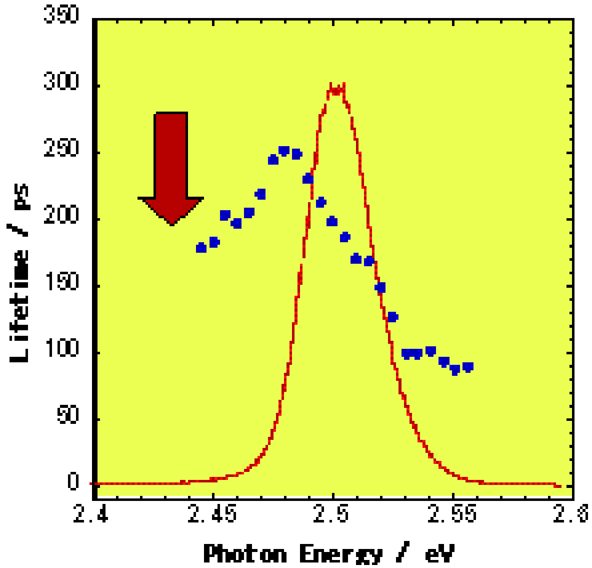

ZnCdSe/ZnMgSSe

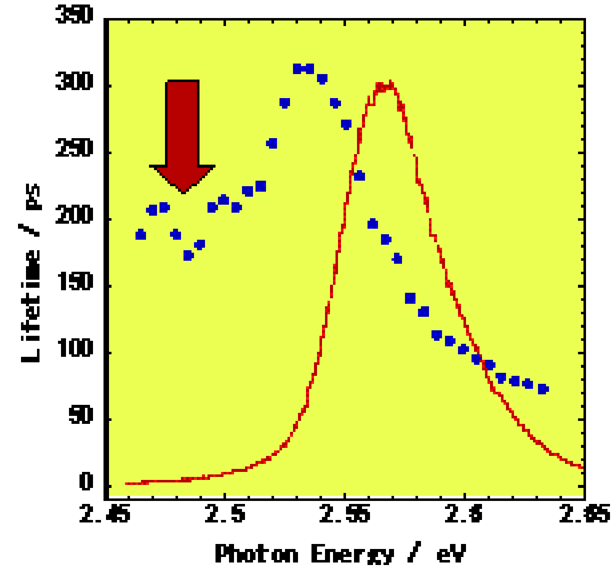

PL lifetimes become shorter not only at shorter wavelength but also at longer wavelength

→ **Another emission process appeared at the longer wavelength region**

Many Body Effect

- Exciton molecule generation
- Exciton-LO Phonon Scattering
- Exciton-Exciton Inelastic scattering

Temperature dependence of the PL

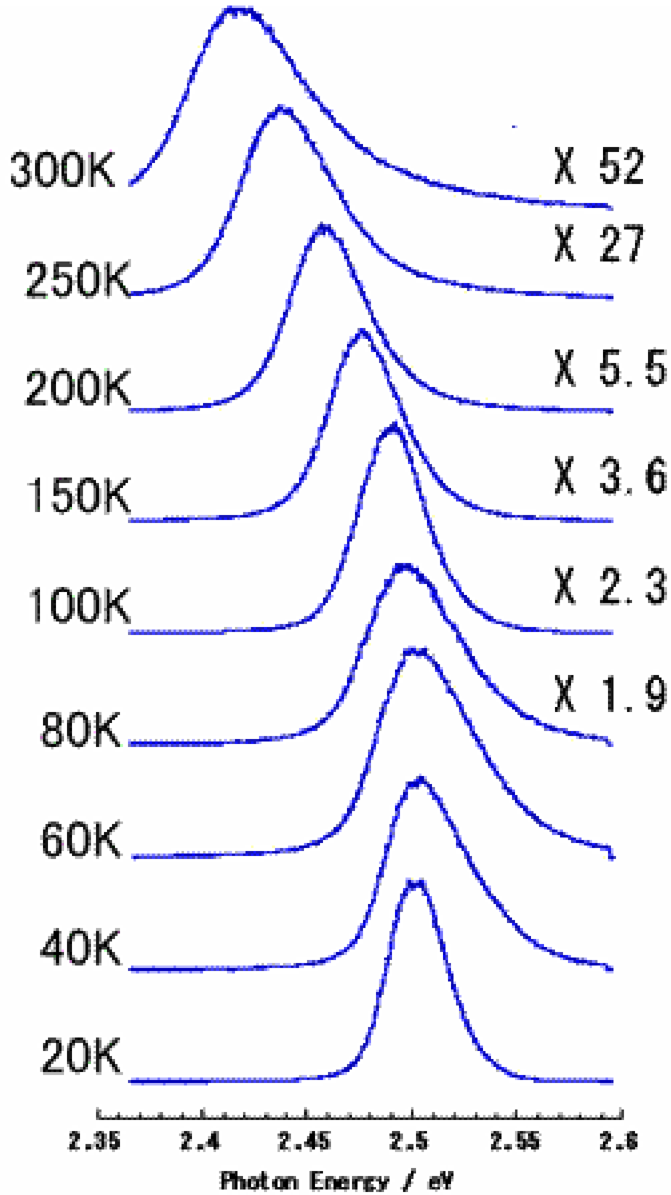

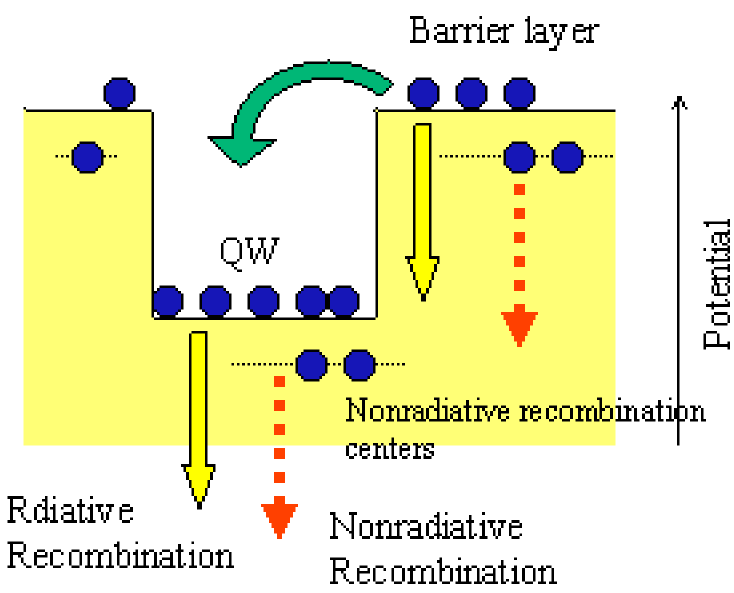

Internal quantum efficiency (η) of emission

$$\eta = \frac{1/\tau_{rad}}{1/\tau_{rad} + 1/\tau_{non}}$$

τ_{rad} ; radiative lifetime

τ_{non} ; nonradiative lifetime

Temperature dependence of the Lifetimes

Weak excitation 1mW ~10^{16} cm^{-3}

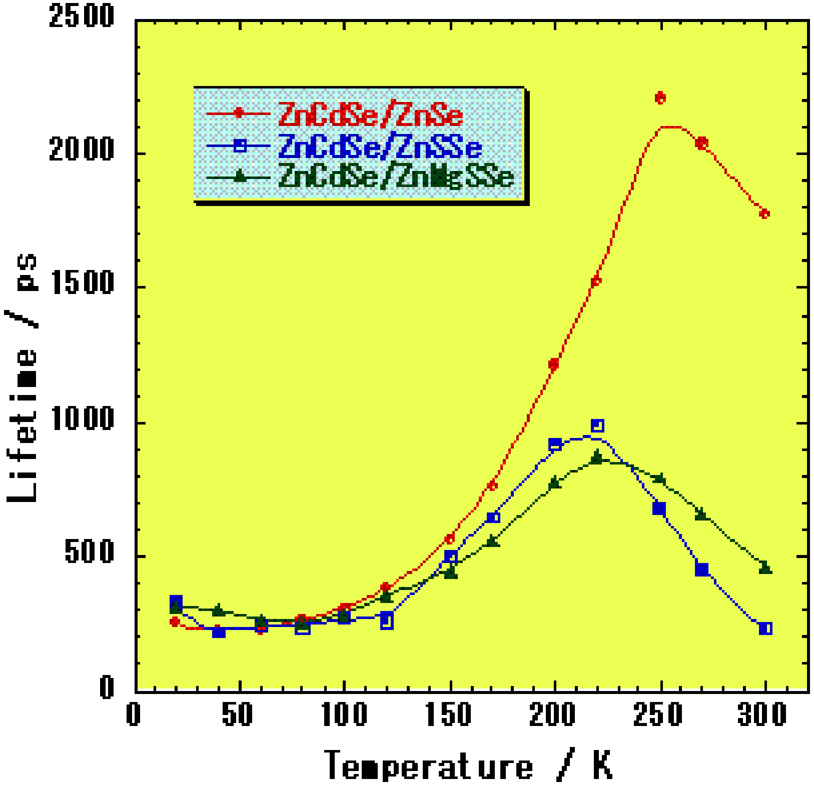

Strong excitation 100 mW ~10^{18} cm^{-3}

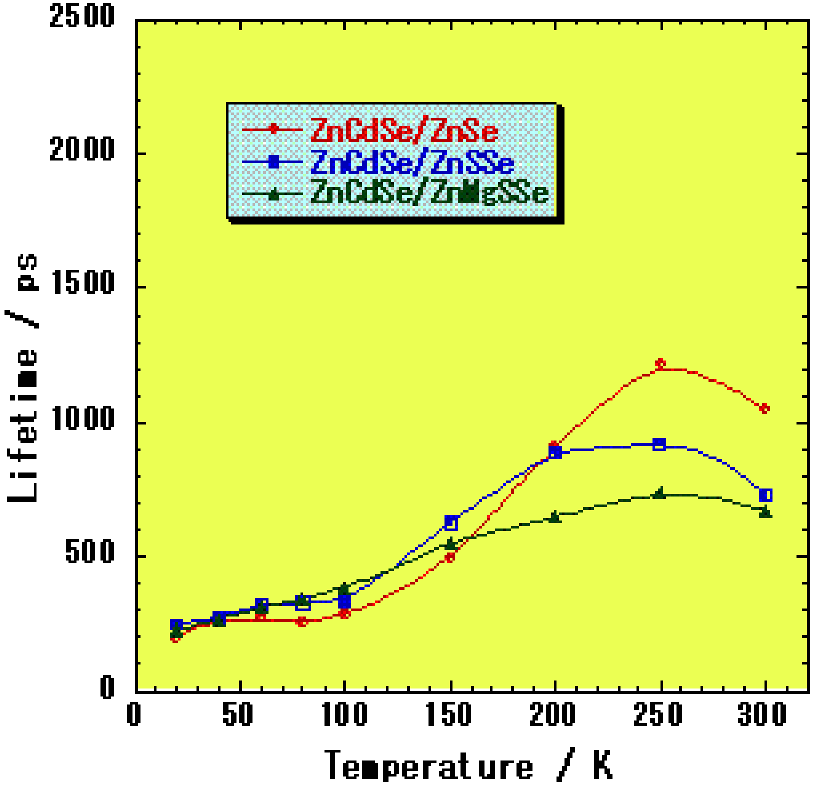

30 mW for ZnCdSe/ZnMgSSe

Internal Quantum Efficiencies

© Koichi Okamoto

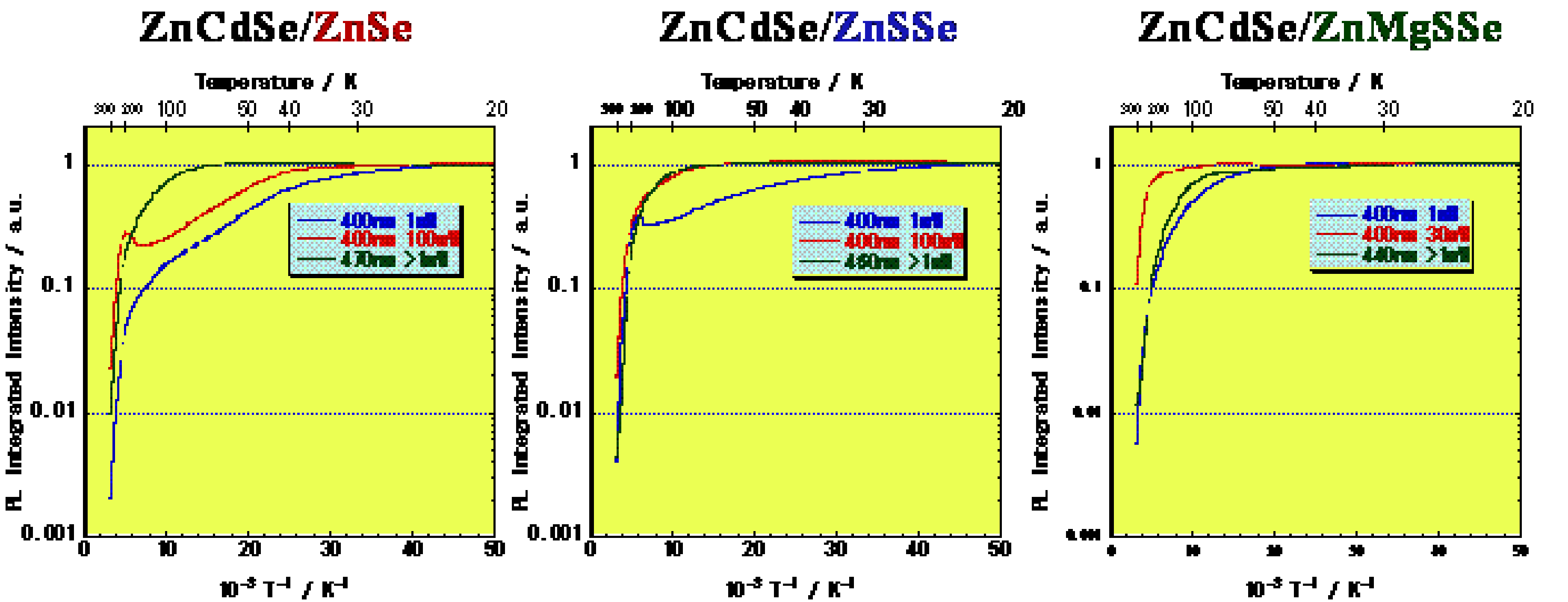

Weak excitation to the barrier layer < Selected excitation to the active layer

< Strong excitation to the barrier

Especially for ZnCdSe/ZnMgSSe

→ What happened?

T-dependence of the recombination rates

Weak excitation 1mW ~10^{16} cm$^{-3$}

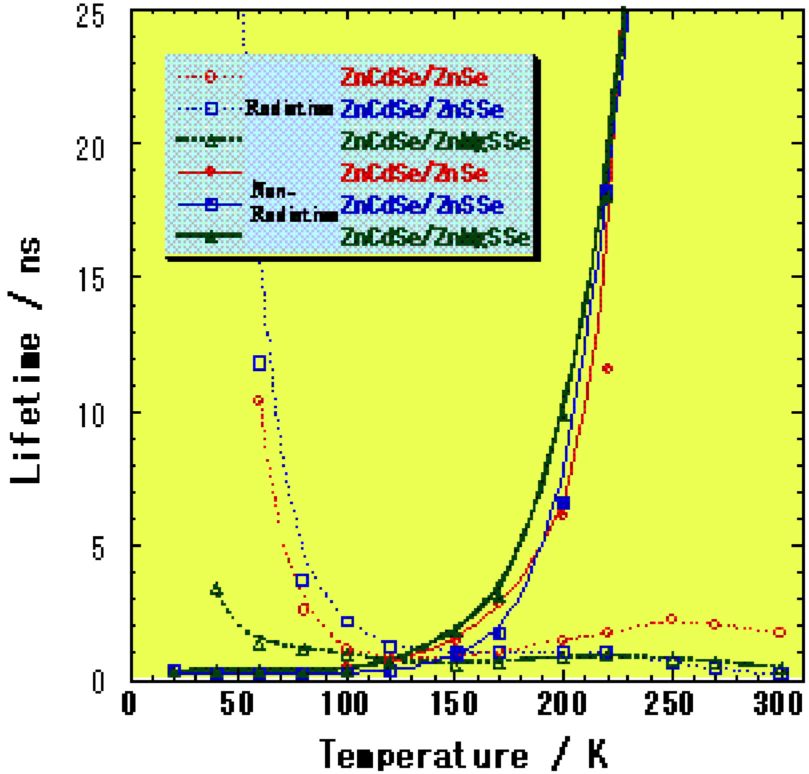

Strong excitation 100 mW ~10^{18} cm^{-3}

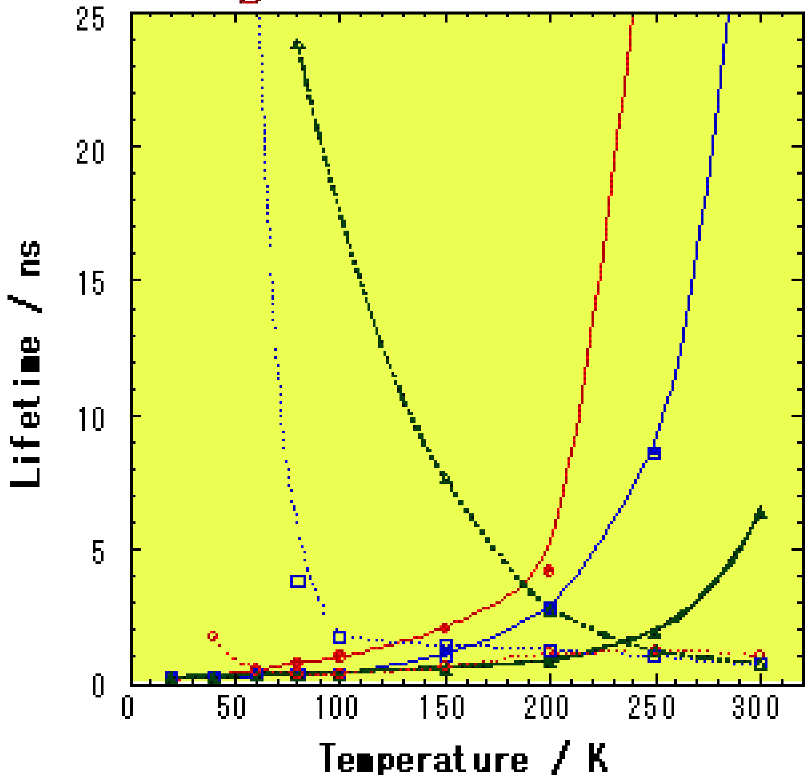

30 mW for ZnCdSe/ZnMgSSe

T-dependence of the localization effect

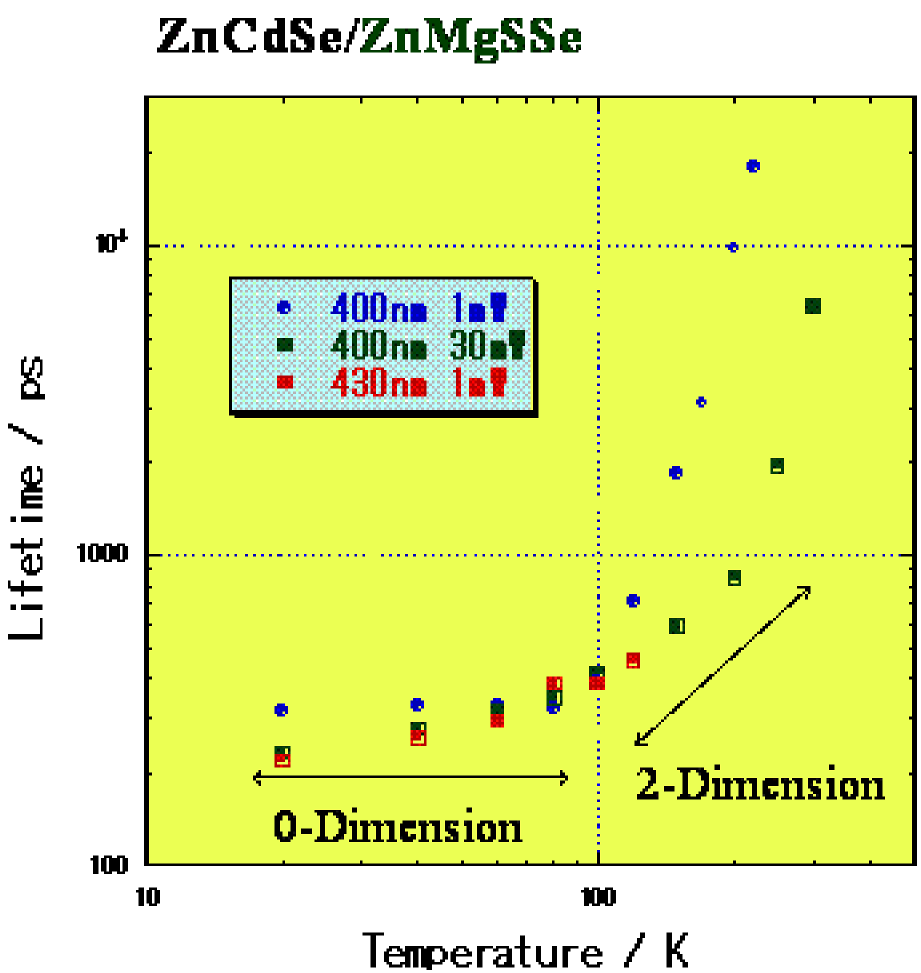

$$\tau_{\mathrm{radiative}} \propto T^{a}$$

when Excitons are located in

3-Dimension, a = 1.5
2-Dimension, a = 1.0
1-Dimension, a = 0.5
0-Dimension, a = 0

0-Dimension = Localized

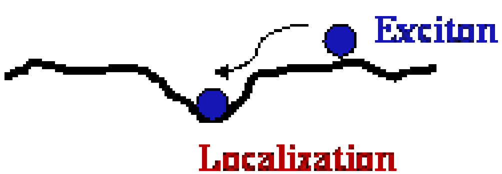

Saturation of the nonradiative recombination

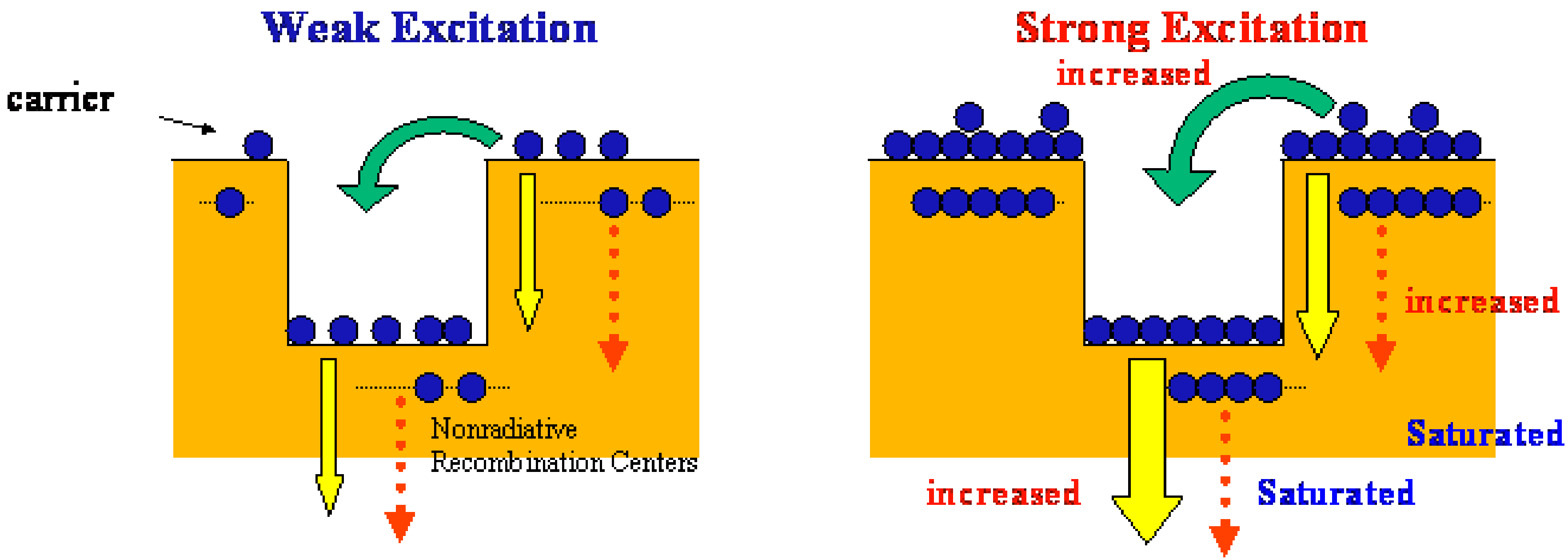

Nonradiative recombination centers (NRC) (defects, dislocations, impurity) in the active layer are saturated by the high density carriers under the strong excitation.

➡ increases the radiative recombination rate in the active layers

➡ NRC in the barrier layer are also saturated

➡ increases the carrier flow into the active layer from the barrier layer

➡ increases the radiative recombination rate in the active layers much more

Power dependence of Arrhenius plots

ZnSe barrier layer is excited by He-Cd laser with 325 nm, 3 Wcm^{-2}

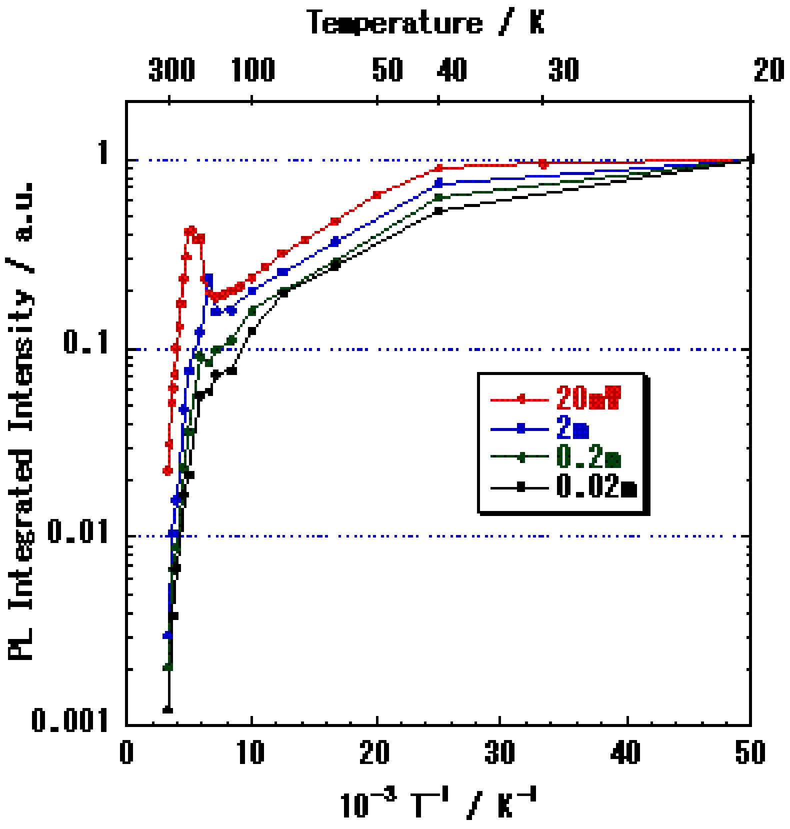

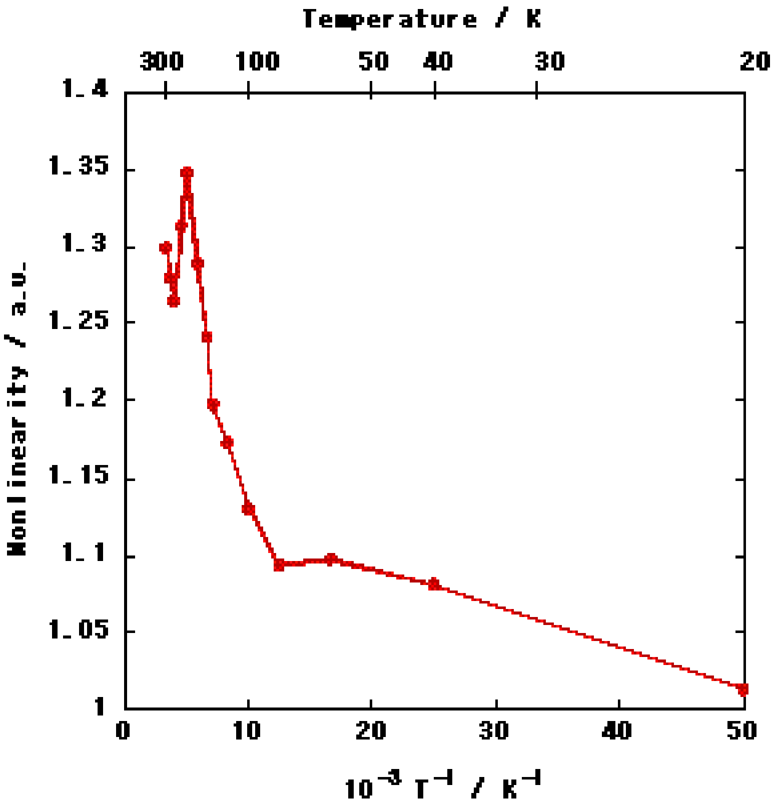

Power dependence of Arrhenius plots

© Koichi Okamoto

ZnCdSe active layer is excited by Ar^+ laser with 488 nm, 3 Wcm^{-2}

ZnCdSe/ZnS

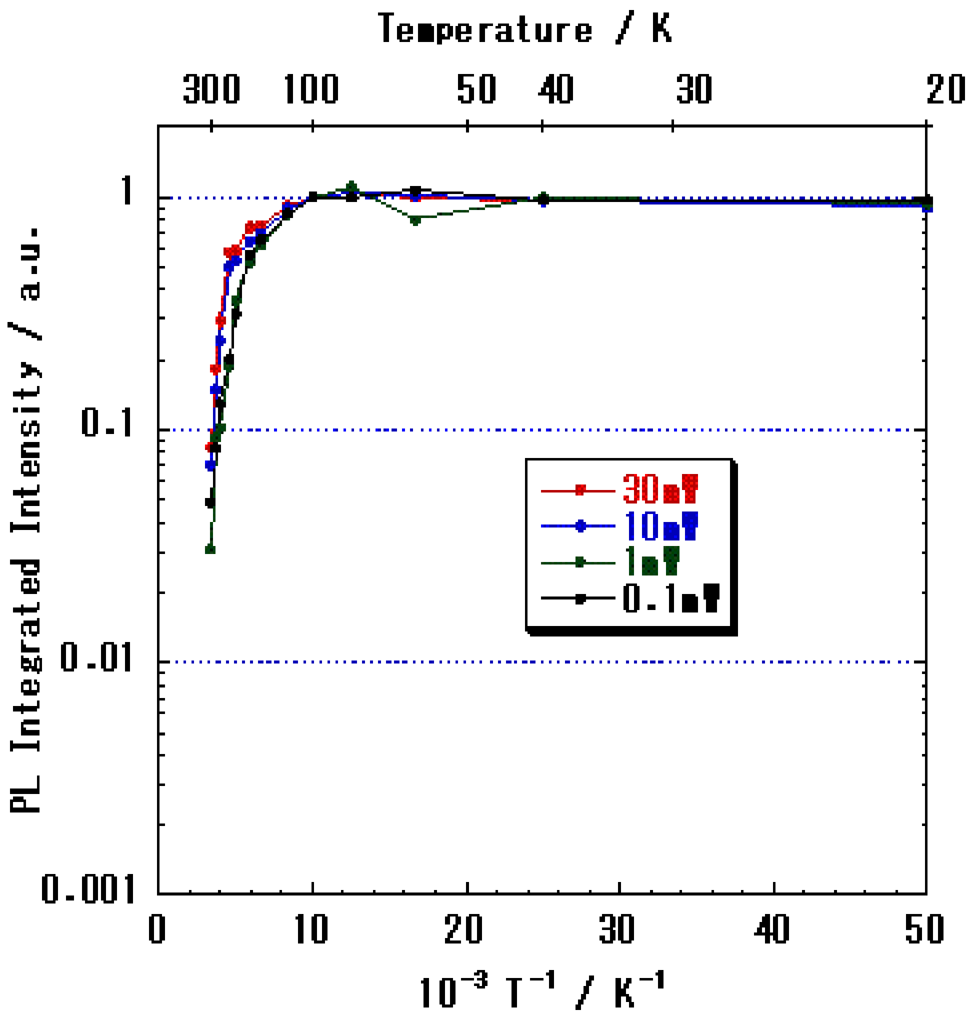

No power dependence

↓

Only when ZnSe barrier layer is excited, unique nonlinear behavior of PL happens

Carrier Dynamics model

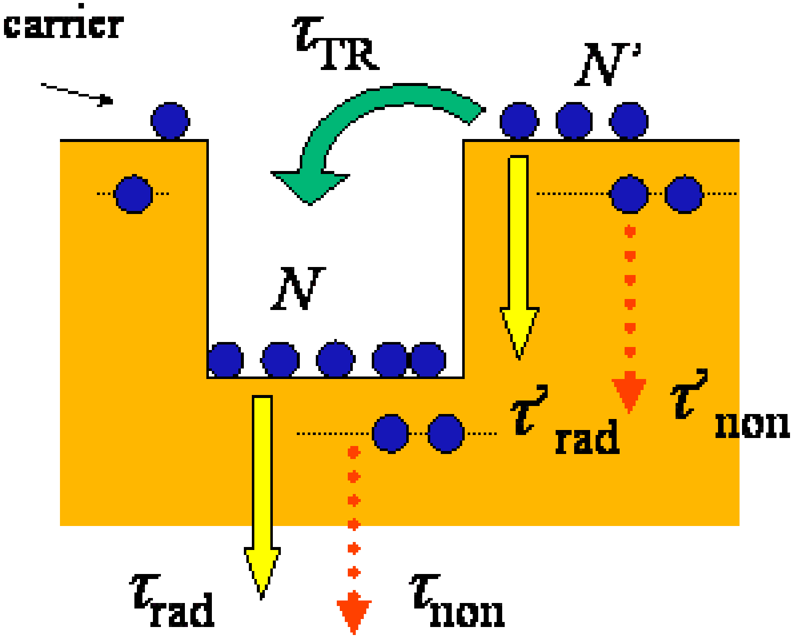

τ'_{rad} : radiative recombination in barrier layer

τ'_{rad} : nonradiative recombination in barrier

τ_{TR} : carrier inflow from barrier into active

τ_{rad} : radiative recombination in active layer

τ_{rad} : nonradiative recombination in active

$$\frac{dN'}{dt} = -\left(\frac{1}{\tau'_{rad}} + \frac{1}{\tau'_{non}} + \frac{1}{\tau_{TR}}\right) N'$$

$$\frac{dN}{dt} = \frac{1}{\tau_{TR}} N' - \left(\frac{1}{\tau'_{rad}} + \frac{1}{\tau'_{non}} + \frac{1}{\tau_{TR}}\right) N$$

Time-resolved PL measurement

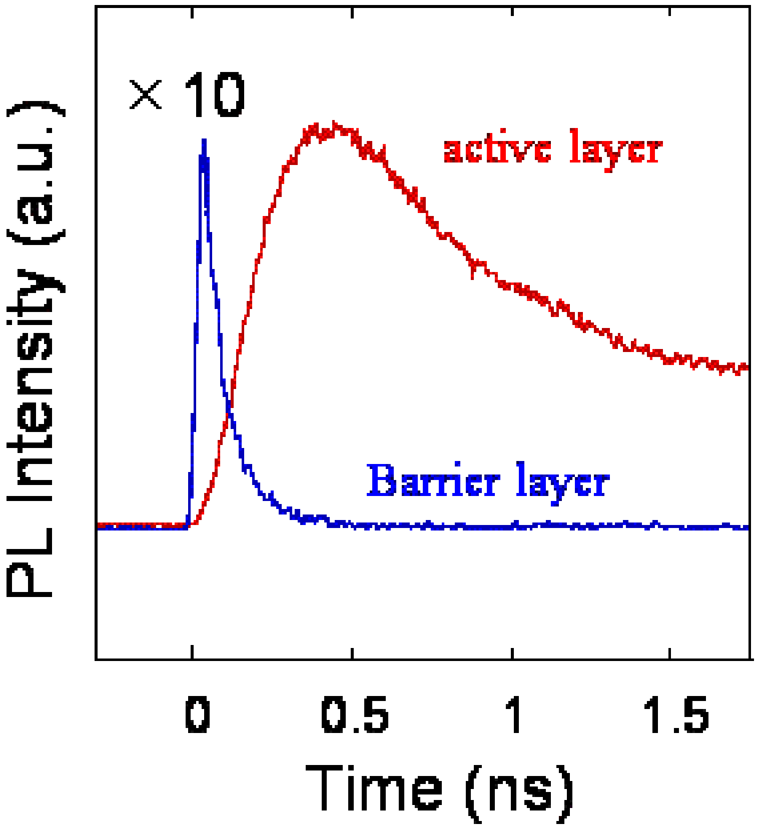

$$N'(t) = N'(0) \exp(-t/\tau'_{PL})$$

$$\frac{1}{\tau'_{PL}} = \frac{1}{\tau'_{rad}} + \frac{1}{\tau'_{non}} + \frac{1}{\tau_{TR}}$$

$$\frac{1}{\tau_{PL}} = \frac{1}{\tau_{rad}} + \frac{1}{\tau_{non}}$$

$$N(t) = \frac{\dfrac{1}{\tau_{TR}}}{\dfrac{1}{\tau'_{PL}} - \dfrac{1}{\tau_{PL}}} N'(0)\left[-\exp(-t/\tau'_{PL}) + \exp(-t/\tau_{PL})\right]$$

Obtained Lifetimes

Power Density ($mJcm^{-2}pulse$)	τ'_{PL}(ps)	τ_{PL}(ps)	τ'_{PL}(ps)
16	127	1.15	104
8	118	1.21	93
1.6	101	1.20	83
0.5	92	1.17	69
0.16	66	1.02	47
0.08	53	1.08	34

$$\frac{1}{\tau'_{PL}} = \frac{1}{\tau'_{rad}} + \frac{1}{\tau'_{non}} + \frac{1}{\tau_{TR}}$$

$$\frac{1}{\tau_{PL}} = \frac{1}{\tau_{rad}} + \frac{1}{\tau_{non}}$$

Power dependence of each parameter

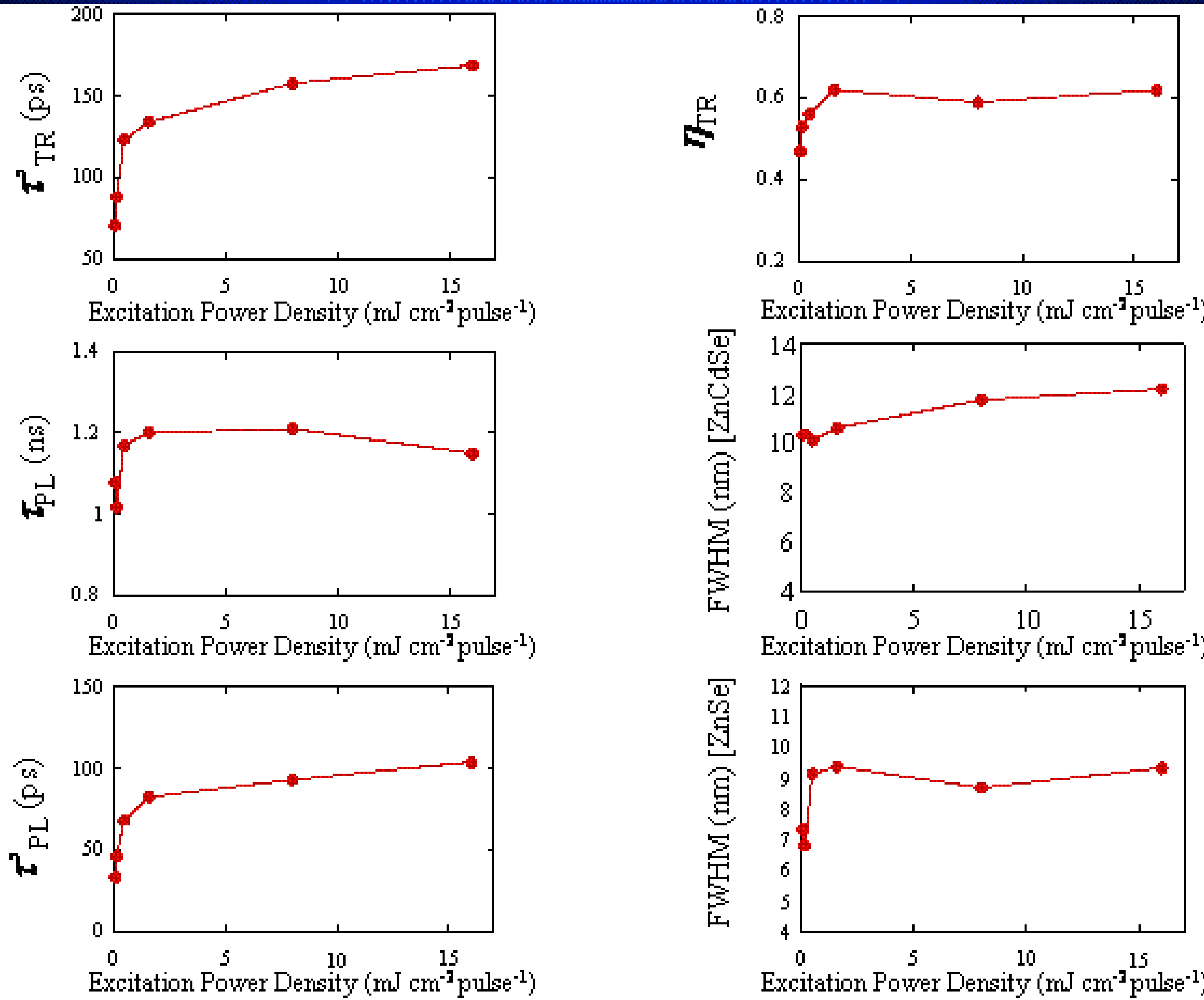

Nonlinearity of PL at 21 K

© Koichi Okamoto

ZnCdSe/ZnSe excited by frequency doubled Al_2O_3:Ti Laser (400nm)

Pulse width 1.5 ps, repetition 80 MHz

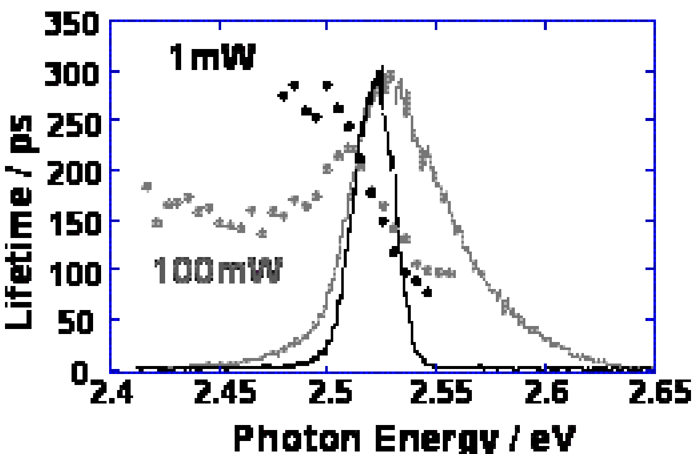

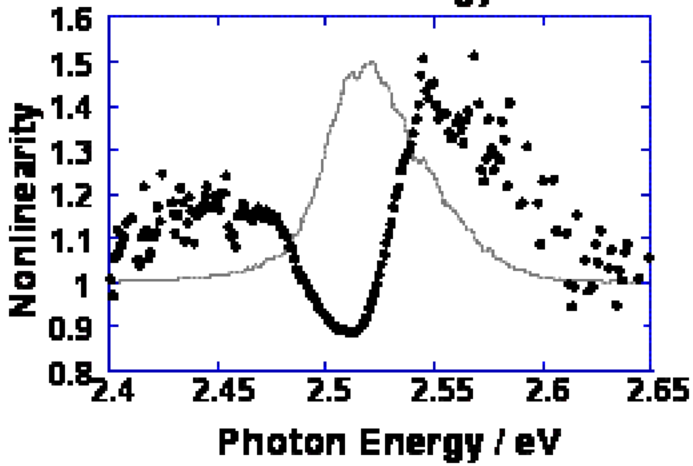

Nonlinearity of PL intensities was observed

(1) High energy side

Saturation of carrier localization

(2) Low energy side

many body effect of excitons

Saturation of localization and many body effect

Saturation of carrier localization

$\tau_r = 290$ ps $E_{me} = 2.528$eV $E_o = 13$meV

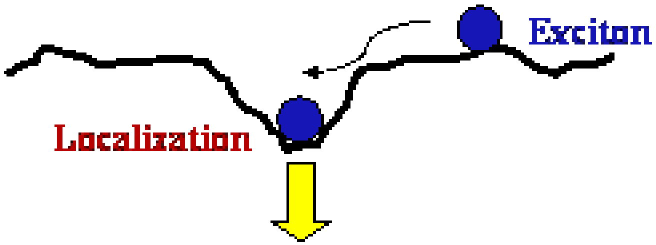

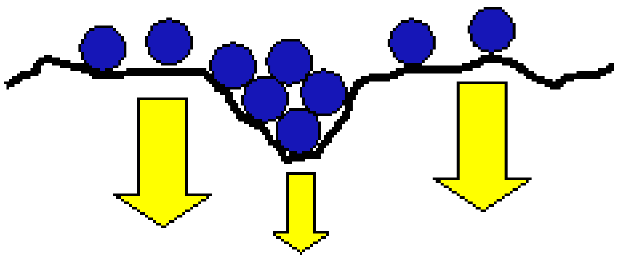

$$\tau(E) = \frac{\tau_r}{1 + \exp[(E - E_{me})/E_o]}$$

τ_r : Lifetime without the localization
E_{me} : Mobility edge
E_o : Localization Energy

Many body effect

- Exciton molecule generation
- Exciton-LO Phonon Scattering
- Exciton-Exciton Inelastic scattering

Emission at low energy side

Energy: 74 meV, line width : 65 meV

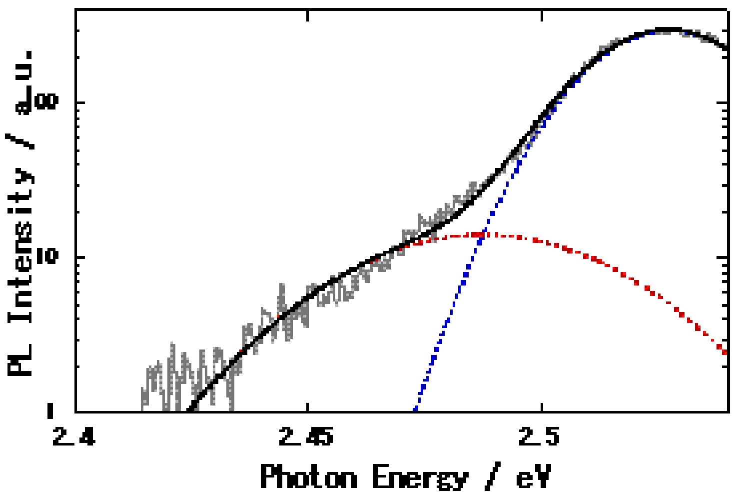

Absorption Saturation with CW- Pump & Probe

© Koichi Okamoto

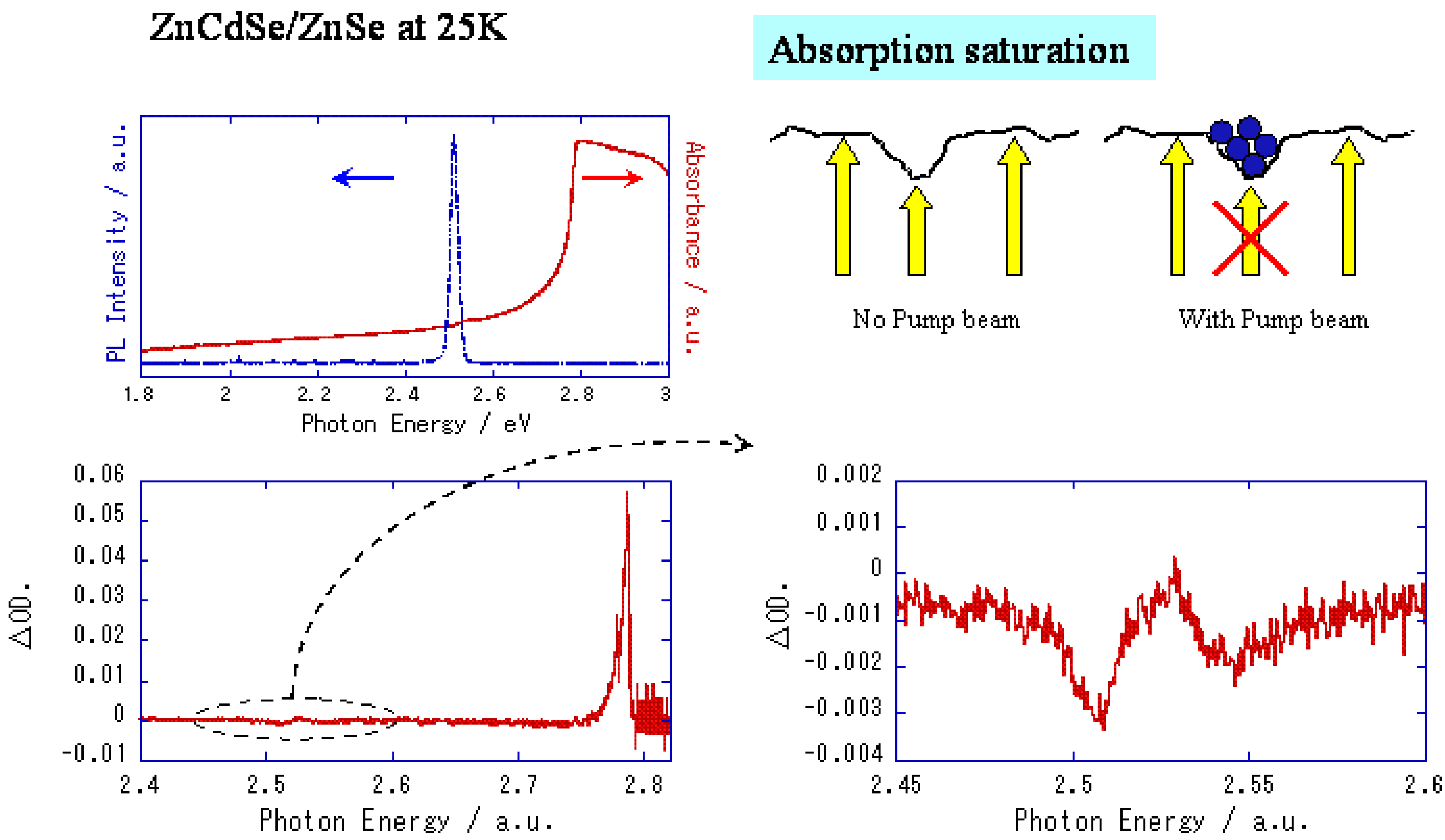

Transient Absorption with TR-Pump & Probe

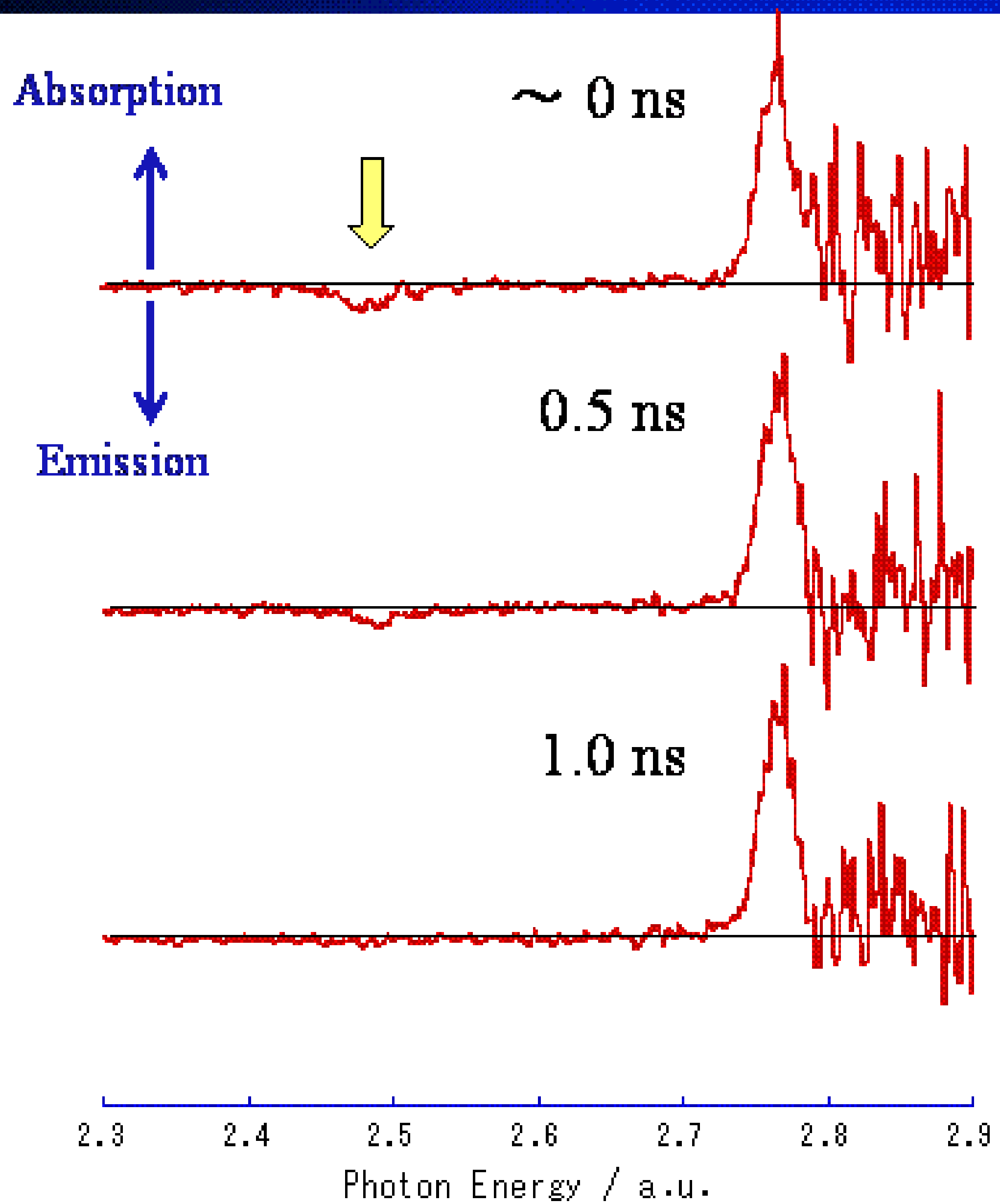

ZnCdSe/ZnSe at 25K

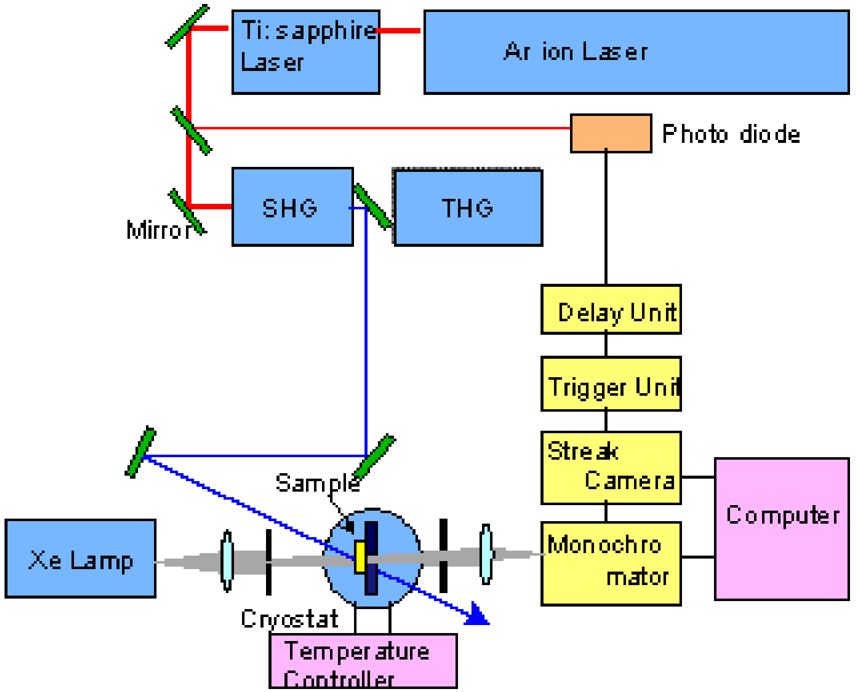

Temperature Increasing estimated by the P&P

© Koichi Okamoto

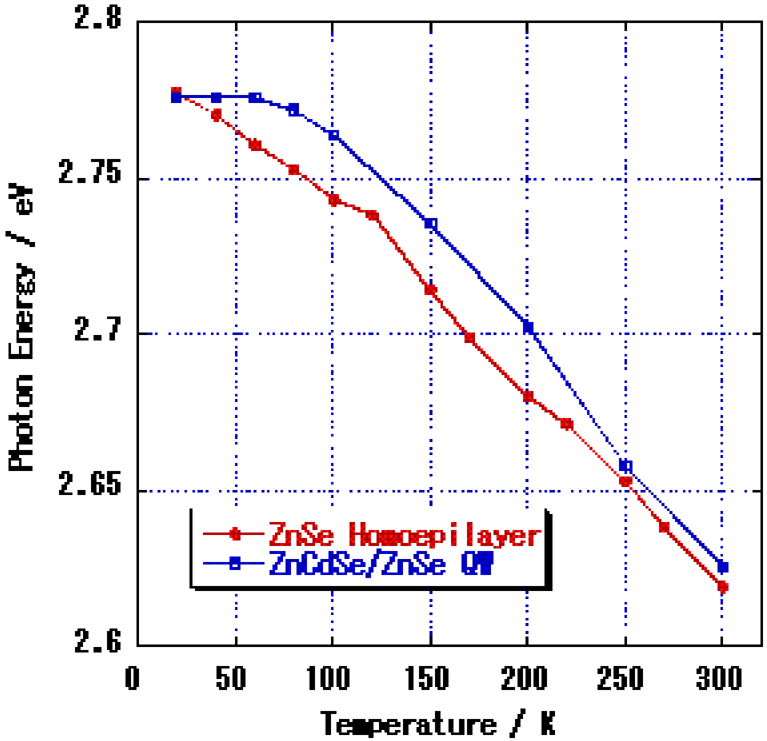

Temperature dependence of the band-edge shift

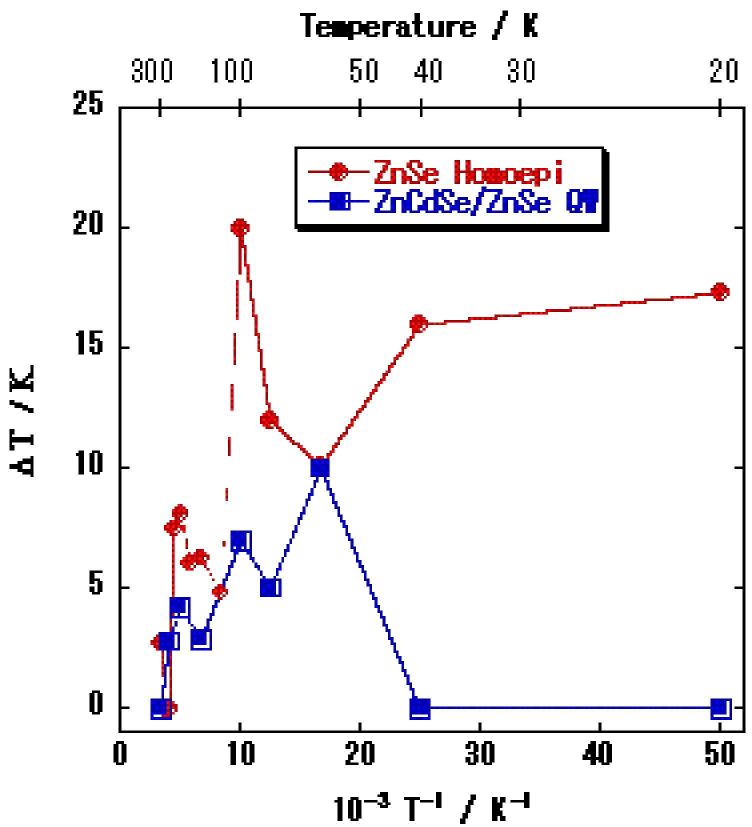

Estimated temperature increasing after excitation

Summary - Nonlinear optics of ZnSe -

- Strong emission of ZnSe homoepitaxial layer should be due to the saturation effect of the nonradiative recombination centers.

- Other various nonlinear optical effects were observed based on the carrier localization dynamics, many body effects, and thermarization process of excitons.

- Such nonlinear optical effects can be applied to various optical devices.

Emission Properties of CdSe quantum dot

Quantum Dot (QD) → Excitons are localized into 0-dimension

various optical functions, optical nonlinearities, unique properties are expected

Applicable to high efficient light-emitting devices or low threshold laser

For InAs/GaAs or Ge/Si materials, Stranski-Krastanov (SK) mode of QDs has been well established by MBE and MOCVD.

In contrast, QD of the wide band gap semiconductors have not so far been established in spite of the large efforts during the last few years.

CdSe/ZnSe quantum dots

CdSe/ZnSe QDs rrown on (110) face of GaAs substrate

Appl. Phys. Lett. **70, 3278, (1997)**

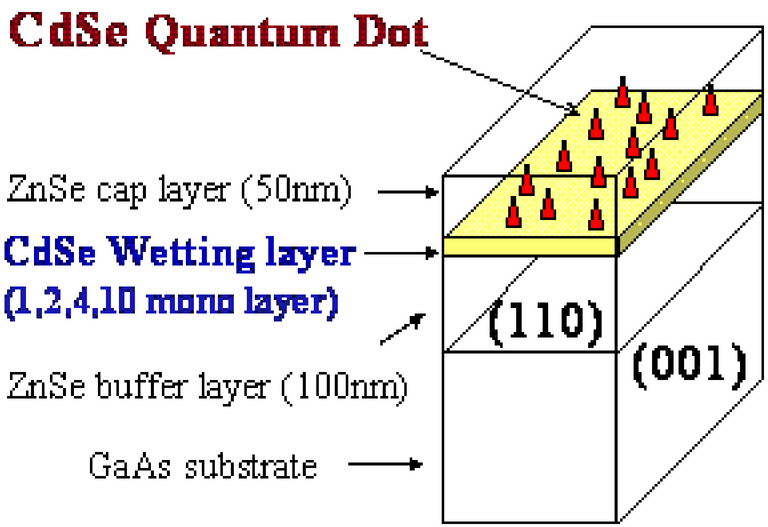

Stranski-Krastanow Mode

Dot density = 1.7 × 10^{12}cm^{-2}

much smaller than that of GaAs-based QDs.

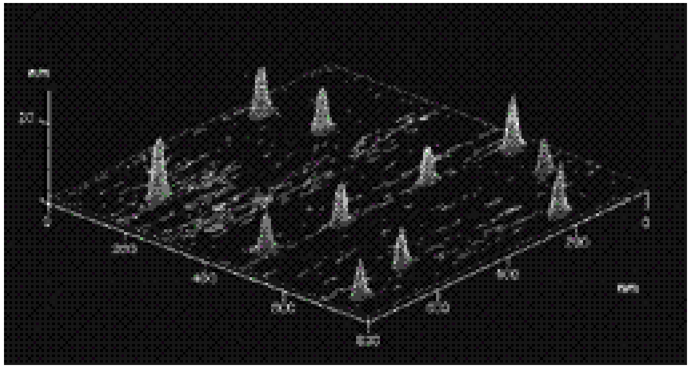

AFM image

Microscopic PL image and spectrum

CdSe(10 MLs)/ZnSe/GaAs(110)

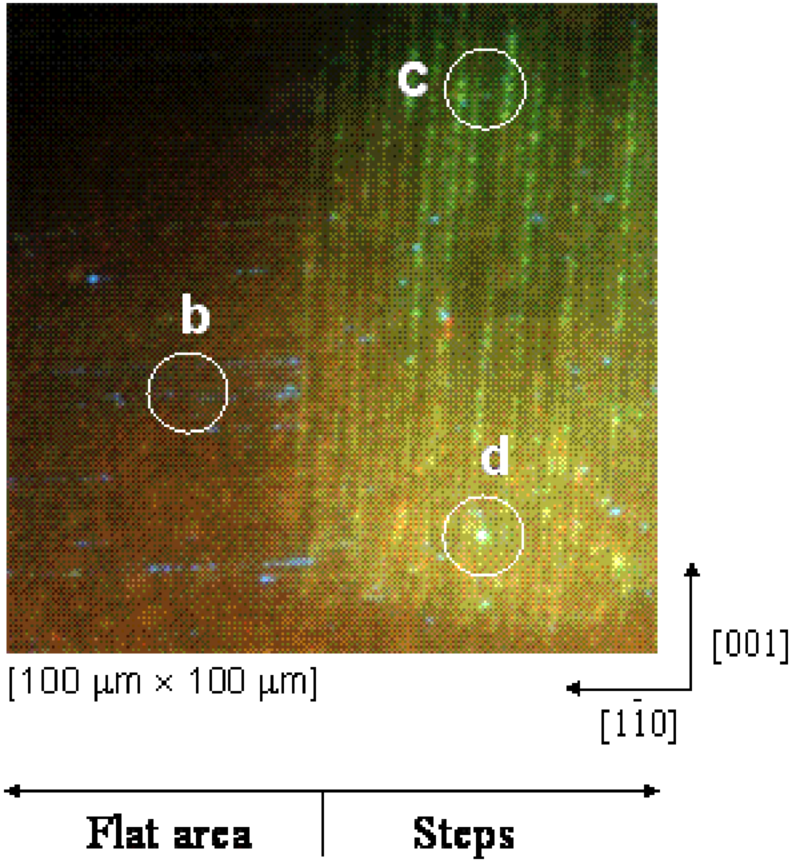

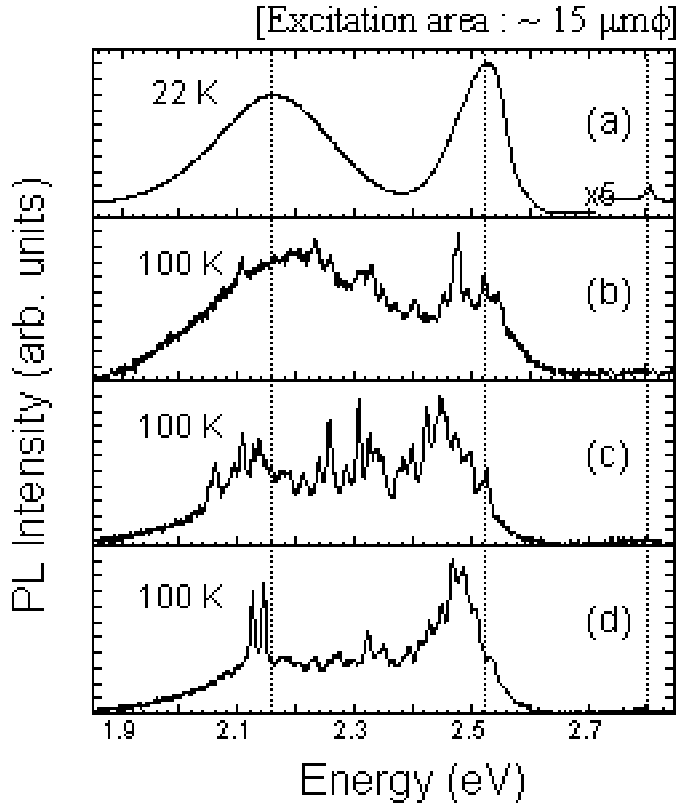

(a) conventional PL
(b)(c)(d) microscopic PL

MicroPL image and spectrum @77K

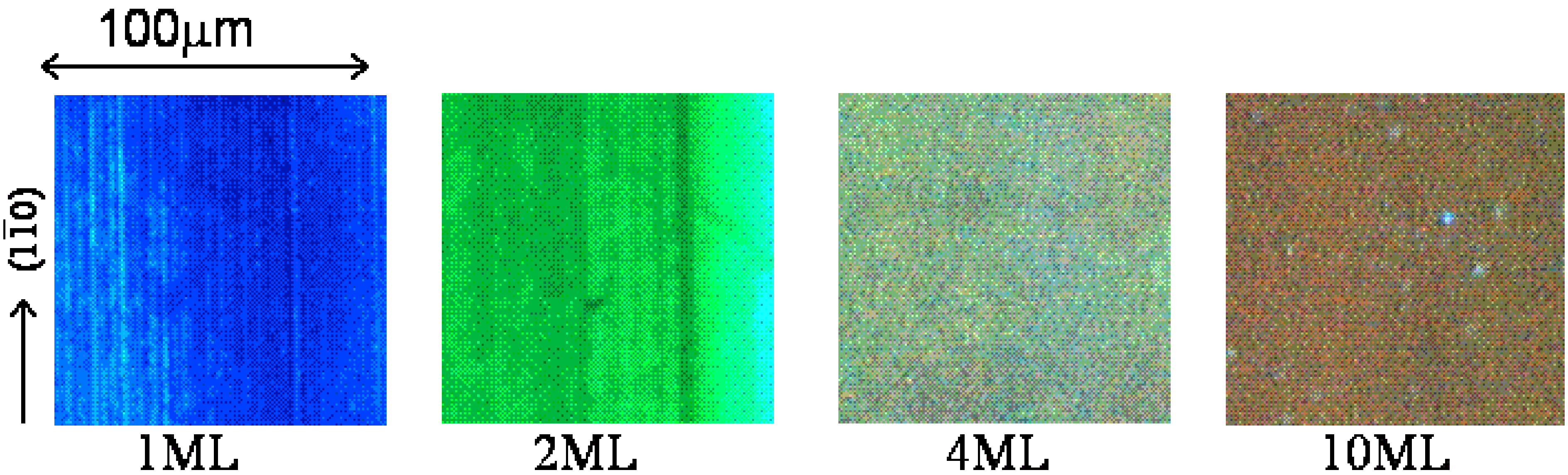

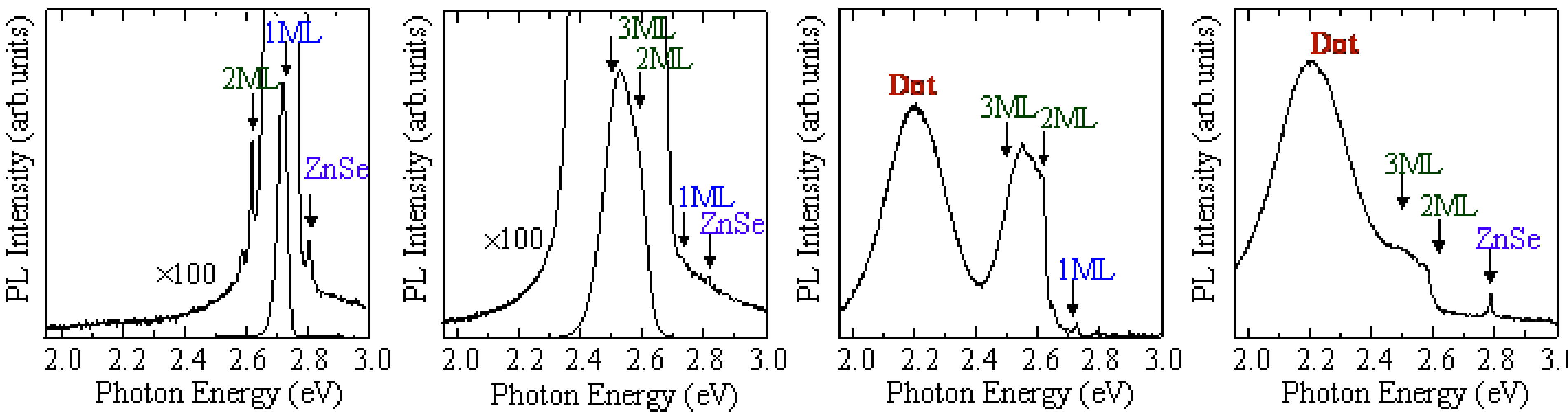

Temperature dependence of PL

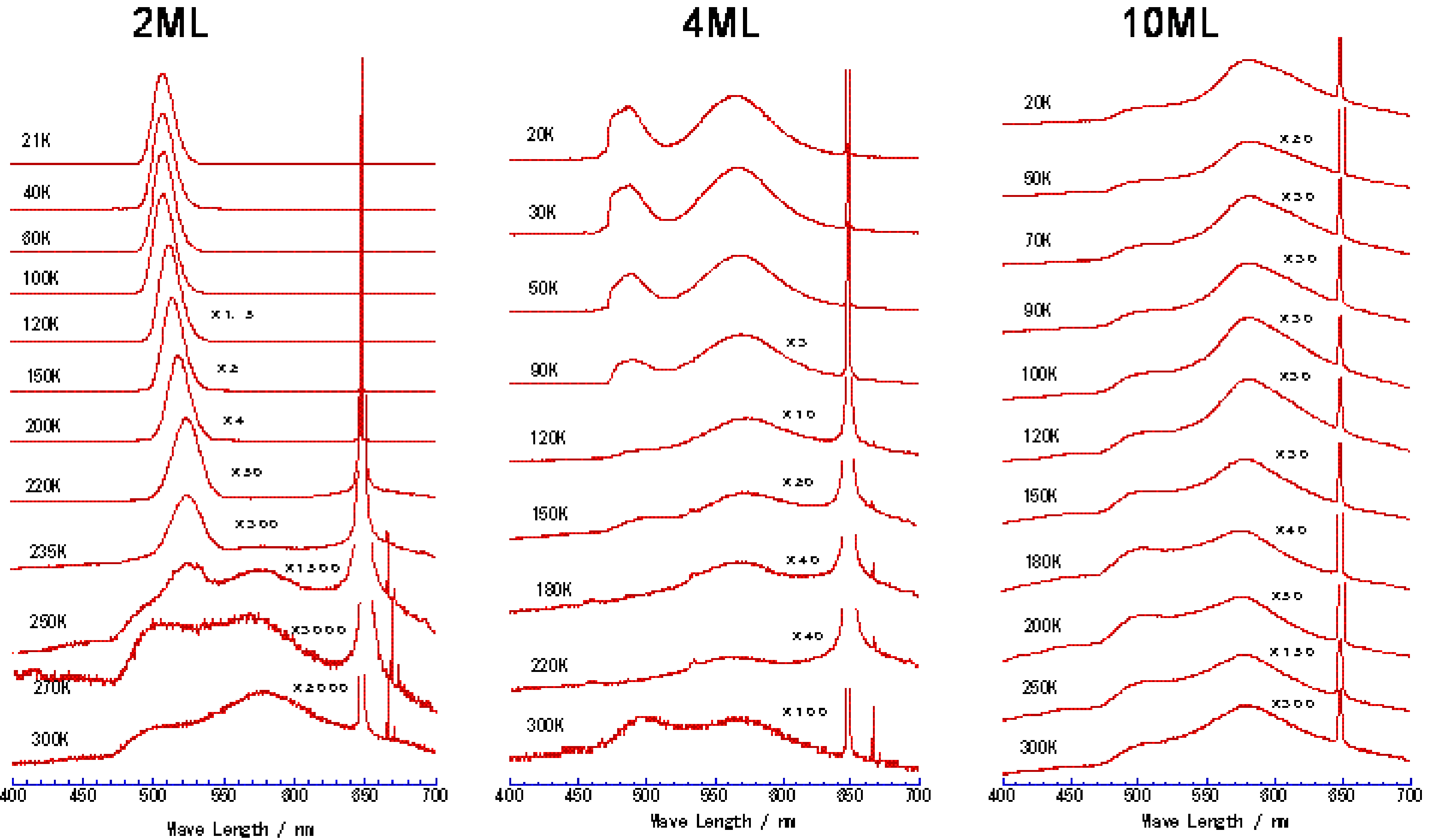

Time-resolved PL for 10ML

© Koichi Okamoto

Power: ~7μJ/cm^2 ,Spot size: ~100μm

@77K

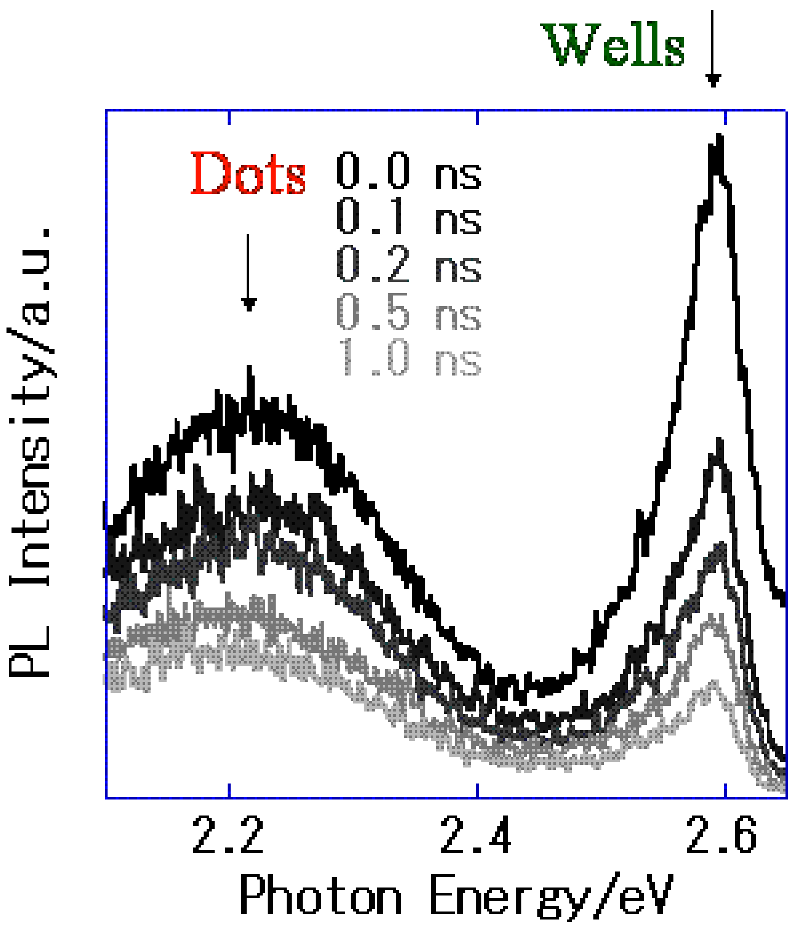

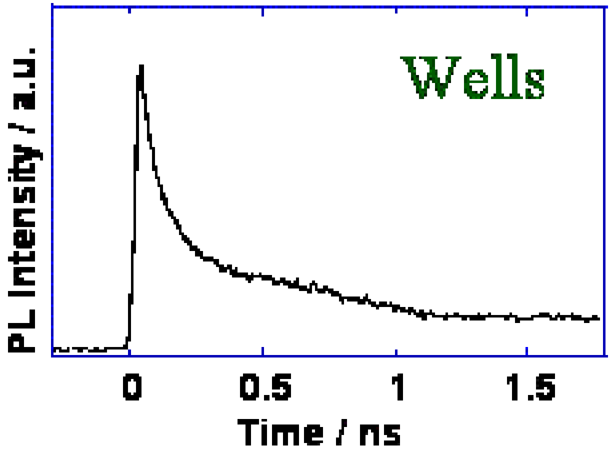

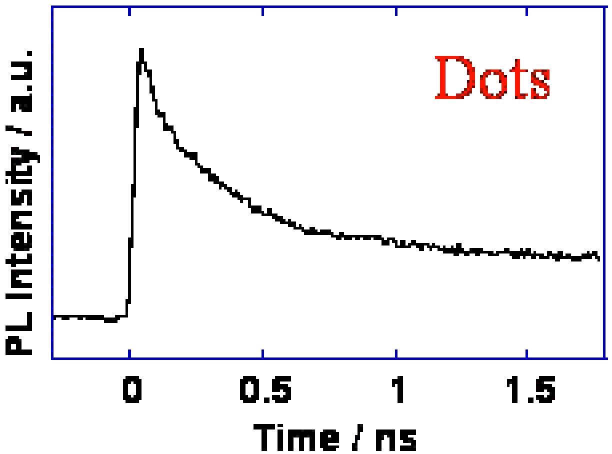

Not a single exponential decay

Time-resolved micro-PL setup

© Koichi Okamoto

Mode locked Al_2O_3:Ti laser
(pumped by Ar^+ laser)
pulse width: 1.5 ps
wavelength: 700~1000 nm
repetition rate: 80MHz
power density: 20µJ/cm^{-2}

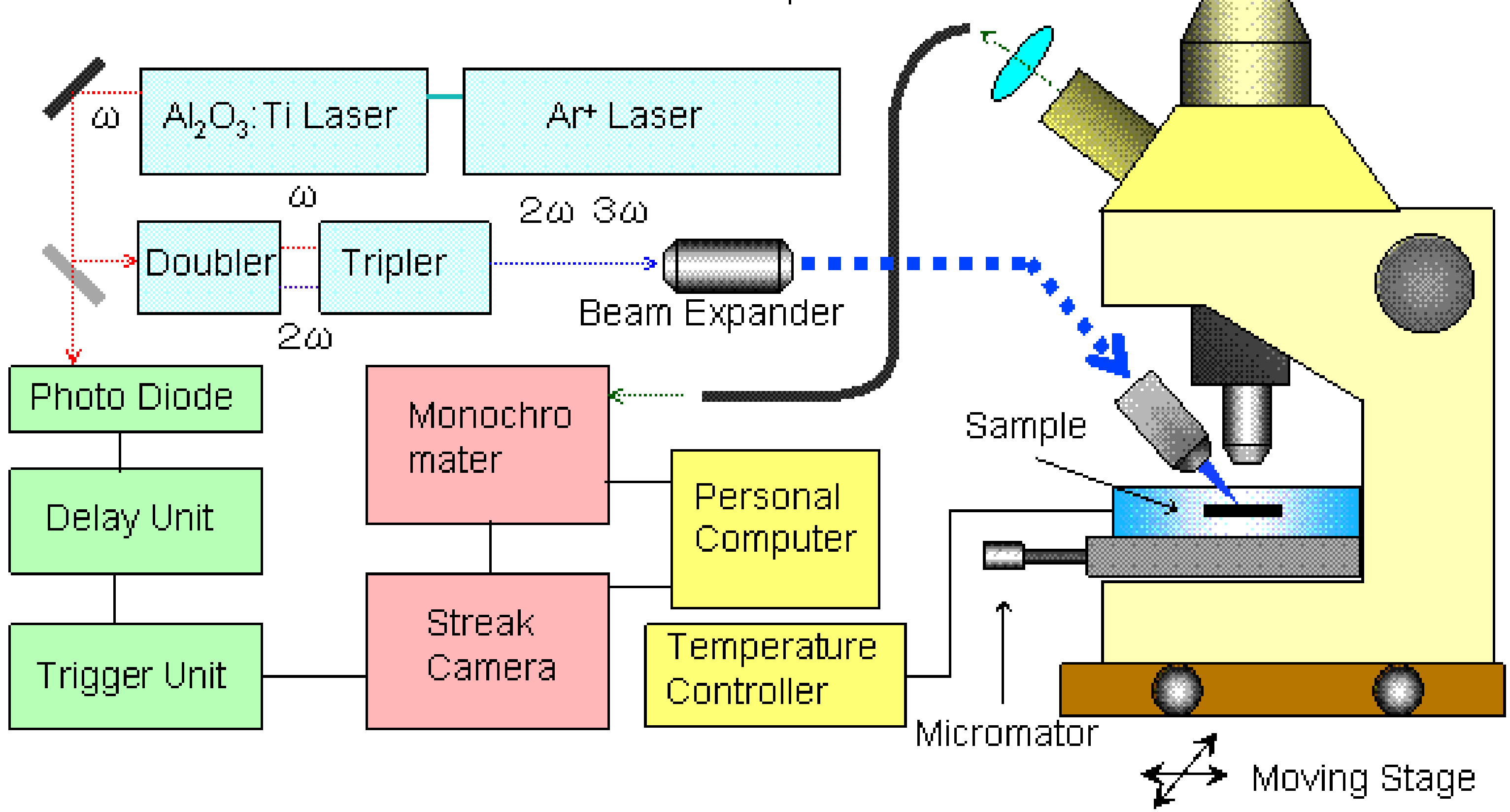

Pictures of the TR-M-PL setup

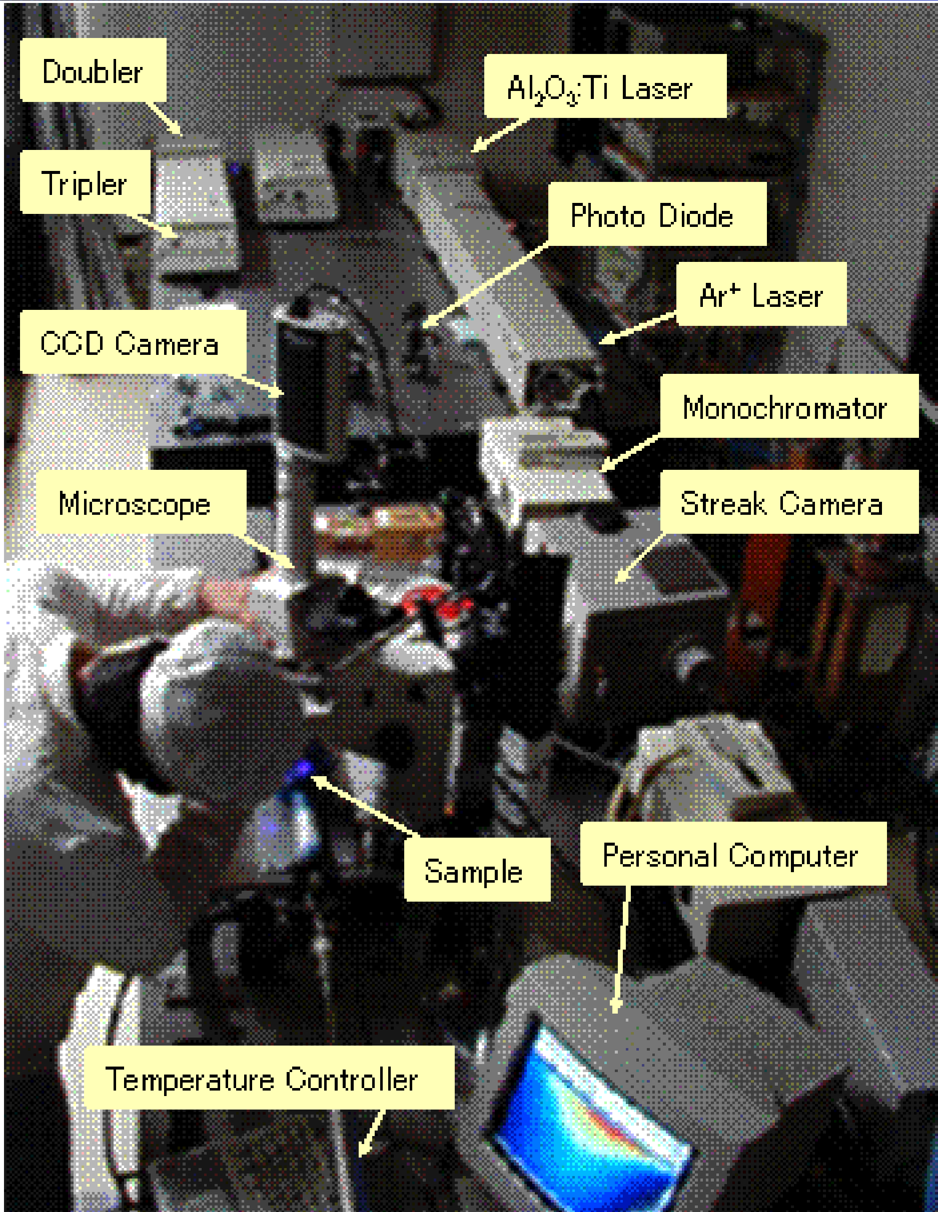

Mode locked Al_2O_3:Ti laser
(pumped by Ar^+ laser)
pulse width: 1.5 ps
wavelength: 700~1000 nm
repetition rate: 80MHz
power density: 20μJ/cm^{-2}

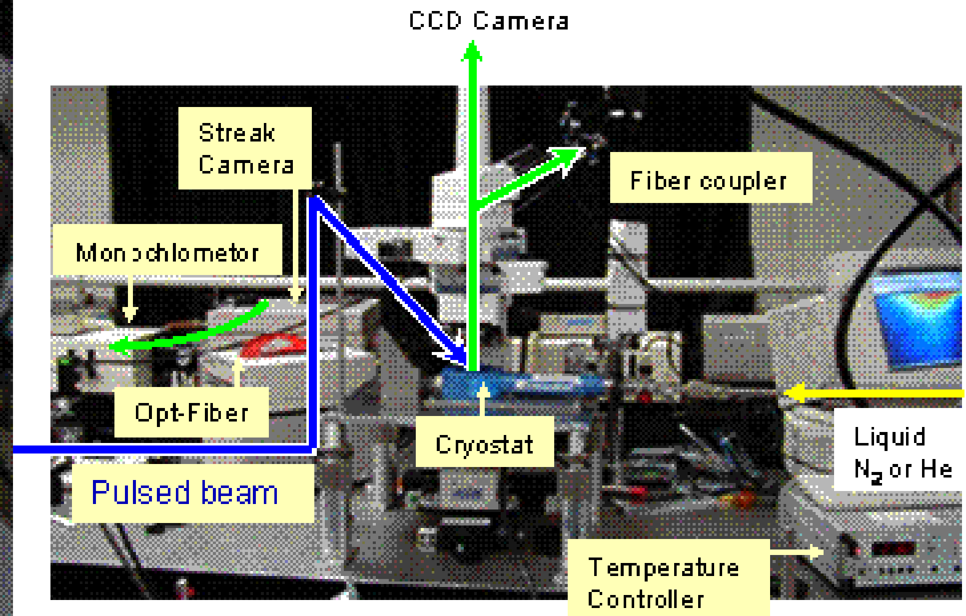

Various colors of emission

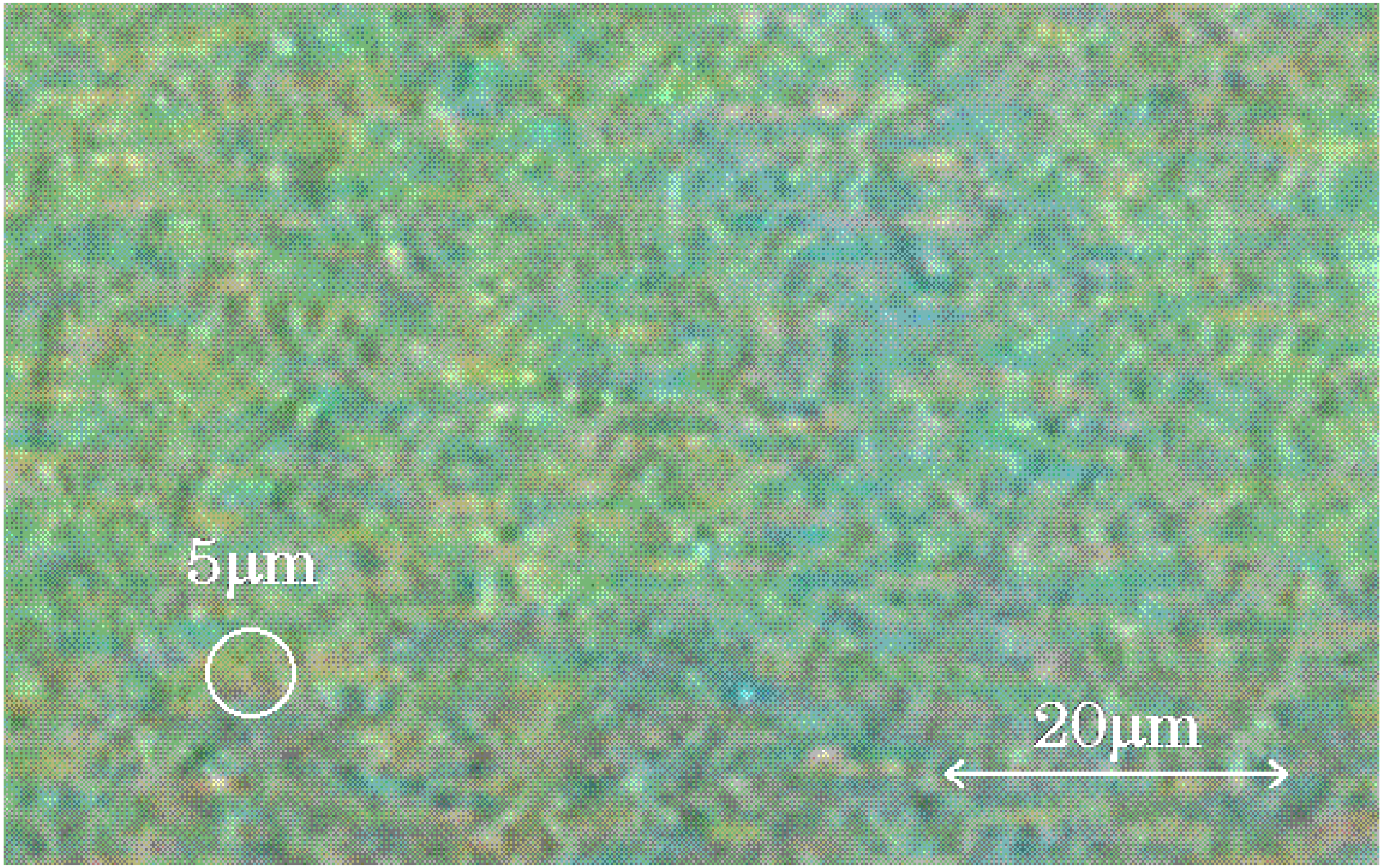

Measurement of emission from single quantum dot is impossible with the current excitation spot size (5μm).

Micro-PL spectra at each spots

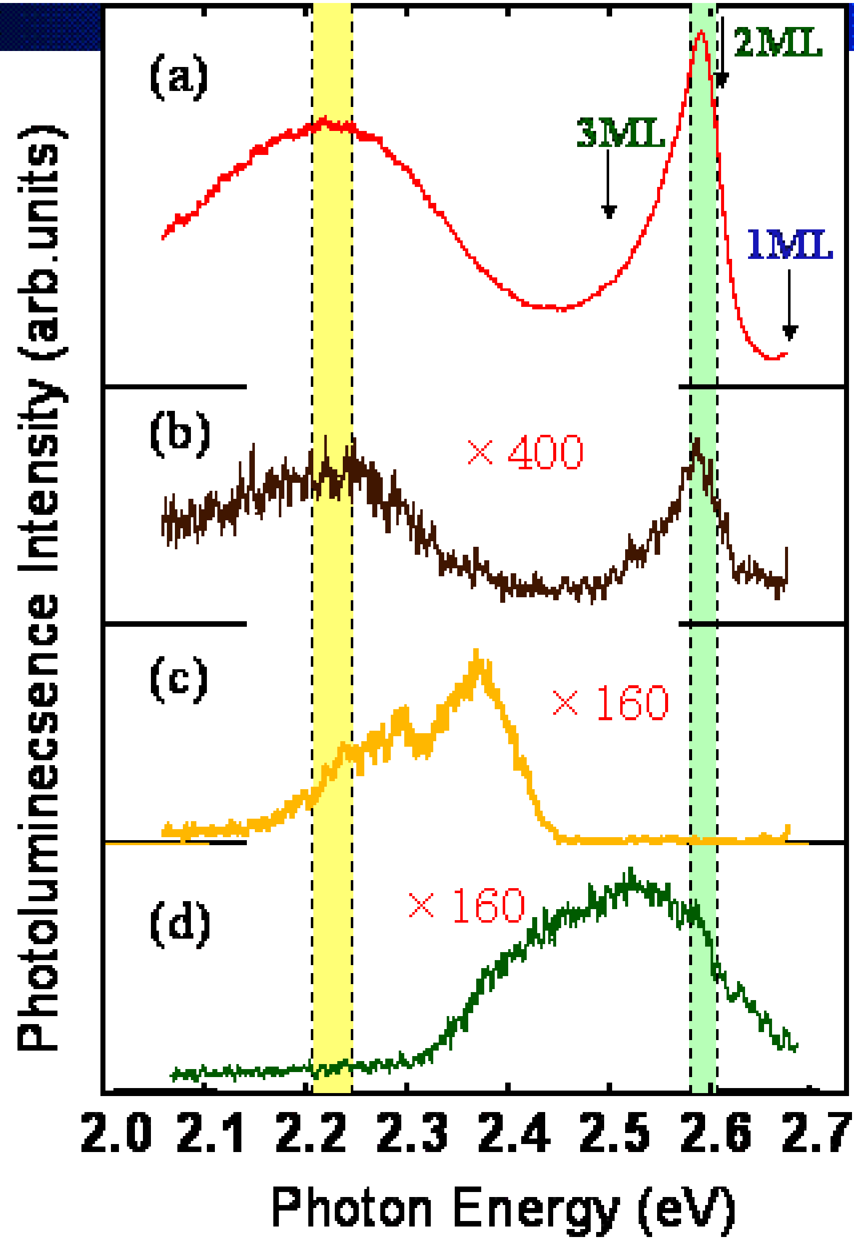

Macroscopic

ϕ_{ex} = 100 μm,
I_{ex} = 7 μJ/cm^2

Microscopic

ϕ_{ex} = 5 μm,
I_{ex} = 7 μJ/cm^2

dark yellow region

yellow bright point

green bright point

From QWs

© Koichi Okamoto

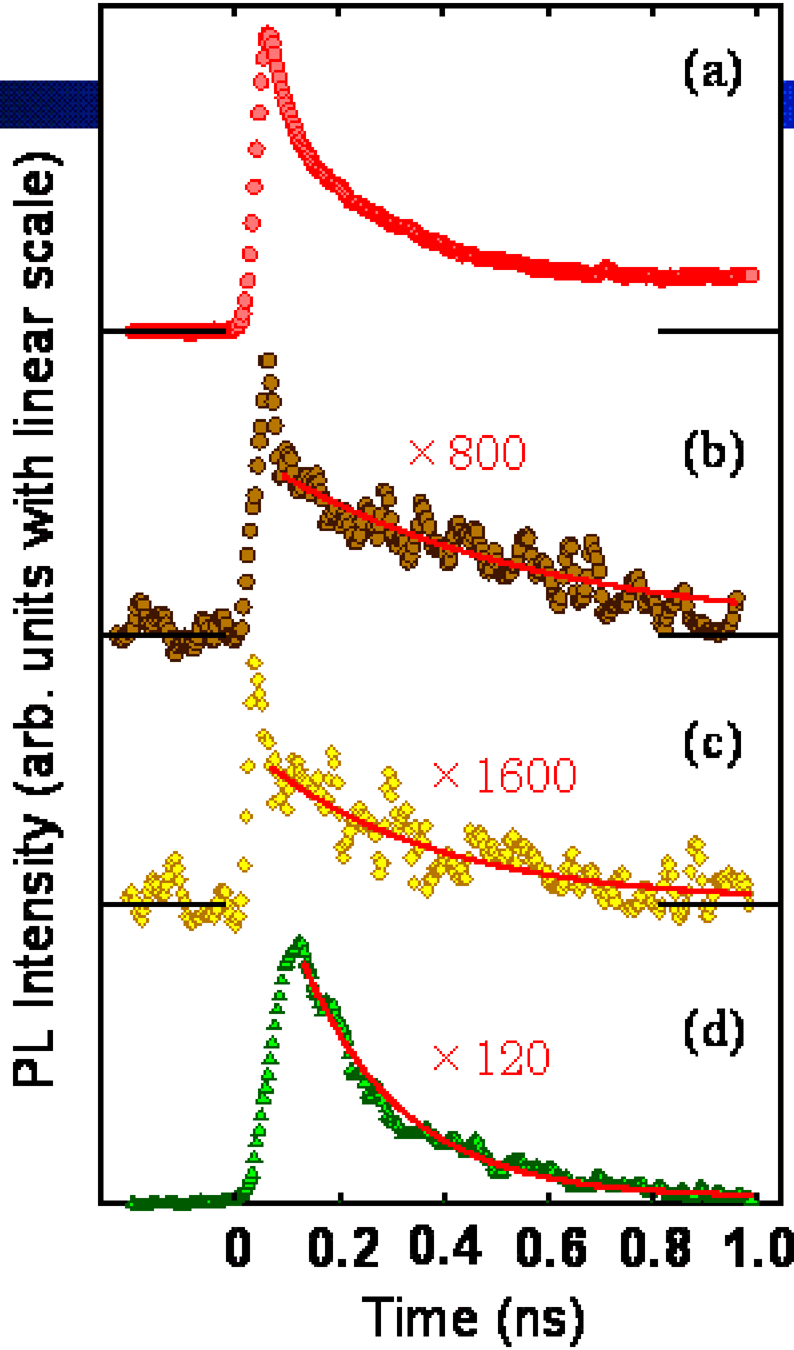

Macroscopic

Non-exponential decay

Multi-exponential decay

Microscopic

Single-exponential decay

$\tau_{PL} = 538 \pm 20$ ps

$\tau_{PL} = 329 \pm 29$ ps

$\tau_{PL} = 194 \pm 3$ ps

From QDs

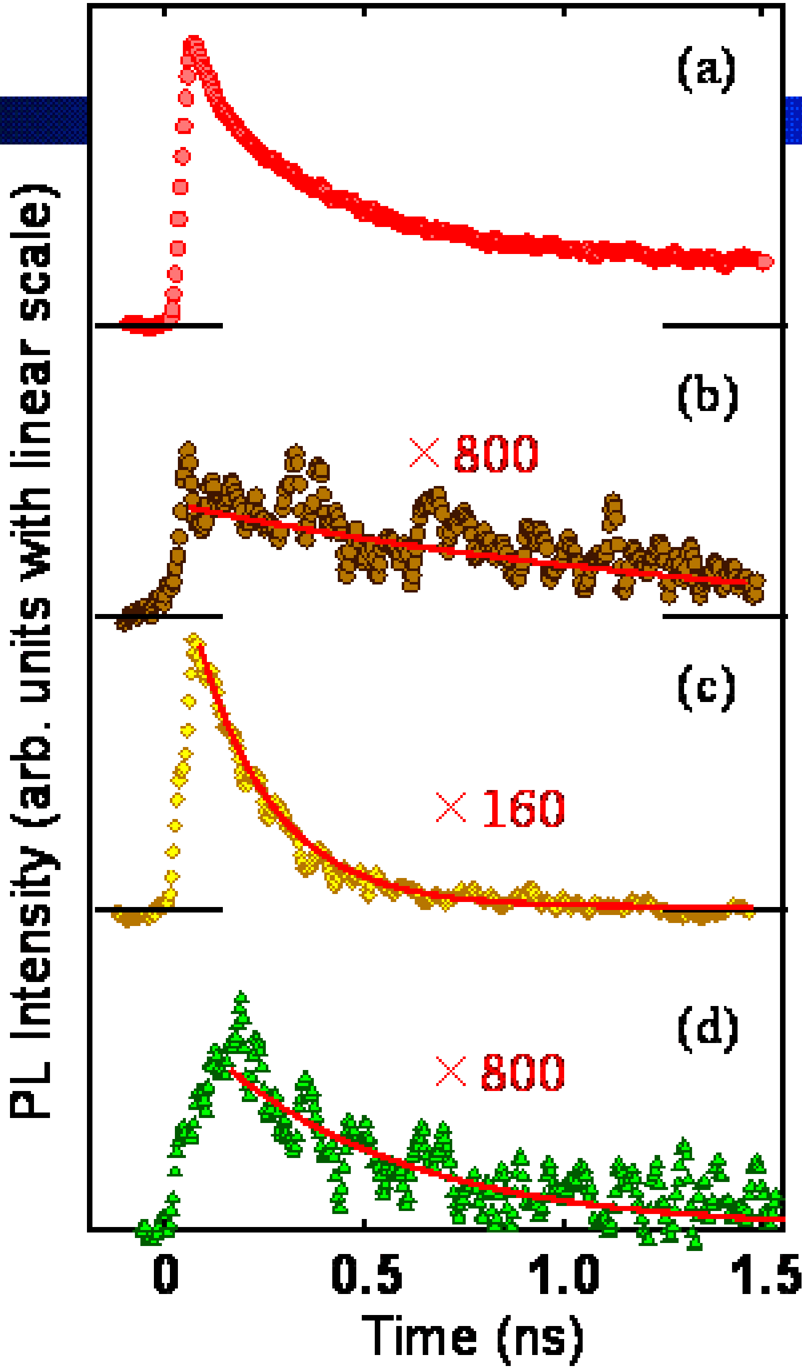

Macroscopic

Non-exponential decay

Multi-exponential decay

Microscopic

Single-exponential decay

$\tau_{PL} = 1.6 \pm 0.6$ ns

$\tau_{PL} = 193 \pm 2$ ps

$\tau_{PL} = 706 \pm 34$ ps

Sharp PL spectra from single QD

10ML @ 77K

Microscopic

$\phi_{ex} = 5\mu m$,
$I_{ex} = 7\ \mu J/cm^2$

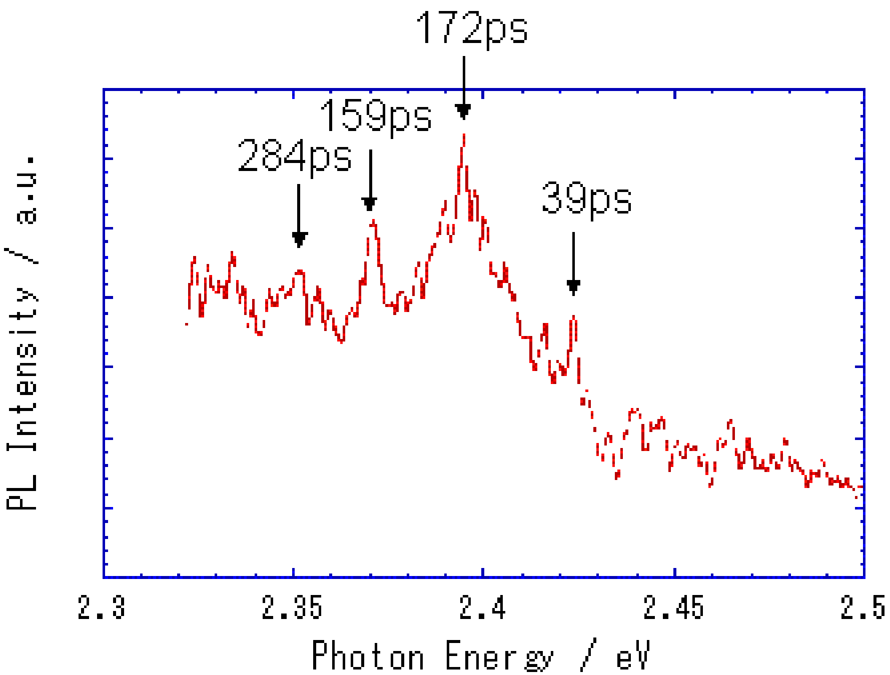

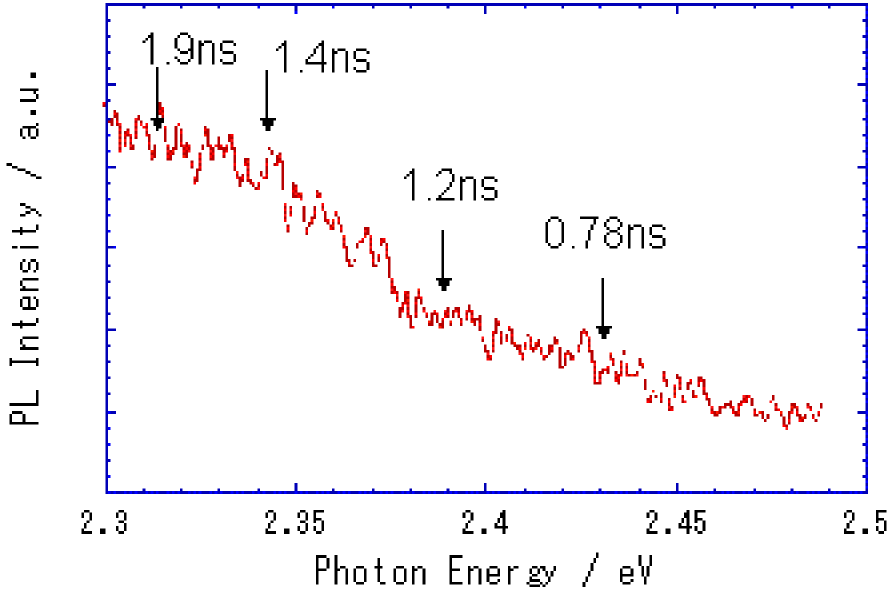

Emission mechanism

$$\frac{1}{\tau_{PL}} = \frac{1}{\tau_{rad}} + \frac{1}{\tau_{nonrad}} + \frac{1}{\tau_{trans}}$$

τ_{PL} : photoluminescence lifetime

τ_{rad} : radiative recombination lifetime

τ_{nonrad} : nonradiative recombination lifetime

τ_{trans} : transfer lifetime from QWs into QDs

(i) PL lifetimes are limited by the nonradiative processes

(ii) radiative lifetimes are changed drastically with the dimensionality of QD-centers

(iii) the situation is the combined e!ect between (i) and (ii) models.

Variation of PL from each QD

Qantum Dot

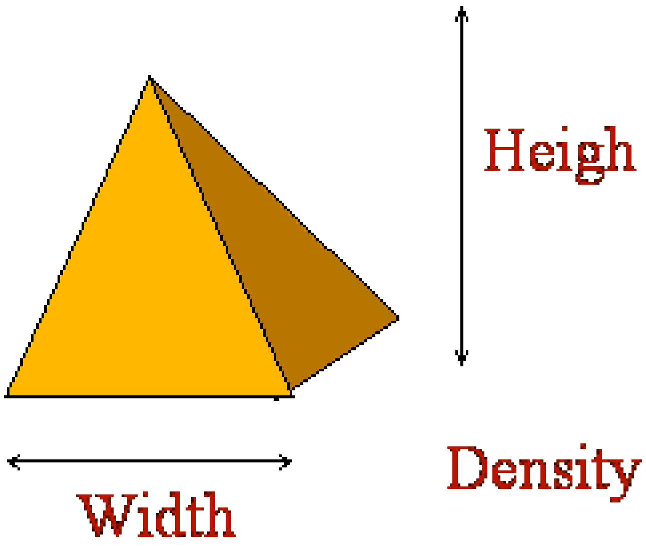

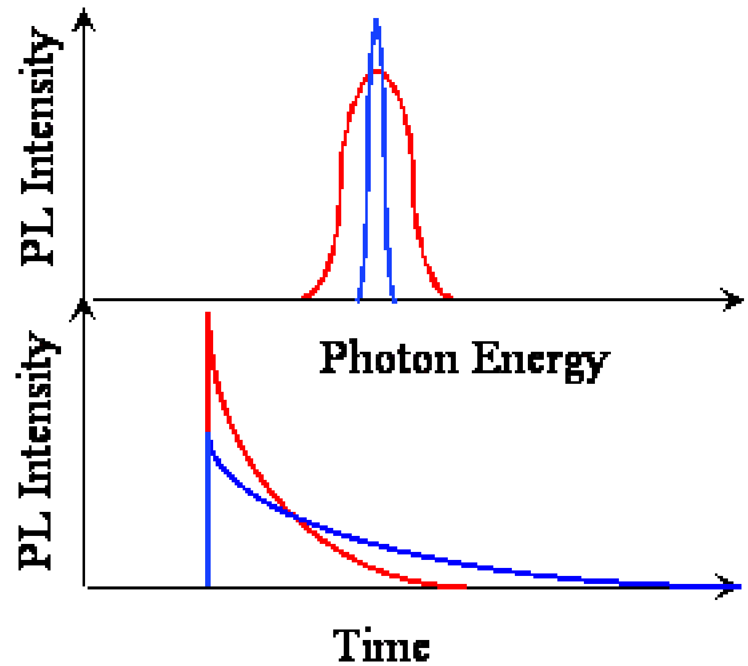

The PL from single QD has various PL lifetime based on the variation of height and width of QD even if the emission wavelength is same

Summary - CdSe QDs emission -

- Recombination mechanism has been assessed for CdSe/ZnSe.
- TRPL spectroscopy was employed at the CdSe(10 ML)/ZnSe sample for emission bands from either QWs (CdSe wetting layers) or QDs (self-formed CdSe QDs) under macroscopic and microscopic excitation.
- It was found that excitons photo-generated at QWs are electively transferred to QDs though the number of transfer channels strongly depends on the number of QDs in the vicinity of microscopic-focus, and that PL lifetimes of emissions from QDs ranged from 193 ps to 1.6 ns at 77 K.

Third order nonlinear optical effect

$\boldsymbol{E}(\boldsymbol{r},t)=\boldsymbol{E}_o\exp[i(\boldsymbol{kr}-\omega t)]$

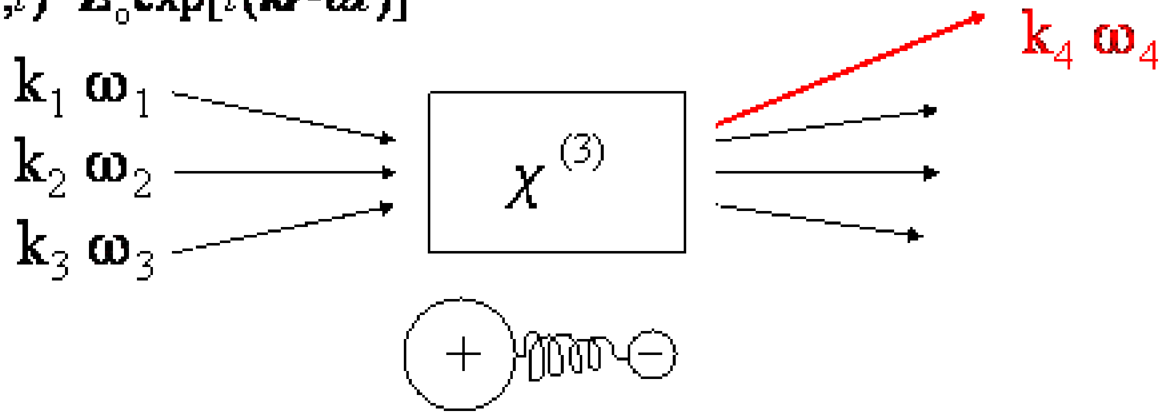

$$\boldsymbol{P}/\varepsilon_o = \sum \chi_{ij}^{(1)}\boldsymbol{E}_j + \sum\sum \chi_{ijk}^{(2)}\boldsymbol{E}_j\boldsymbol{E}_k + \sum\sum\sum \chi_{ijkl}^{(3)}\boldsymbol{E}_j\boldsymbol{E}_k\boldsymbol{E}_l + \cdots$$

$\chi^{(3)}$ may be changed by internal dynamic processes without direct photon transfer.
Examples,

femto — pico — micro — mili — second — mint — hour → **Time**

Electronic polarization
Electron transfer
Energy transfer
Carrier Dynamics
Excitation Dynamics
Molecular vibration

Thermal dynamics
Volume, structure change
Density change
Ultrasonic, Acoustic wave
Chemical reaction
Molecular translation

Clustering, Aggregation
Molecular harmonic effect
Nana particle growth
Crystal growth
Phase Transfer
Metal diffusion

Principle of the TG method

$$\Lambda = \frac{\lambda_e}{2\sin(\theta/2)} \qquad q = \frac{2\pi}{\Lambda}$$

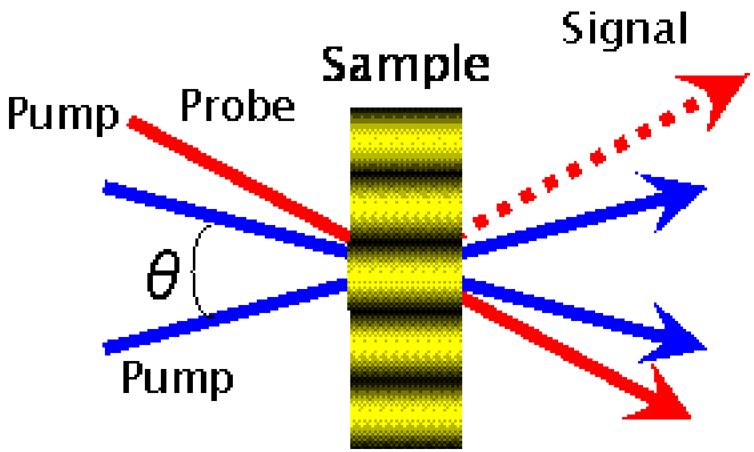

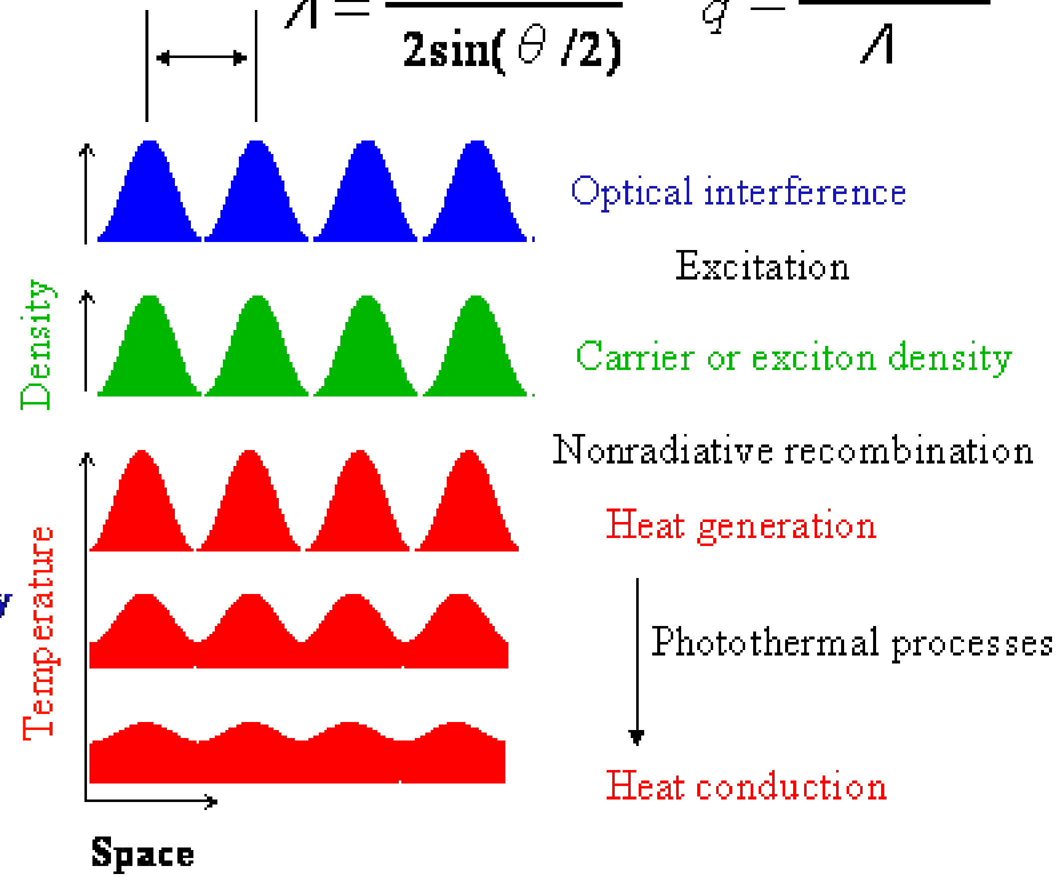

One of the 3rd-order nonlinear spectroscopy

Pump by the interference pattern created by crossing two beams

Create the grating (moderation of the carrire and/or exciton densities or temperature)

Probe by the diffracted beam

High sensitivities, high accuracy, high time resolution, and high spatial resolution

Setup for the TG method (ns)

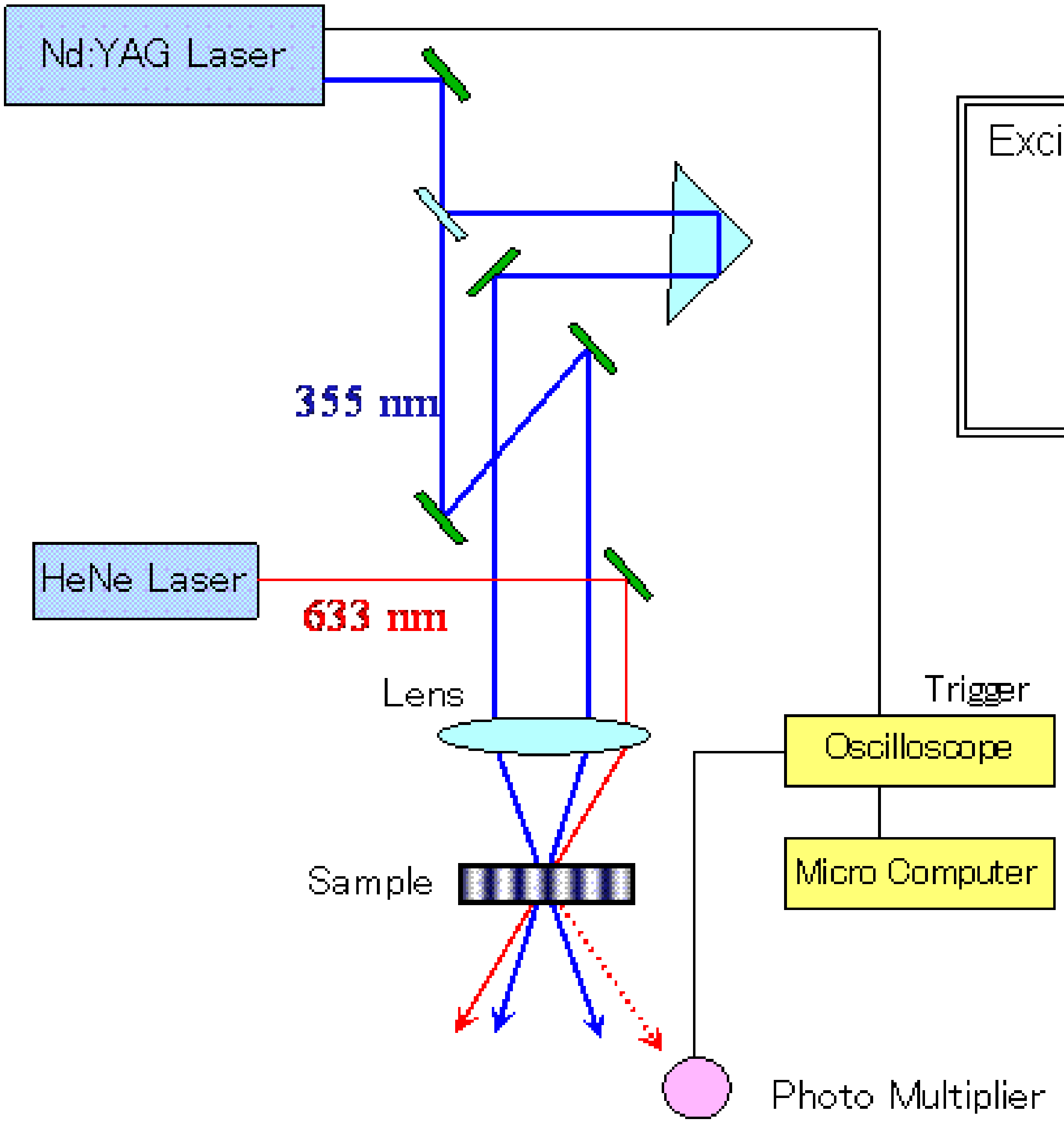

Excitation Laser
Nd:YAG laser
frequency tripled beam
pulse width: 10 ns
wavelength: 355 nm
repetition rate:5 Hz

Obtained TG signals @23°C

© Koichi Okamoto

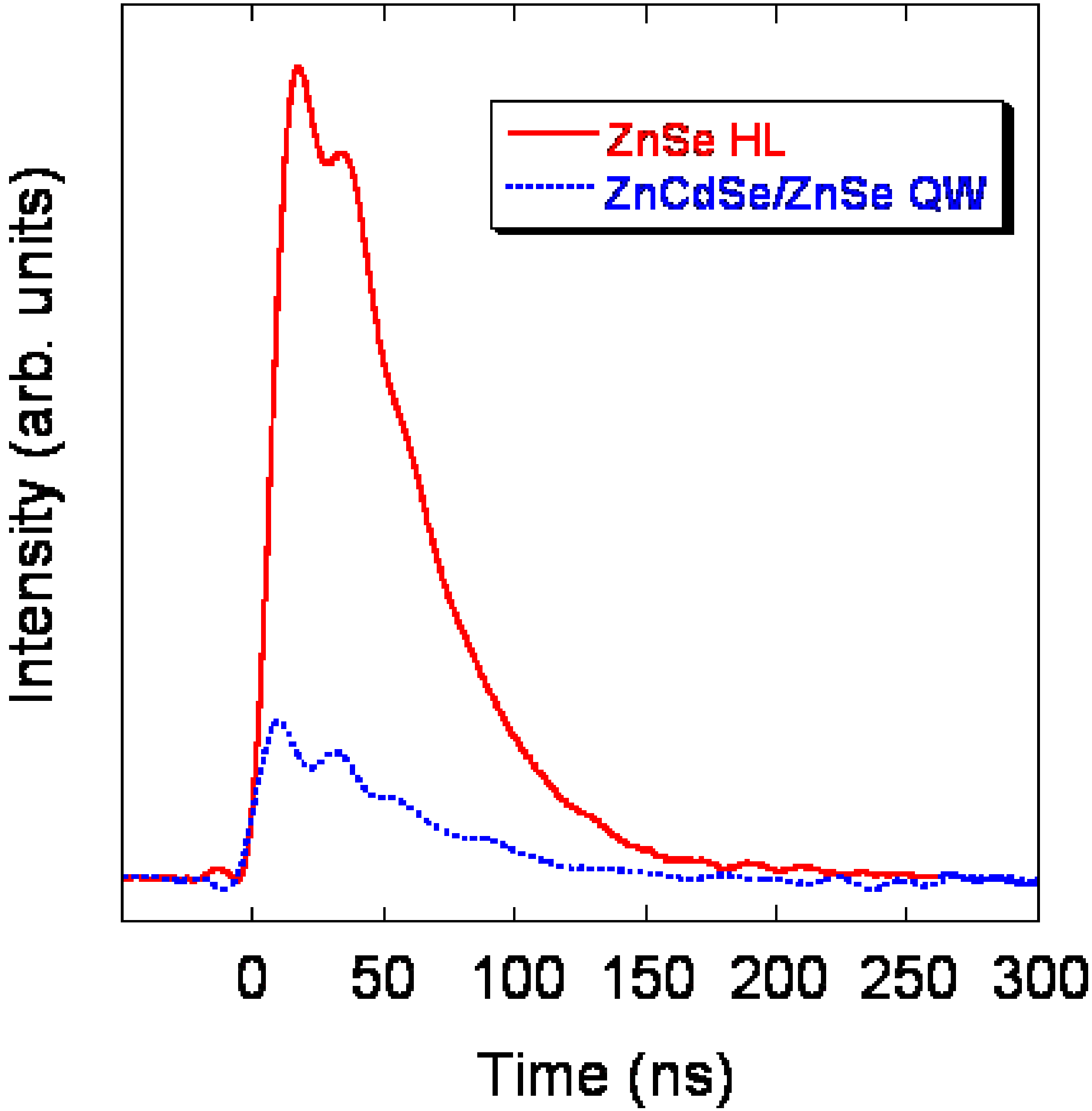

Analysis

From the couple-wave theory, diffracted efficiency is given by

$$I_{TG} / I_o = \delta n^2 + \delta k^2$$

Refractive-index change (Δn) due to the temperature increasing (ΔT) by the nonradiative recombination processes of carries are given by

$$I_{TG}^{1/2} \propto \delta n = \left\{ \left(\frac{\partial n}{\partial r} \right)_T \frac{\partial r}{\partial T} + \left(\frac{\partial n}{\partial T} \right)_r \right\} \delta T$$

Temporal and spatial dependence of the temperature change $\delta T(x,t)$ is given by the following rate equation

$$\frac{d\,\delta T(x,t)}{dt} = D_{th} \frac{d^2\,\delta T(x,t)}{dx^2}$$

where D_{th} is the thermal diffusivity.

$D_{th} = \lambda / C_p \rho$ (λ: thermal conductivity, C_p; thermal capacity, ρ, density)

$$I_{TG}^{1/2}(q,t) \propto \delta T(q,t) = \exp(-D_{th} q^2 t)$$

The time-profile of TG signals decay exponentially

TG decay rate (k) vs. grating constant (q)

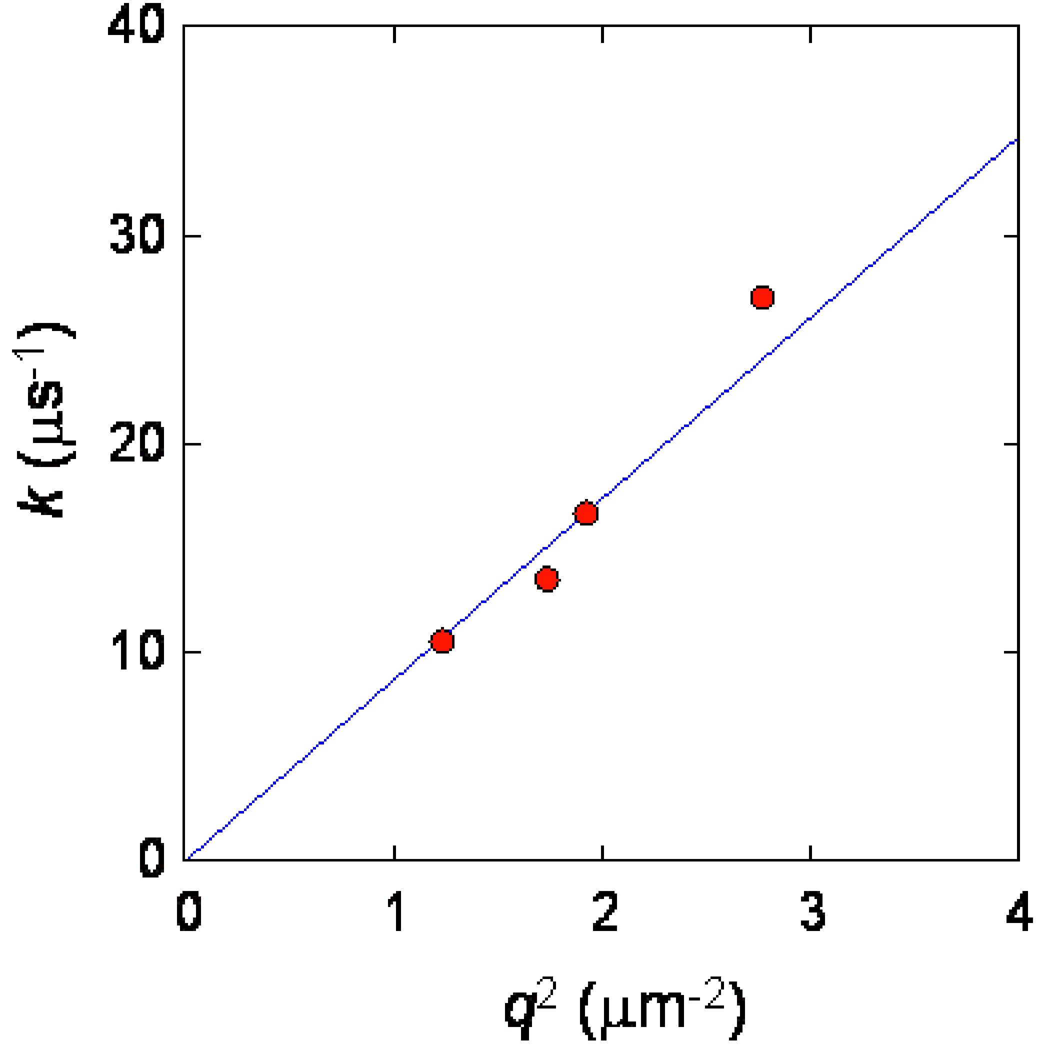

Obtained thermal diffusivity

From the relationship between k and q,

$$k = D_{th} q^2$$

D_{th} is obtained by the slop of the k-q^2 plot

(Experimental) $D_{th} = 0.84 \pm 0.11 \times 10^{-5}\ m^2 s^{-1}$

ZnSe; $\lambda_c = 0.19\,Wcm^{-1}K^{-1}$, $C_p = 0.086\,calg^{-1}K^{-1}$, $\rho = 5.266\,gcm^{-3}$

(Calculated) $D_{th} = 1.00 \times 10^{-5}\ m^2 s^{-1}$

Excellent agreement!

We concluded that the obtained TG signal is due to the thermal processes by the nonradiative recombination of carriers.

Excitation power density dependence

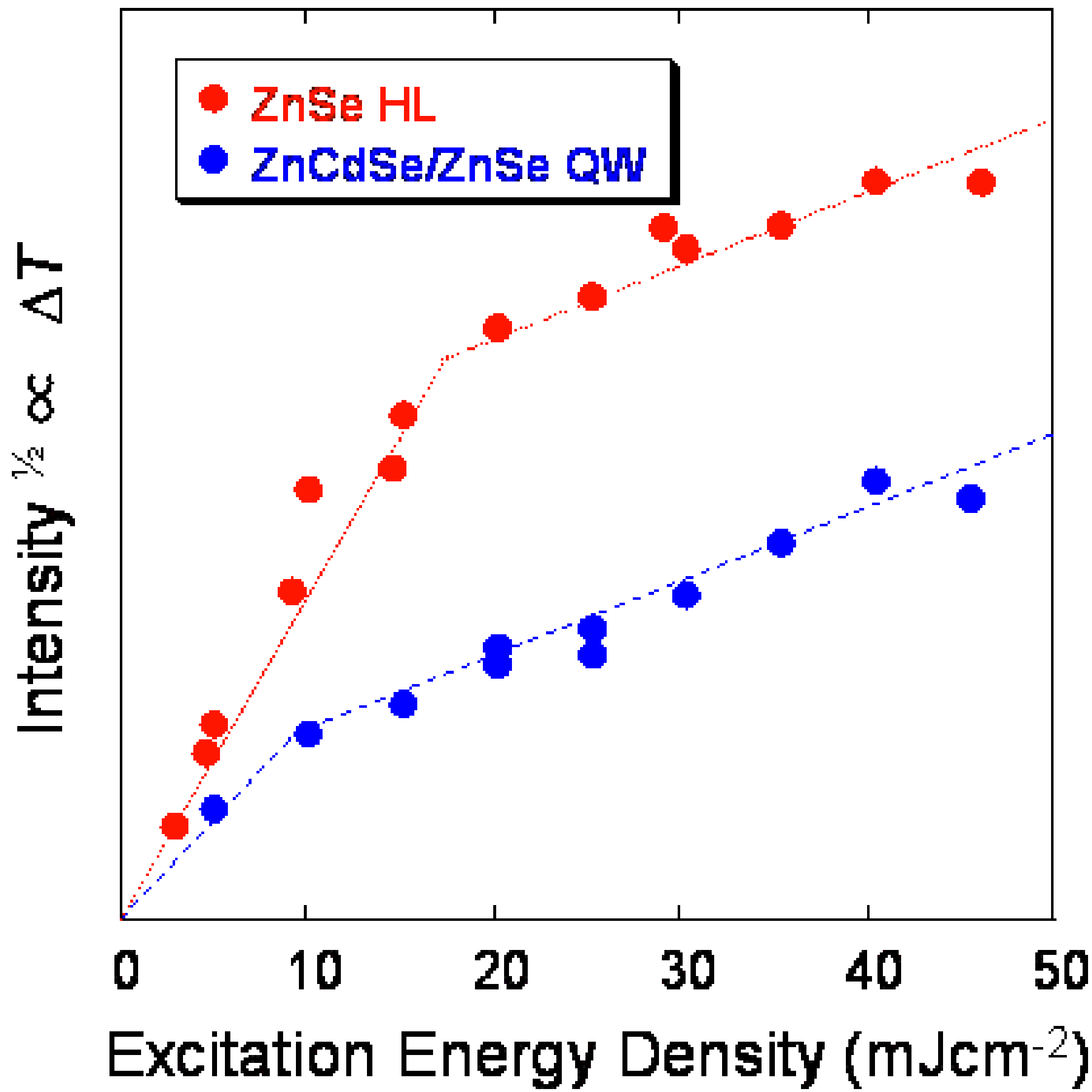

Setup of the transient lens (TL) method

© Koichi Okamoto

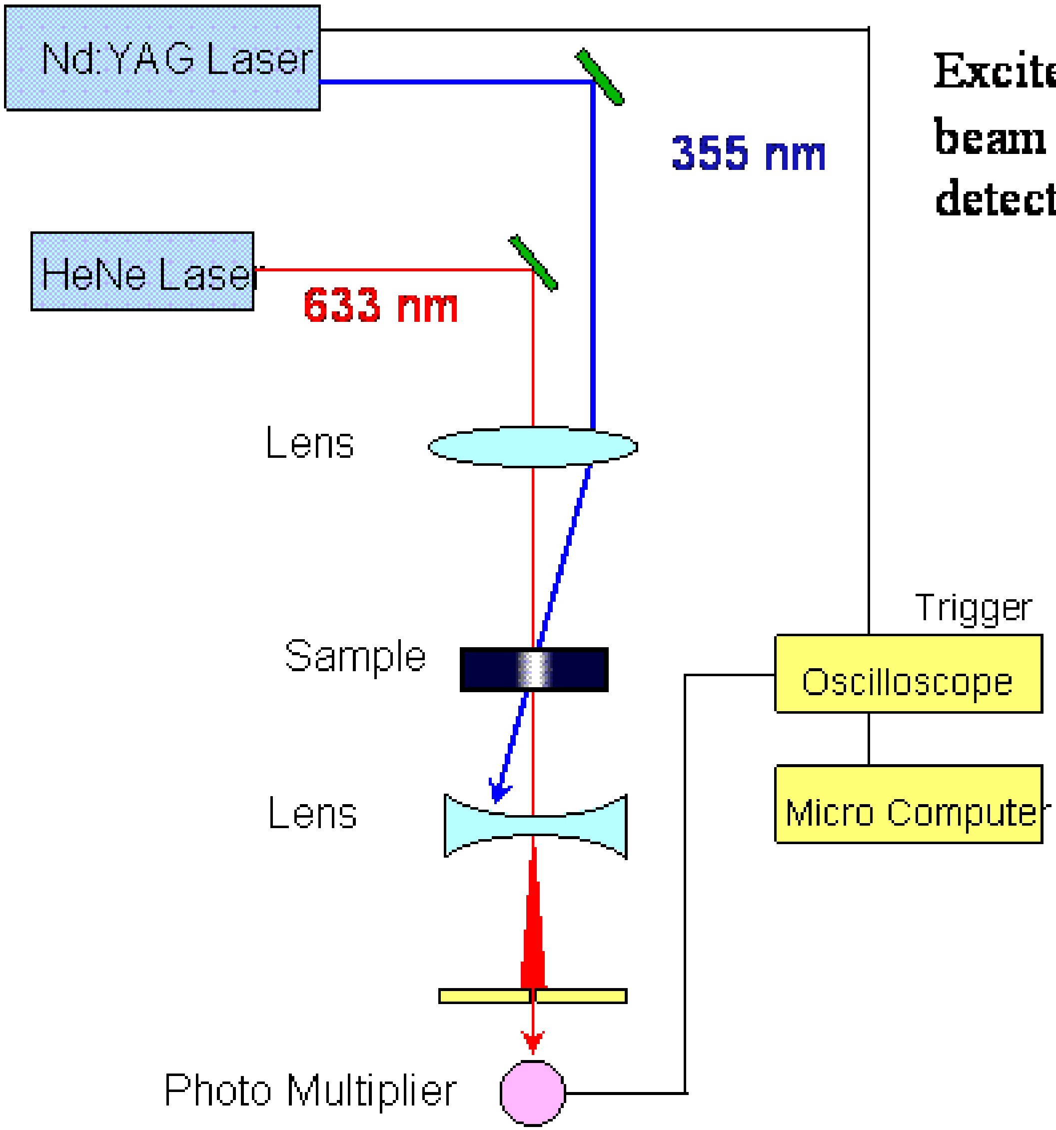

Excite samples by Gaussian shaped beam spot and measure $\chi^{(3)}$ by detecting the dispersion of light

Obtained TL signals

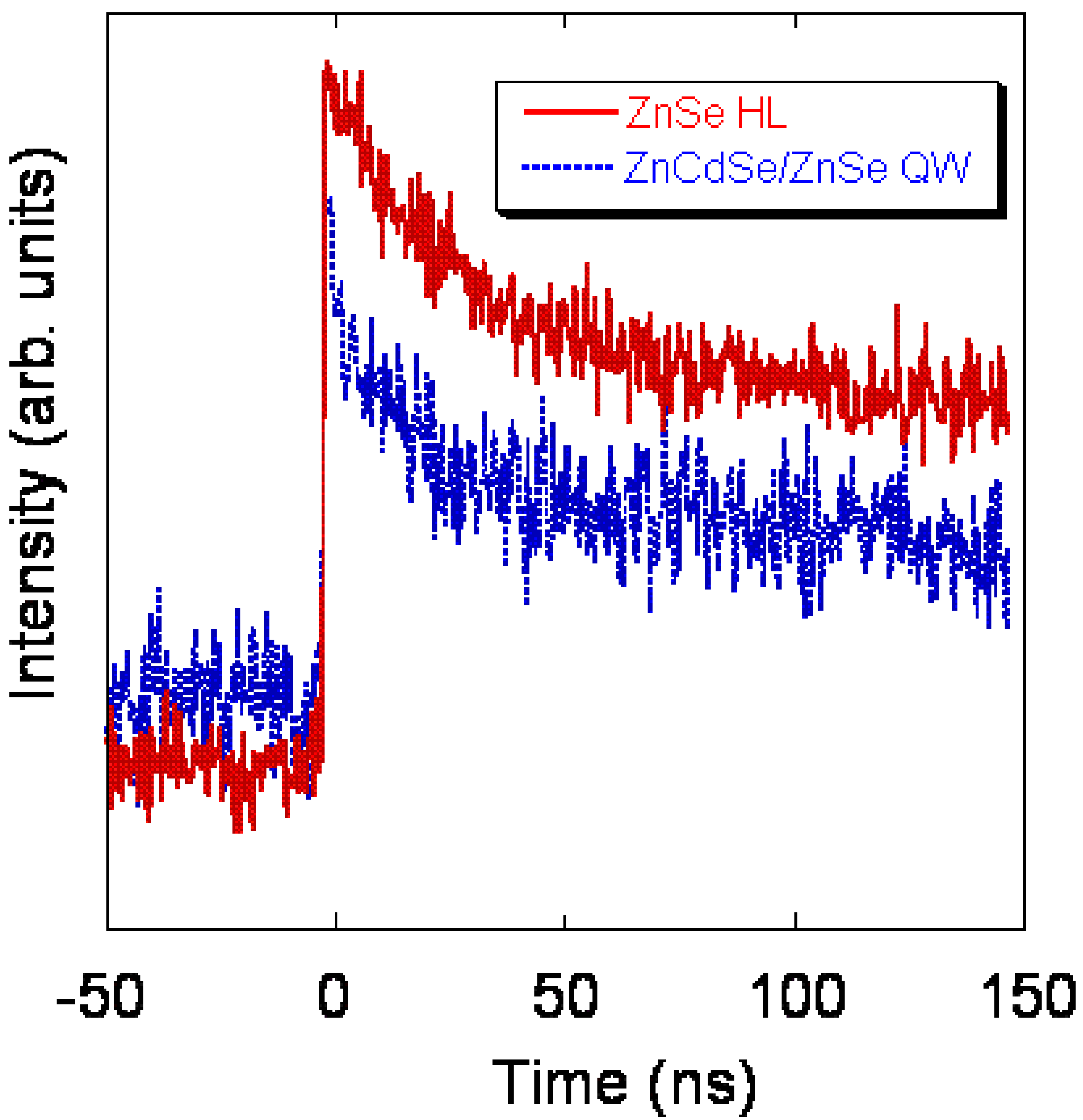

Comparing with GaN and ZnSe

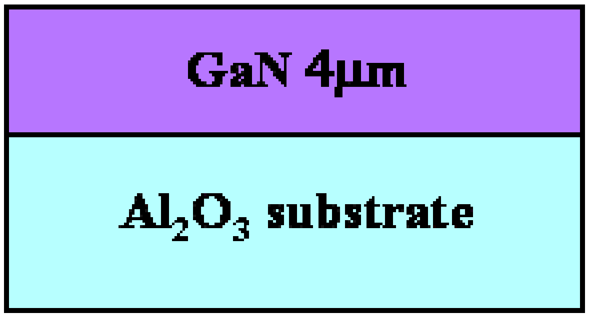

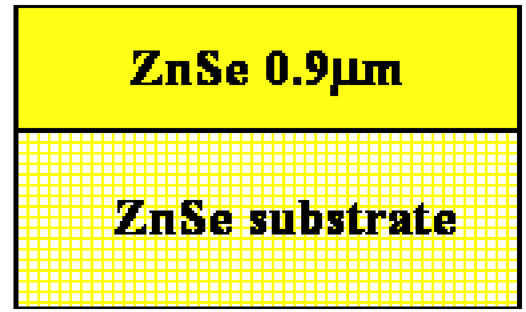

GaN heteroepitaxial layer

grown by metalorganic chemical vapor deposition (**MOCVD**).

Dislocation 10^8 - 10^{10} cm^{-2}

ZnSe homoepitaxial layer

grown on ZnSe substrate by molecular beam epitaxisy (**MBE**).

Dislocation $<10^4$ cm^{-2}

Result: Time profile of the TG signals (ns)

@R.T.

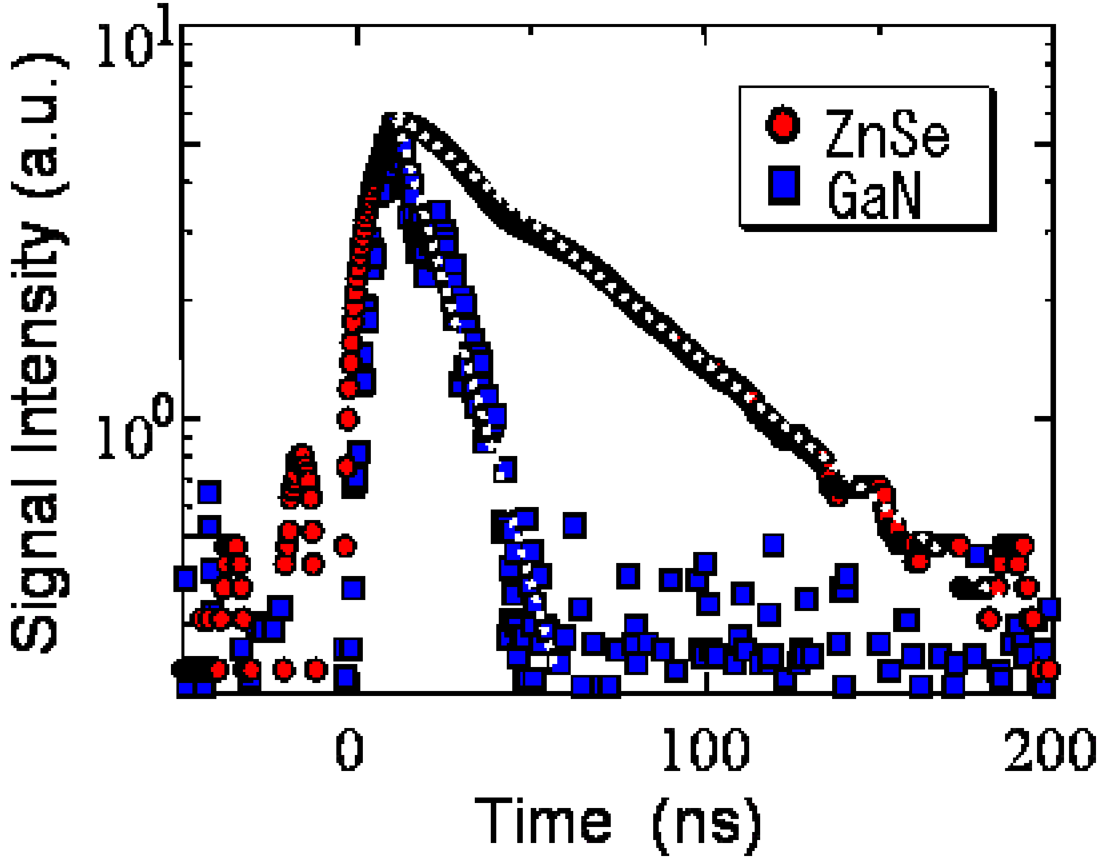

- These signals rise immediately within the excitation pulse (few nanosecond) and decay within few tens nanosecond.

$$I_{TG}^{1/2}(t) = A \exp(-k\ t)$$

- Decay rate constant (k / μs^{-1}) of GaN is about 5 times larger than that of ZnSe

Analysis

The TG signal intensity is given by the sum of the square of the refractive index change (Δn) and absorbance change (Δk)

$$I_{TG} / I_o = \alpha\, \delta n^2 + \beta\, \delta k^2$$

In this time, $I_{TG}^{1/2} \propto \delta n$

The time and spacial dependence of $\Delta n\,(x, t)$ depend on the dynamics of carrier and/or exciton

$$\delta n\,(x, t) = \left(\frac{\partial n}{\partial N}\right) \delta N\,(x, t) + \left(\frac{\partial n}{\partial T}\right) \delta T\,(x, t)$$

Carrie/exciton density change $\Delta N\,(x, t)$ and the temperature change $\Delta T\,(x, t)$ are giveb by the diffusion equations

$$\frac{\partial\, \delta N\,(x, t)}{\partial t} = D \frac{\partial^2 \delta N\,(x, t)}{\partial t} - \left(\frac{1}{\tau_{rad}} + \frac{1}{\tau_{non}}\right) \delta\, \delta N\,(x,t)$$

$$\frac{\partial\, \delta T\,(x, t)}{\partial t} = \frac{1}{\tau_{mn}} \delta N\,(x, t) + D_{th} \frac{\partial^2 \delta T\,(x, t)}{\partial t}$$

By solving this equations,

$$I_{TG}^{1/2}\,(q, t) = \left(\frac{\partial n}{\partial N}\right) \delta N\,(q, 0) \exp\left[-(1/\tau_{rad} + 1/\tau_{non} + D q^2)\, t\right]$$

Term of the population grating

$$+ \left(\frac{\partial n}{\partial T}\right) \frac{\delta T\,(q, 0) \quad 1/\tau_{non}}{1/\tau_{rad} + 1/\tau_{non} + D q^2} \left(-\exp\left[-(1/\tau_{rad} + 1/\tau_{non} + D q^2)\, t\right] + \exp\left(-D_{th}\, q^2\, t\right)\right)$$

Term of the thermal grating

Excitation beam angle dependence

© Koichi Okamoto

GaN@R.T.

$$I_{TG}^{1/2}(q,t) \propto \delta n_{N}^{\circ} \exp\left[-\left(1/\tau_{rad} + 1/\tau_{non} + D q^2\right) t\right]$$

Term of the population grating

$$+ \delta n_{th}^{\circ} \frac{1/\tau_{non}}{1/\tau_{rad} + 1/\tau_{non} + D q^2} \left(-\exp\left[-\left(1/\tau_{rad} + 1/\tau_{non} + D q^2\right) t\right] + \exp\left(-D_{th} q^2 t\right) \right)$$

Term of the thermal grating

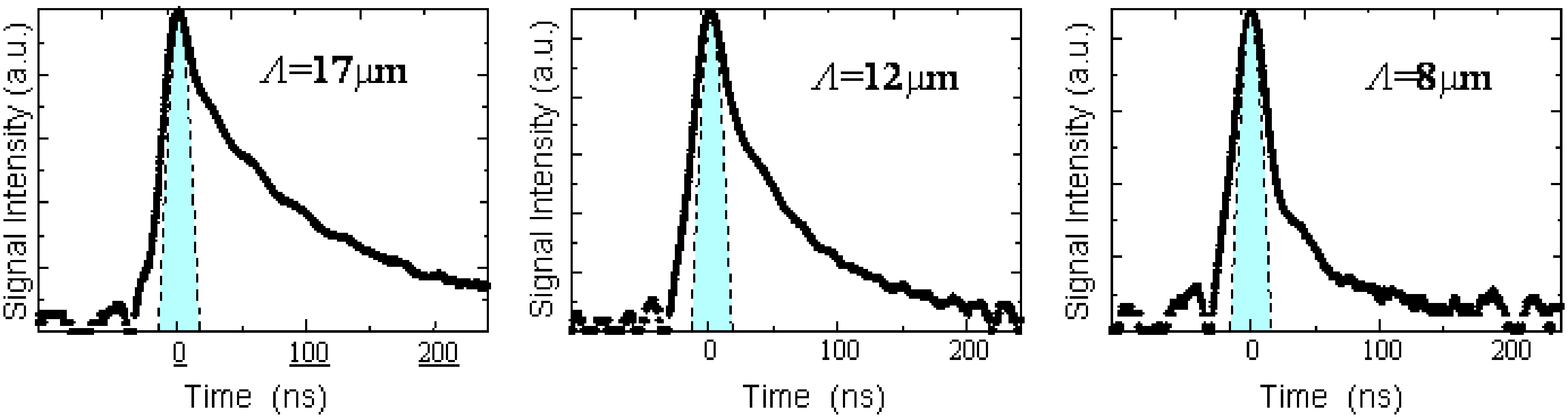

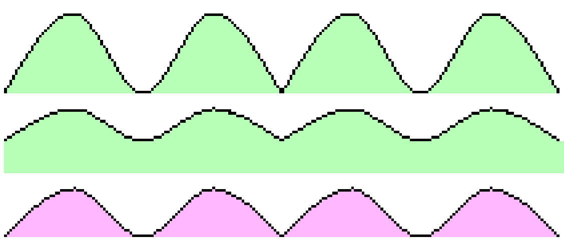

Thermal grating is well generated

Fast decay component

→ **attribute to the population grating**

Slow decay component

→ **attribute to the thermal grating**

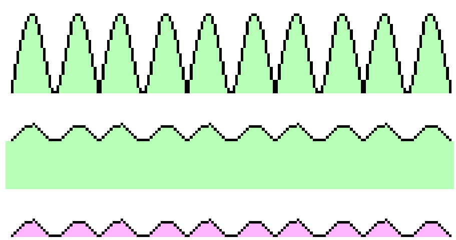

Population grating is relaxed before the thermal grating is generated

Relationship between TG decay rate constant (k/μs^{-1}) and the grating constant (q^2/μm^{-2})

@R.T.

Term of the thermal grating

(By theory)

$$I_{TG}^{1/2}(t) \propto \delta T^0 \exp(-D_{th} q^2 t)$$

D_{th} : thermal diffusion constant ($D_{th}=\lambda_c/\rho C_p$)

(ρ : density C_p, : heat capacity λ_c : heat conductivity)

(By fitting)

$$I_{TG}^{1/2}(t) = A \exp(-k\, t)$$

$$k = D_{th}\, q^2$$

$$A \sim \delta T$$

Experimental values

D_{th} = 0.43 cm^{2}s^{-1} (GaN) 0.084 cm^{2}s^{-1} (ZnSe),

Calculated values

D_{th} = 0.44 cm^{2}s^{-1} (GaN) 0.10 cm^{2}s^{-1} (ZnSe),

(λ_c=1.3 Wcm^{-1}K^{-1}, ρ=6.095 gcm^{-3}, C_p=9.745 calmol^{-1}K^{-1} :GaN
λ_c=0.19 Wcm^{-1}K^{-1}, ρ=5.266 gcm^{-3}, C_p=0.0086 calg^{-1}K^{-1} :ZnSe,)

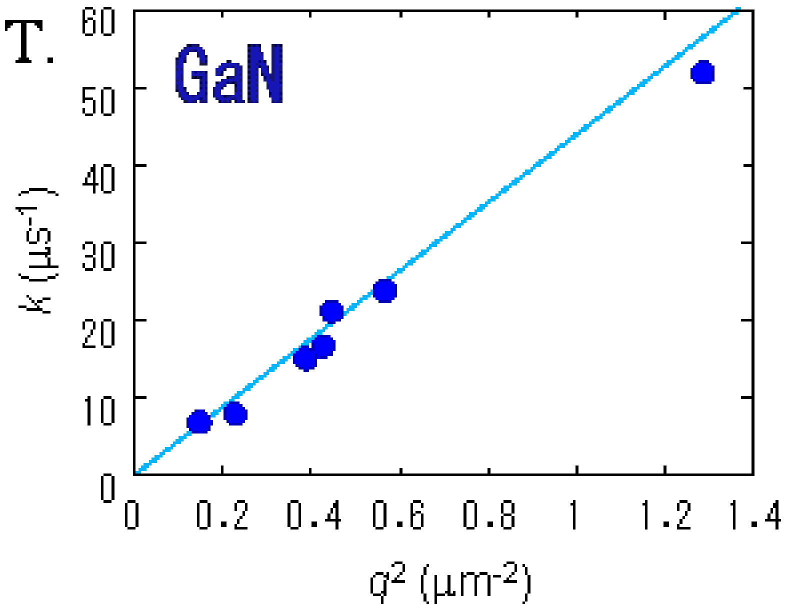

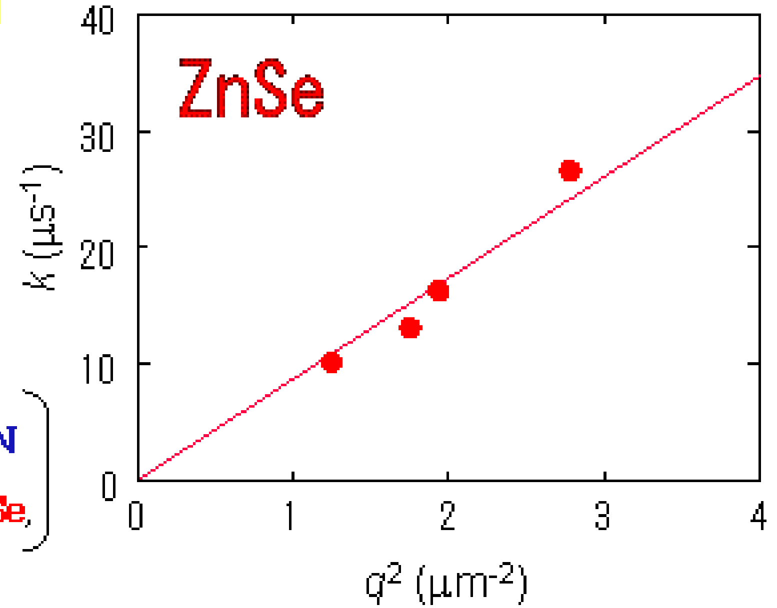

Excitation energy dependence

@R.T.

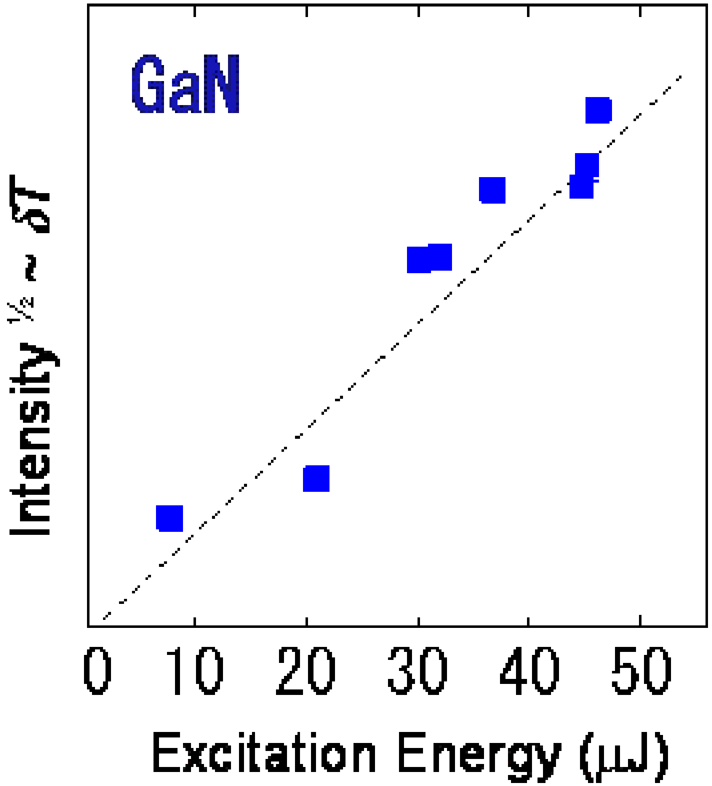

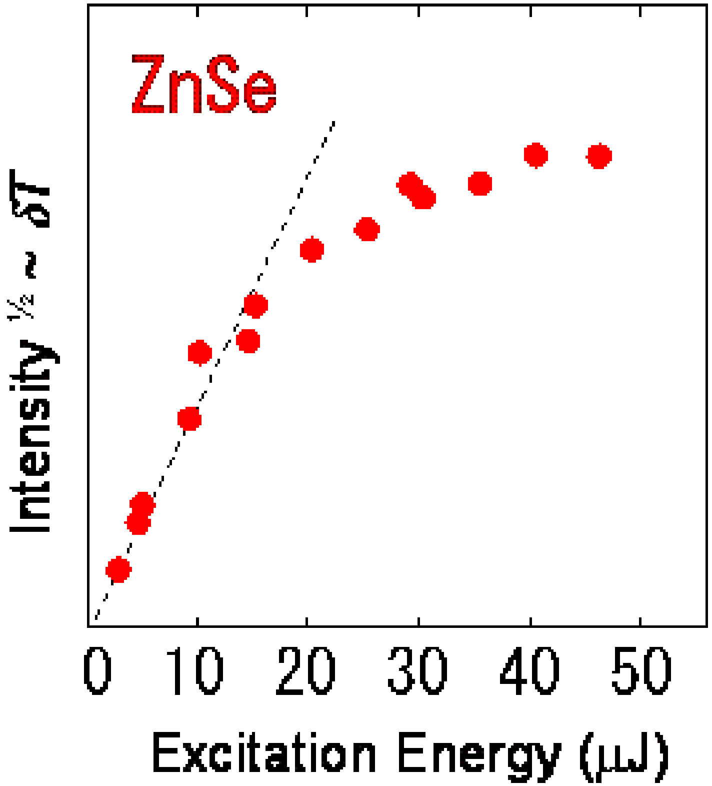

It was found that the heat generation (nonradiative recombination processes) in **GaN** was not saturated, which is different from the reported case of **ZnSe**.

Model

ZnSe

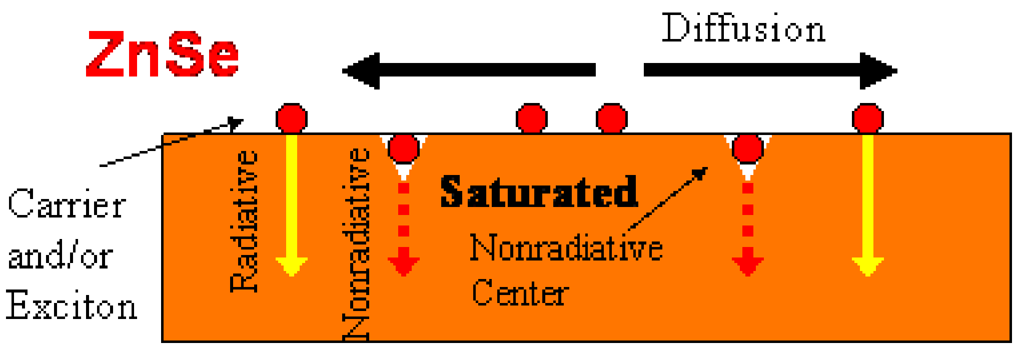

Dislocation $<10^4$ cm^{-2}

GaN

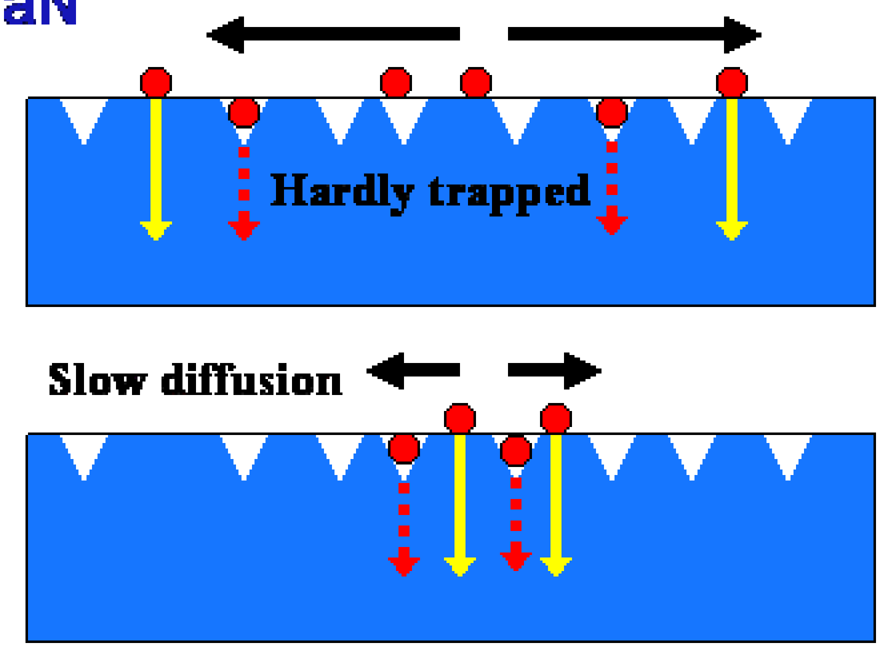

Dislocation 10^8 -10^{10} cm^{-2}

$$1/\tau_{\text{non-rad}} = N_t \, \sigma \, v_{th}$$

N_t : density of non-radiative recombination center (NRC)
σ : cross section captured to NRC
v_{th} : thermal velocity

Nonradiative centers are easily saturated.

N_t is low

Radiative recombination should be enhanced.

Nonradiative centers are not saturated.

Model-1

Carrie and/ or exciton are hardly trapped in the nonrdiative centers.

σ is low

Model-2

Diffusion of carrie and/ or exciton are very slow.

v_{th} is low

Model-1 and/or model-2 should be the reason of the strong emission character of GaN

Setup for the TG method (ps)

© Koichi Okamoto

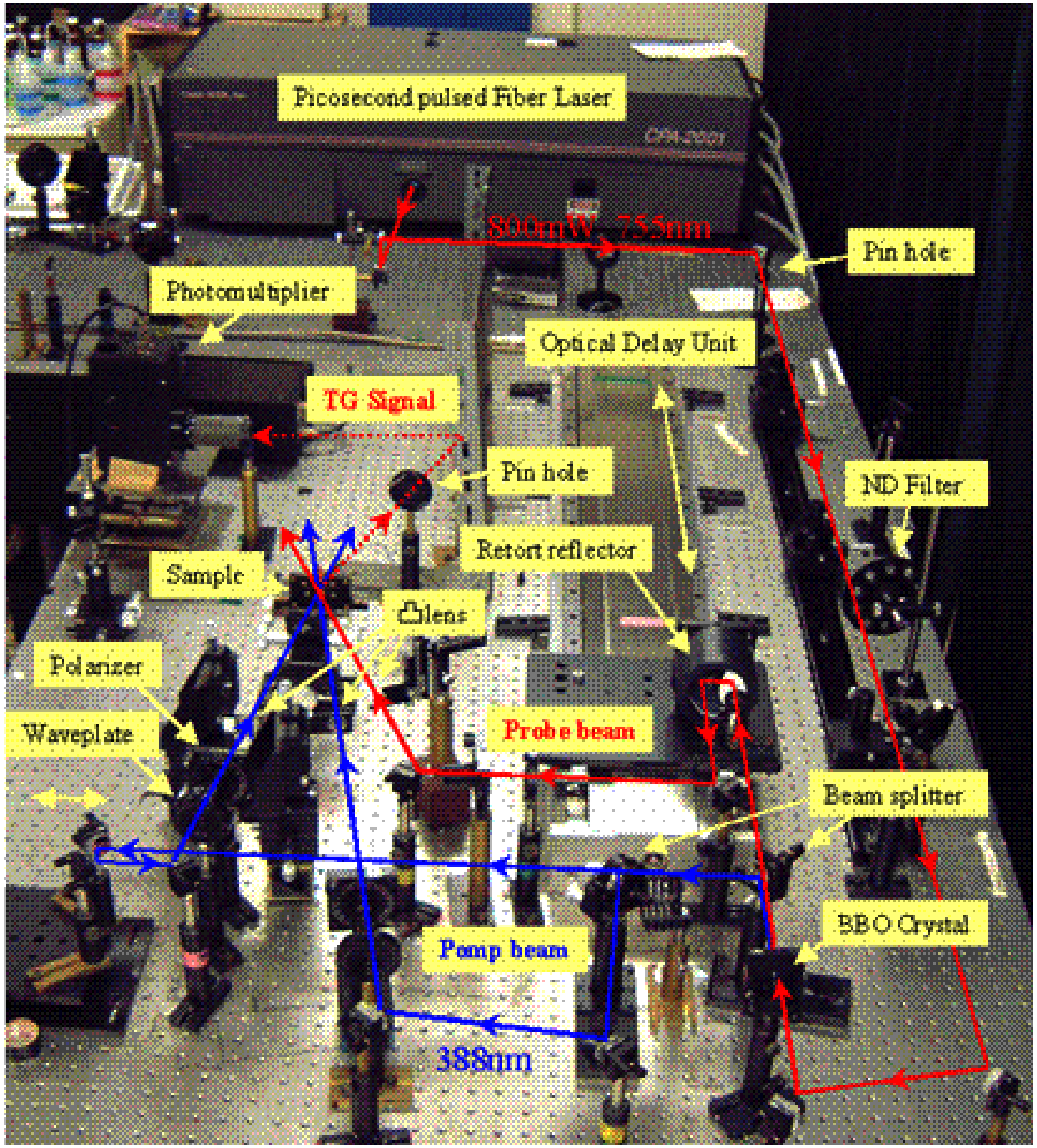

Excitation Laser
- Mode locked Fiber laser
- frequency doubled beam
- pulse width: 0.5 ps
- wavelength: 388 nm
- repetition rate: 1 kHz

Probe fundamental beam

Time profile of the TG signals (ps)

$$I_{TG}^{1/2}(q,t) \propto \delta N(q,0)\exp[-(1/\tau_{rad} + 1/\tau_{non} + Dq^2)t]$$

Term of the population grating

$\Lambda = 0.7\mu m$

@R.T.

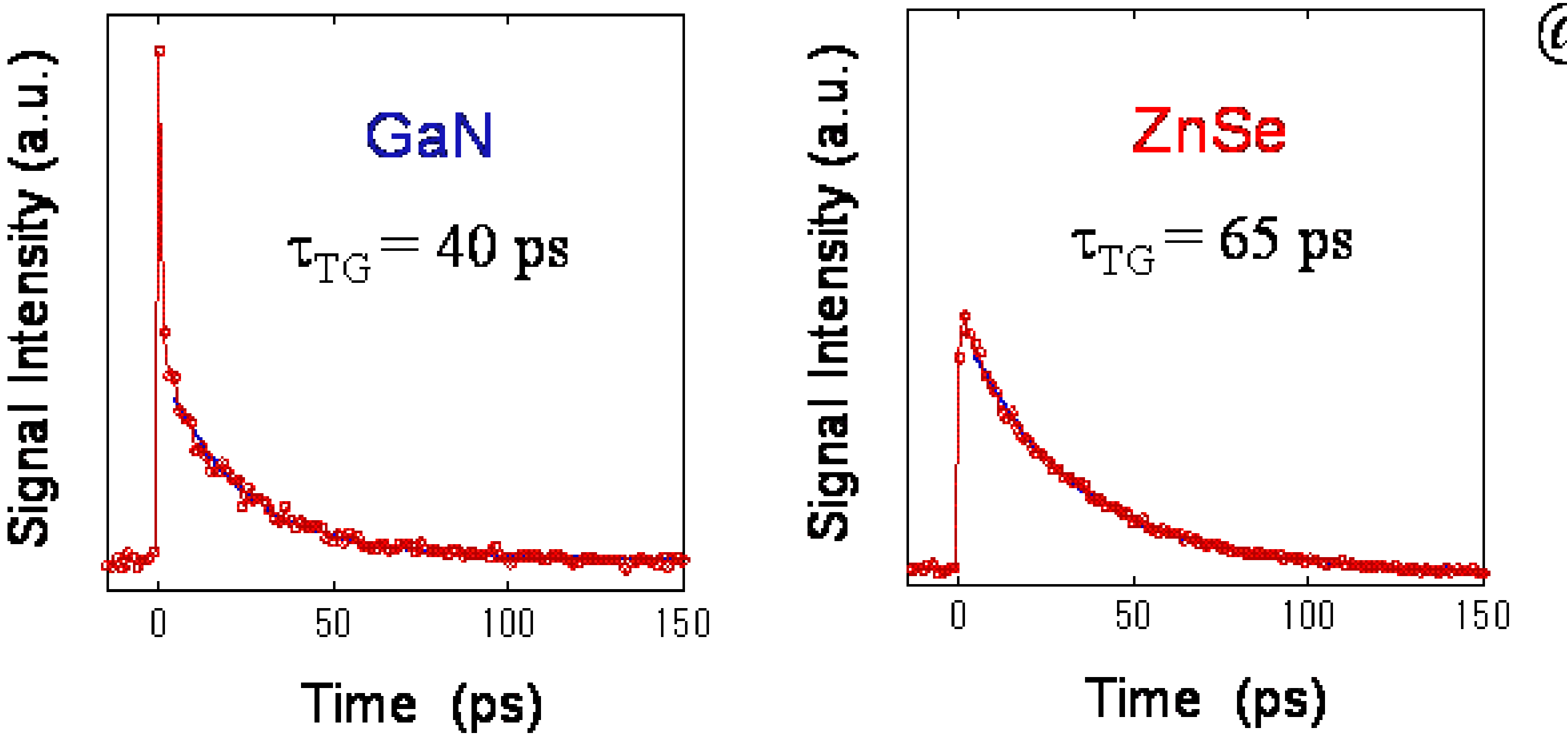

Decay rates are controlled by the **diffusion** and **recombination** processes of carrier/exciton

→ Diffusion constants (D) of carrie/exciton would be obtained by separating these two processes

Detail results and discussion should be published in the next opportunity

Summary - TG measurements -

- Transient Grating (TG) method is the powerful tool to detect the thermal dynamics of nonradiative recombination and the diffusion processes of carries and/or excitons in semiconductors.
- Thermal diffusivity in GaN obtained by the decay rate constant of the TG signals (D_{th} = 0.41 cm^{2}s^{-1}) was close to the calculated one (D_{th} = 0.44 cm^{2}s^{-1}).
- We found that the nonradiative dynamics of GaN is different from that of ZnSe, though the radiative dynamics (quantum efficiency) is similar.

It is important to note that detailed information on the optical properties such as the ratio between internal quantum efficiency and external one by comparing nonradiative and radiative processes. Such an approach is in progress.

Acnowlegements

This work was partly supported by the Kyoto University-Venture Business Laboratory Project, Research Foundation for Opto-Science and Technology, Konica Imaging Science Foundation and a Grant-in- Aid for Scientific Research from the Japan Society for the Promotion of Science and Ministry of Education, Science and Culture.

Microscopic Patterning on the Polysilane Films

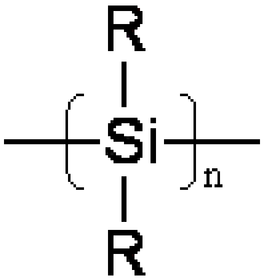

Polysilane compounds are easily oxidized by UV irradiation in air and properties (refraction index, polarization, or hydrophilic character, etc.) are drastically changed.

The microscopic pattern of the polysilane thin films

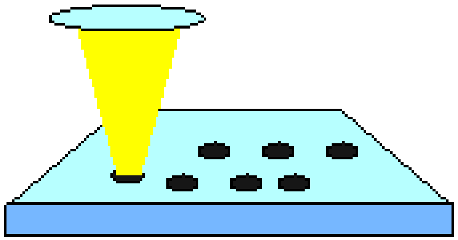

optical memory

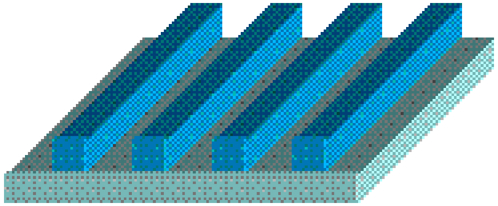

photonics bandgap

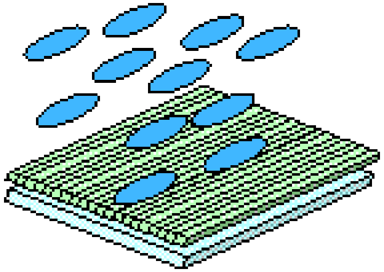

alignment plate

<u>Such the microscopic patterns have been created by the etching technique</u>

We created and observed the microscopic pattern on the polysilane thin films by using the nanosecond pulsed laser induced optical grating.

Sample structure

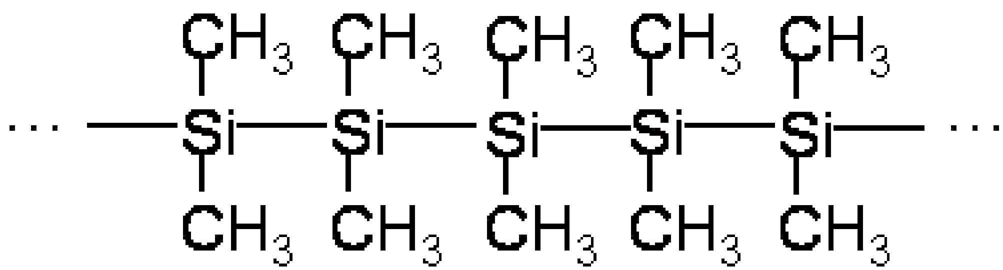

Poly-dimethyl-silane

n=10-20

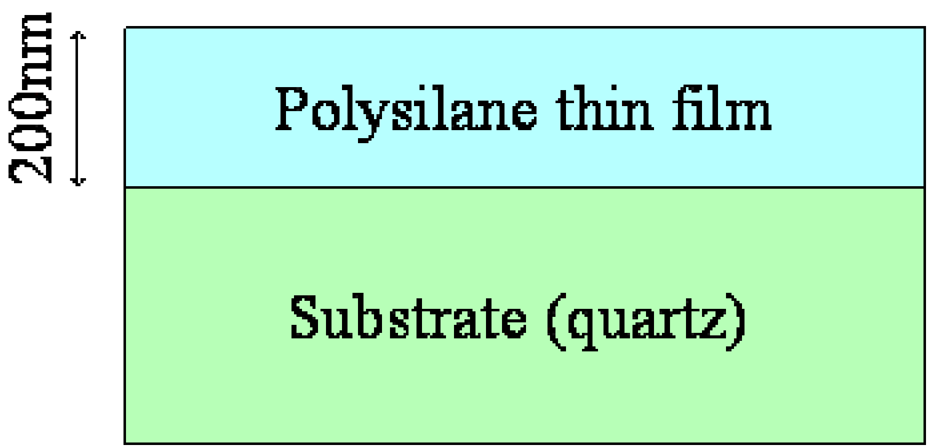

Grown by the high vacuum deposition

Thickness: 200 nm
Presser: 10^{7}-10^{8} Torr
Flow rate: 1-10 nm/s

Result: Time profile of the TG signals

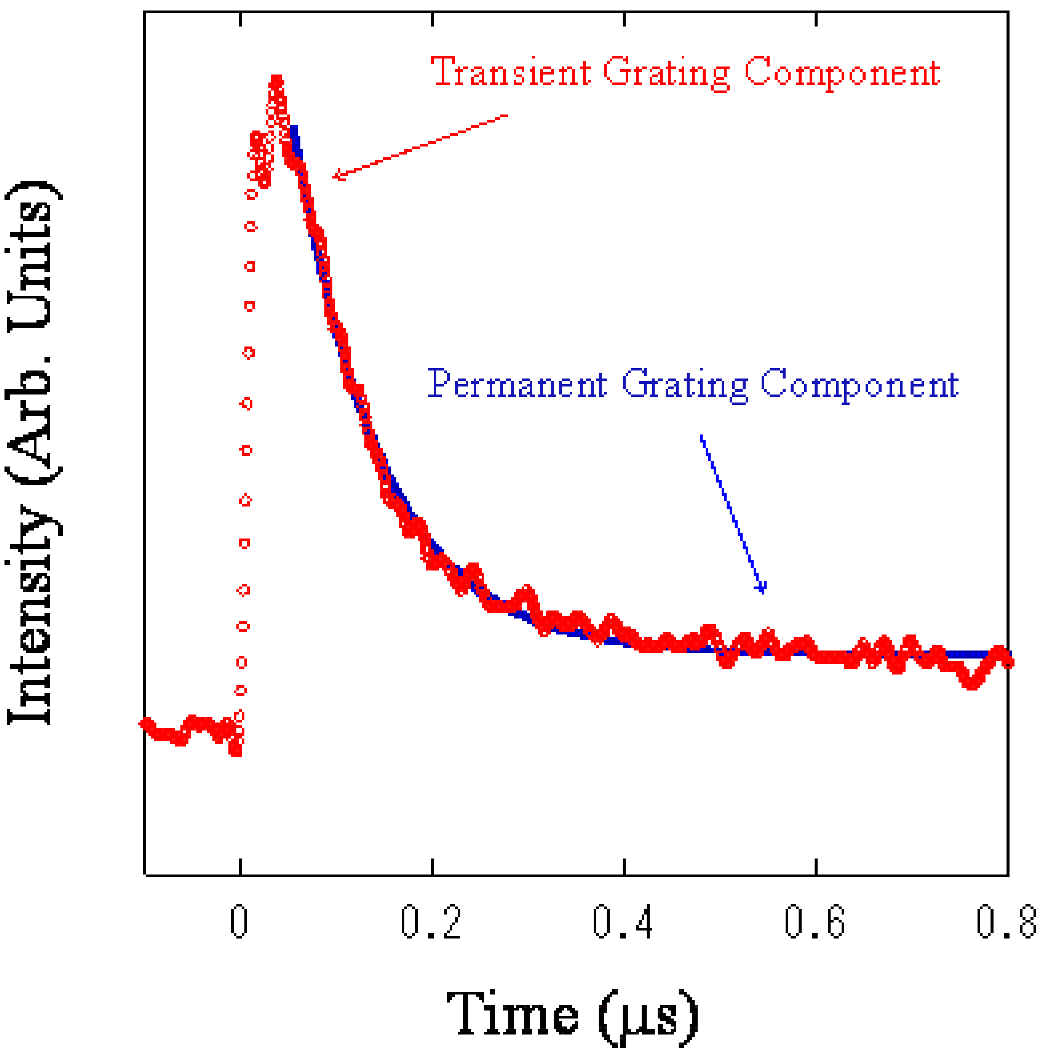

Analysis

The TG signal intensity is given by the sum of the square of the refractive index change (δn) and absorbance change (δk)

$$I_{TG} / I_o = \alpha\, \delta n^2 + \beta\, \delta k^2$$

In this time, $I_{TG}^{1/2} \propto \delta n$

The time and spacial dependence of $\delta n\,(x, t)$ depend on the heat dynamics and chemical reaction

$$\delta n\,(x, t) = \left(\frac{\partial n}{\partial T}\right)\delta T\,(x, t) - \left(\frac{\partial n}{\partial N_R}\right)\delta N_R\,(x, t) + \left(\frac{\partial n}{\partial N_P}\right)\delta N_P\,(x, t)$$

$\delta T\,(x, t)$ are given by the following diffusion equations

$$\frac{d\delta T\,(x, t)}{d\,t} = \frac{Q\,(x, t)}{\rho C_P} + D_{th} \frac{d^2 \delta T\,(x, t)}{dx^2}$$

By solving this equations,

$$\delta T\,(q, t) \propto \delta T\,(q, 0) \exp(-D\, q^2\, t)$$

Therefore, time profile of the TG signal are given by

$$I_{TG}(t)^{1/2} \propto \delta n = \left(\frac{\partial n}{\partial T}\right)\delta T\,(0) \exp(-D\, q^2\, t) - \left(\frac{\partial n}{\partial N_R}\right)\delta N_R + \left(\frac{\partial n}{\partial N_P}\right)\delta N_P$$

Transient Grating Component

Permanent Grating Component

δT : temperature change

δN_R : density change of reactant

δN_P : density change of product

Q : released heat amount

ρ : density

C_P: heat capacity

D_{th}: thermal diffusion constant

q : grating constant

Laser shot dependence of the TG signals

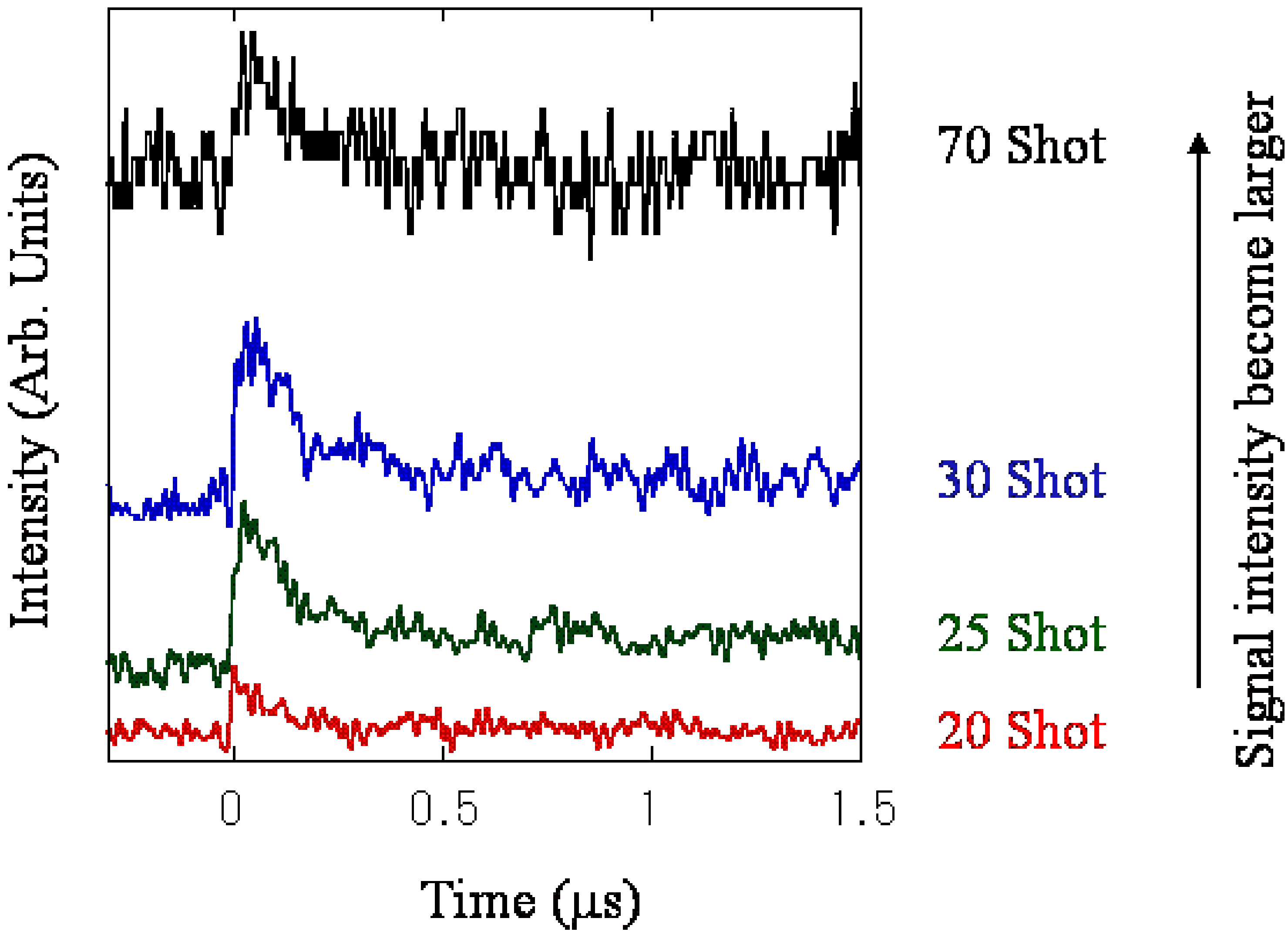

Laser shot dependence of the permanent grating

© Koichi Okamoto

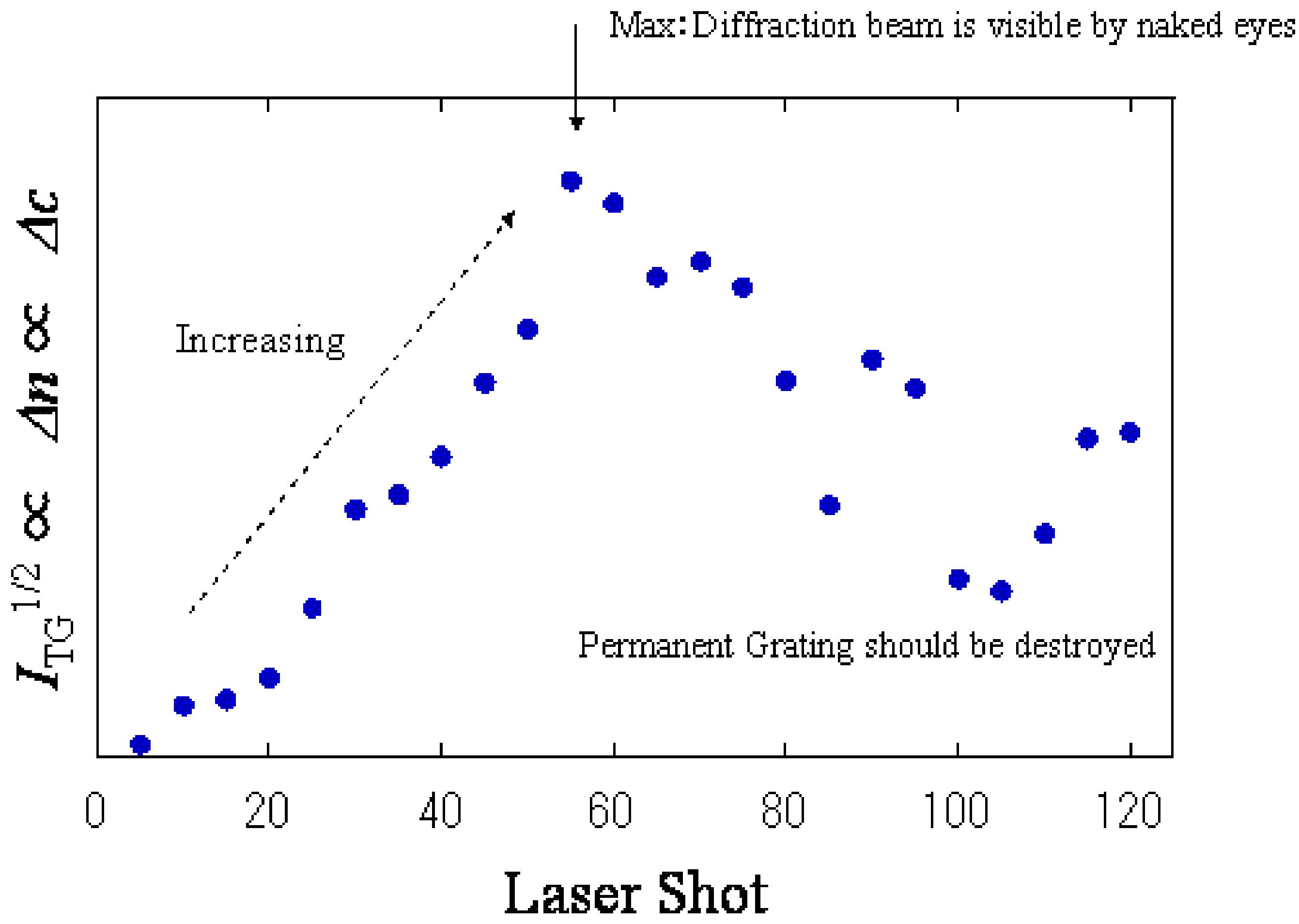

Images of the Microscope

Before

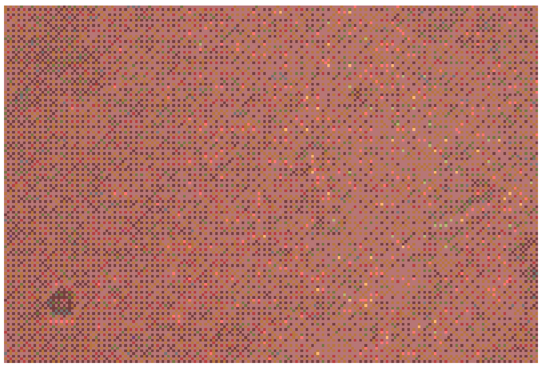

50 Shot

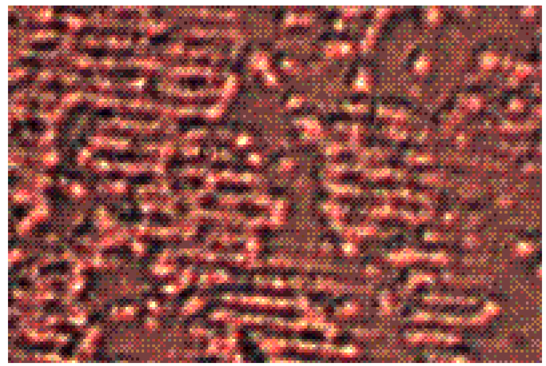

100 Shot

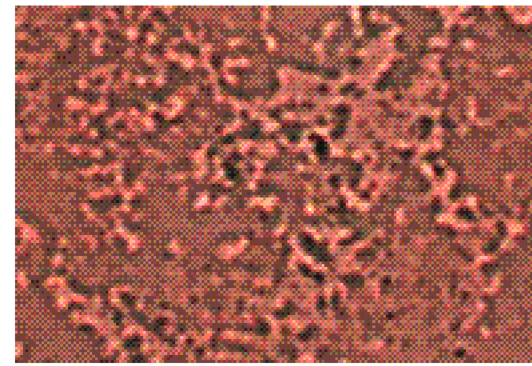

10μm

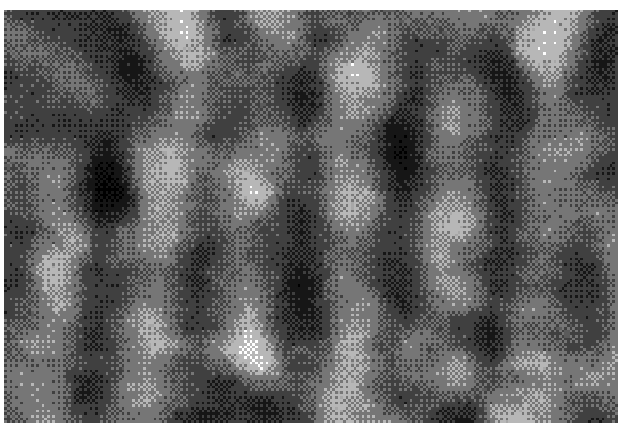

5μm

Microscopic pattern can be observed after 50 shot.

This pattern should be destroyed after 100 shot.

Model

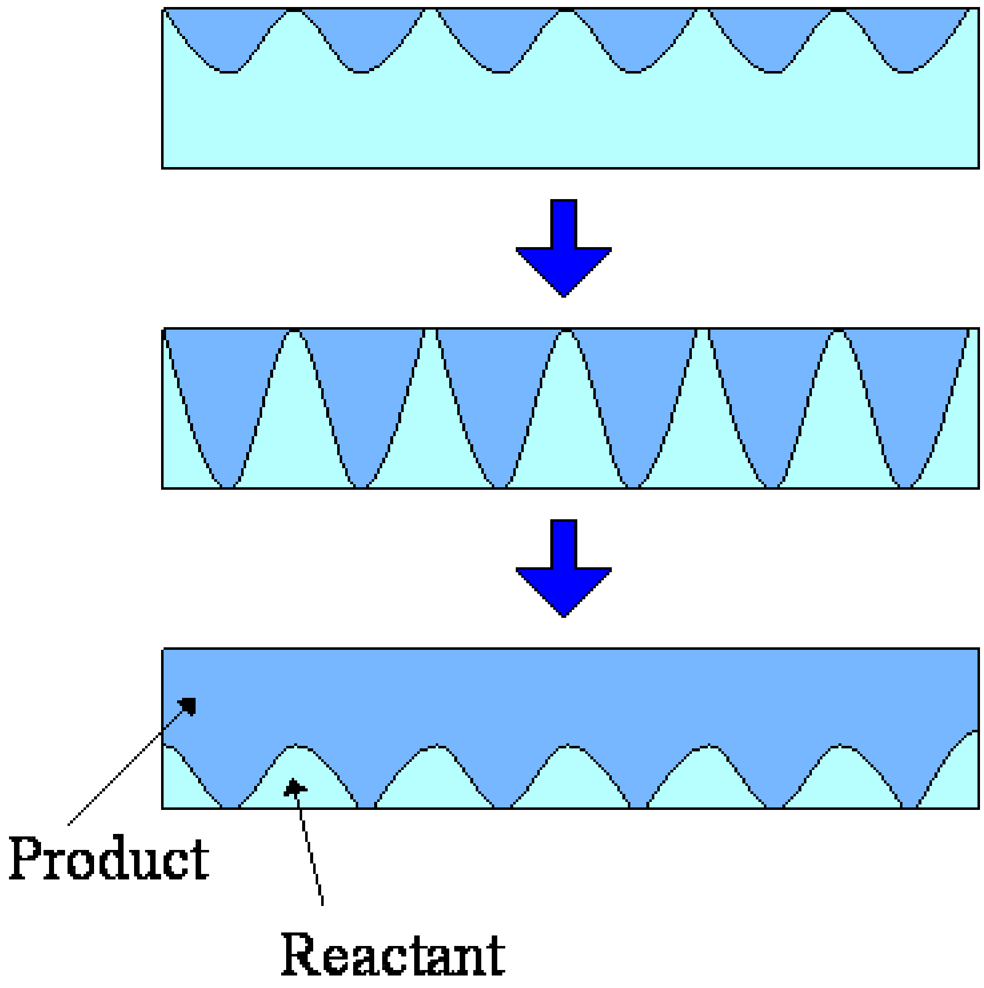

Before the max point

Pattern is created

Diffraction signal increase

Max point (50 laser shot)

Pattern is well created

Diffraction signal is max (visible)

After the max point

Pattern is destroyed

Diffraction signal decrease

Summary - TG micro patterning -

- Transient Grating (TG) method can create and, at the same time, observe the microscopic pattern on the polysilane thin films.
- Firstly, the microscopic pattern is created, and after the max point, pattern is destroyed by the laser radiation shot.
- This method is simple and convenient to create and observe the microscopic pattern than the ordinary techniques.
- Theoretically, the fringe size can be archived as small as half of the excitation wavelength. (in this condition, 133nm)

Other Application – Dynamics of Dopamine -

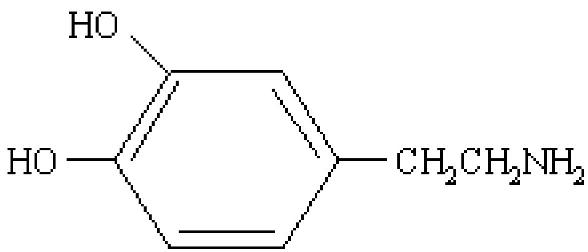

Dopamine

Understanding o f the photoexcitaion, photoreaction, molecular dynamics of Dopamine is very important to elucidate dynamics and mechanism of living body

Time-profile of the TG signal taken for Dopamine/DMF

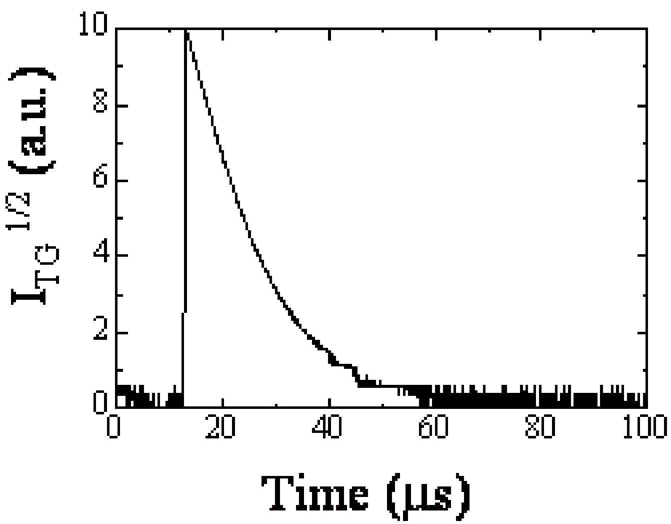

Thermal grating signal of Dopamine

➡ Excitation and reaction mechanics

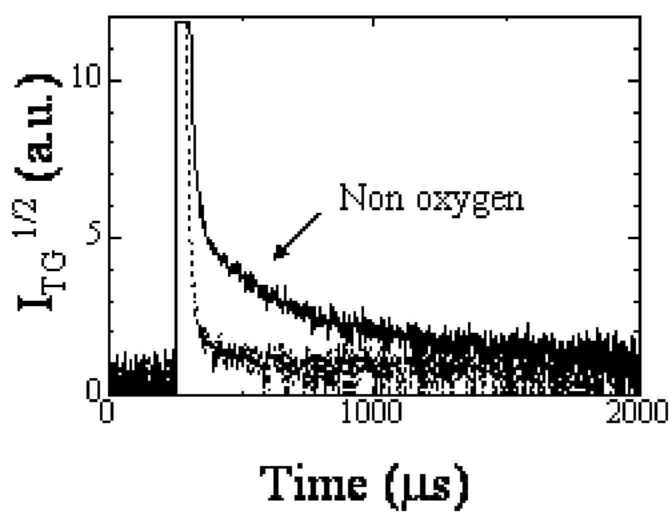

Population grating signal of Dopamine

➡ Molecular dynamics

Other Application – Nano Metal Particles -

Nano Metal Particles → catalyst materials, electrical and optical devices

$$PtCl_6^{2-} + 4e \xrightarrow[\text{(restoration)}]{\text{UV irradiation}} Pt + 6Cl^-$$

$$nPt \xrightarrow[\text{(clustering)}]{} Pt_n$$

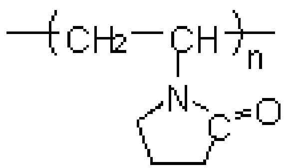

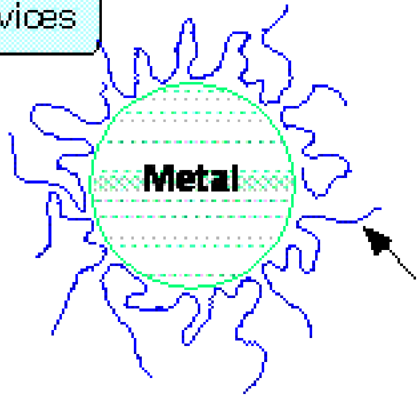

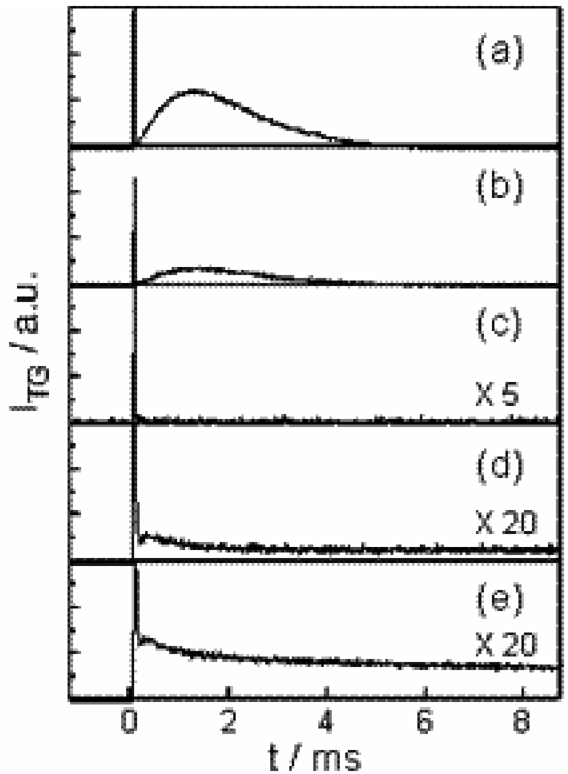

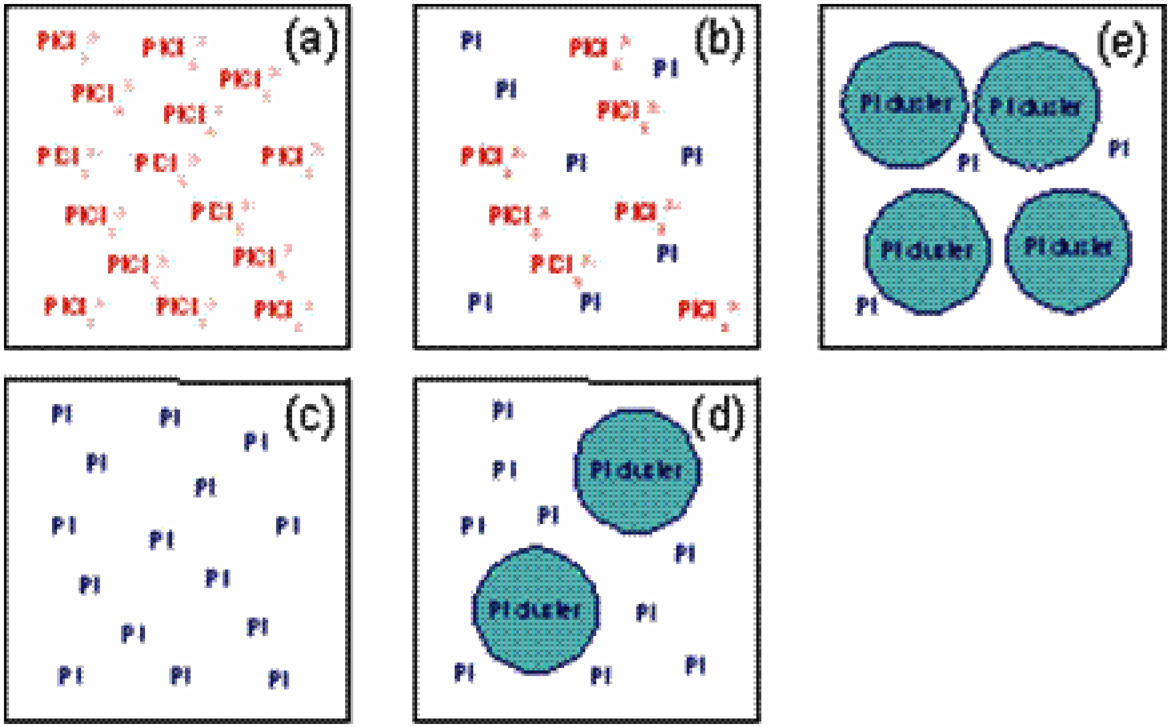

Acknowledgement

Special Thanks to

Prof. Kazumi Matsushige (Kyoto University- VBL director)

Prof. Shigeo Fujita (Electro. Sci. & Eng., Kyoto University)

Prof. Yoichi Kawakami (Electro. Sci. & Eng., Kyoto University)

Prof. Masahide Terazima (Chemistry, Kyoto University)

Prof. Hirokazu Tada (Institute of Molecular Science)

Ex-PD members of Kyoto University-VBL

Prof. Hyun-Chul Ko, (Present; University of South Alabama)

Prof. Masafumi Harada (Present; Nara Women's University)

Prof. Michiaki Mabuchi (Present; Niihama National College of Technology)